Real-Time Rainfall-Runoff Model of the Carraízo-Reservoir Basin in Puerto Rico

By Nicasio Sepúlveda, Francisco Pérez-Blair, Lewis L. DeLong, and Dianne López-Trujillo

---

U.S. GEOLOGICAL SURVEY

Water-Resources Investigations Report 95-4235

Prepared in cooperation with the

PUERTO RICO AQUEDUCT AND SEWER AUTHORITY

San Juan, Puerto Rico
1996

U.S. DEPARTMENT OF THE INTERIOR
BRUCE BABBITT, Secretary

U.S. GEOLOGICAL SURVEY
Gordon P. Eaton, Director

For additional information write to:

District Chief
U.S. Geological Survey
GSA Center, Suite 400-15
651 Federal Drive
San Juan, Puerto Rico 00965

Copies of this report can be purchased from:

U.S. Geological Survey
Branch of Information Services
Box 25286
Denver, CO 80225-0286

CONTENTS

ILLUSTRATIONS

TABLES

CONVERSION FACTORS AND ACRONYMS

Multiply	By	To obtain
foot	0.3048	meter
inch	2.540	centimeter
mile	1.6093	kilometer
inch per hour	0.00071	centimeter per second
square mile	2.5916	square kilometer
foot per day	0.3048	meter per day
cubic foot per second	0.028317	cubic meter per second
acre-foot	1,233.5	cubic meter

Acronyms used in report:

Automated Data Processing System (ADAPS)

National Weather Service (NWS)

Puerto Rico Aqueduct and Sewer Authority (PRASA)

Puerto Rico Civil Defense (PRCD)

Puerto Rico Department of Natural and Environmental Resources (PRDNER)

United States Geological Survey (USGS)

Real-Time Rainfall-Runoff Model of the Carraízo-Reservoir Basin in Puerto Rico

By Nicasio Sepúlveda, Francisco Pérez-Blair, Lewis L. DeLong, *and* Dianne López-Trujillo

ABSTRACT

The methodology used to develop a rainfall-runoff model of the Carraízo-reservoir basin in Puerto Rico based on real-time data is presented. The time period covered by the simulation begins when the sum of rainfall unit values from all stations in the basin exceeds a pre-specified threshold value and ends at a simulation time equal to six hours after the unit value time corresponding to the most recent rainfall data available. Unit values are used in this report to denote values given at 15-minute intervals. The rainfall-runoff model presented herein has two components. The first component consists of a watershed model based on the Green-Ampt infiltration equations and the geomorphic unit hydrograph (GUH) algorithm. The second component is a hydraulic routing model based on the computer code HYDRAUX, which uses a finite-element collocation method with a hermitian interpolation technique to numerically solve the unsteady one-dimensional flow in networks of open channels.

The delineation of the Carraízo-reservoir basin resulted in 10 independent subbasins and 5 intervening subbasins. The calibrated Green-Ampt infiltration parameters are used to compute excess rainfall unit values from the rainfall hyetograph for all subbasins. The GUH is convolved with the excess rainfall hyetograph to produce the GUH-estimated direct runoff hydrograph for each of the 10 independent subbasins within the overall basin. The excess rainfall hyetograph computed for each dependent subbasin is used to compute the lateral inflow unit values at these subbasins. An estimated base flow is added to the GUH-estimated direct runoff hydrograph to supply an upstream boundary condition to the hydraulic routing model whenever a measured discharge hydrograph is not available for any one of the independent subbasins. The hydraulic routing model uses as input the lateral inflow unit values, the upstream boundary conditions, and the river channel geometries and hydraulic properties to generate the routed discharge hydrographs at each dependent subbasin.

The performance of the calibrated Green-Ampt infiltration parameters is evaluated for each subbasin by comparing computed excess rainfall volumes with direct runoff volumes computed from a hydrograph separation technique applied to measured hydrographs for large rainfall events. These verification events are also used to determine the accuracy of the GUH algorithm. The performance of HYDRAUX is assessed by comparing simulated and measured hydrographs for events where lateral inflow to the river channels was mainly contributed by base flow. The watershed and the hydraulic routing components of the real-time rainfall-runoff model were determined to be reasonably accurate and reliable because most of the differences between the computed and measured hydrographs could be attributed to the spatial and temporal variations in rainfall. The overall performance of the model was assessed by comparing measured and simulated discharge hydrographs for two large rainfall events. The results show the overall model is a reliable tool for estimating discharge hydrographs from raingage data.

INTRODUCTION

The development of a real-time rainfall-runoff model for the Carraízo-reservoir basin in Puerto Rico has been conducted by the U.S. Geological Survey (USGS) in cooperation with the Puerto Rico Aqueduct and Sewer Authority (PRASA). The Carraízo reservoir (fig. 1), completed in 1953 by the PRASA, is one of the major sources of water supply for the San Juan metropolitan area. The towns of Aguas Buenas, Gurabo, Juncos, Las Piedras, and San Lorenzo, as well as the city of Caguas lie within the Carraízo-reservoir basin boundary (fig. 1). The total area of the basin draining into the reservoir is about 208 square miles.

The Puerto Rico Department of Natural and Environmental Resources (PRDNER) and the Puerto Rico Civil Defense (PRCD) are the leading agencies responsible for issuing flood warnings and responding to flood emergencies. The PRDNER and PRCD depend on the flood warning bulletins issued by the National Weather Service (NWS). The NWS, in turn, depends on the real-time raingage and river stage data obtained by the USGS from stations operating upstream of the Carraízo reservoir. During major rainfall events, the streamflow of the lower section of the Río Grande de Loíza has affected flood-prone areas downstream from the dam where about 40,000 residents live, even though it is regulated by volumetric discharges from the dam. Recent major floods occurred in 1960, 1961, 1970, 1979, 1985, 1987, and 1992. The peak discharges for Río Grande de Loíza at the damsite were 170,000 and 160,000 cubic feet per second for the floods of 1960 and 1970, respectively (National Dam Safety Board, 1979). The Carraízo dam could be more effectively used as a flood-control structure if more timely runoff volumes were available.

The data collection platforms installed at each of the Carraízo-reservoir stations transmit data that are stored in the National Water Information System (NWIS) using the Automated Data Processing System (ADAPS) software program installed on the PRIME computer. All stored data pertaining to any particular rainfall event can then be retrieved from ADAPS. The rainfall and discharge data used in the analysis and testing of the real-time rainfall-runoff model presented herein is in 15-minute interval format. This format is called unit values. Data values for a day of rainfall or discharge require 96 unit values. It should be noted that not all stations transmit their recordings at the same time which may cause the number of unit values stored for each station to be different. The number of unit values is expected to be the same only if all stations are operating in the emergency mode. All streamgage and raingage data are grouped as unit values; that is, discharge and rainfall data are grouped in 15-minute intervals. The data search, data regrouping in 15-minute intervals, as well as data transfer to the computer workstation where the model runs, are done in a UNIX-system V Bourne shell executable program that makes these processes transparent to the model's user. The commands for this shell program are listed in Appendix 1. In addition, all executable commands needed to run the rainfall-runoff model are listed in this shell program.

This report explains the methodology and usage of a real-time rainfall-runoff model of the Carraízo-reservoir basin using a watershed model component and a hydraulic routing component. The hydraulic component is based on the computer program HYDRAUX (DeLong, 1995). The model estimates volumetric discharges at the reservoir as a function of time during rainfall events. In addition, the model estimates what the recession curve of the discharge hydrograph would be if rainfall were to cease after the most recent rainfall data available. The addition of a stochastic rainfall-prediction component to the rainfall-runoff model presented herein, which is strictly deterministic, is beyond the scope of this study.

The presentation of the theoretical components of the rainfall-runoff model is followed by a discussion of how these components were implemented. A description of the Carraízo-reservoir basin is followed by a discussion of its division into independent and intervening subbasins. The main soil categories present in the basin are then presented. The theory of the watershed and the hydraulic routing models are presented in the REAL-TIME RAINFALL-RUNOFF MODEL section. The watershed modeling theory, covering the Green-Ampt infiltration equations, the hydrograph

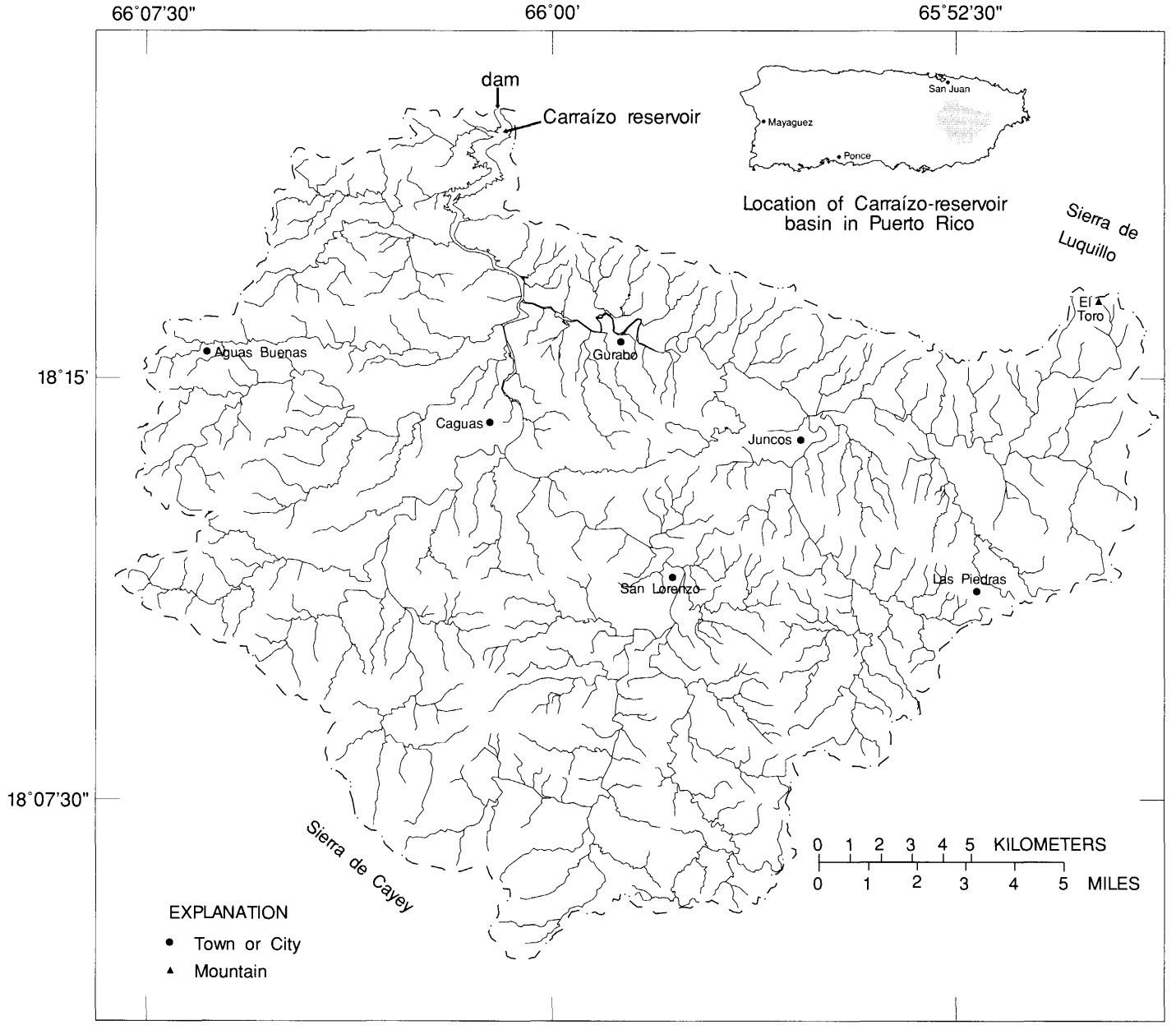

Figure 1. Location and drainage area of Carraízo-reservoir basin in Puerto Rico.

separation technique developed particularly for this model, and the methodology used to develop the geomorphic unit hydrograph (GUH) equations, are presented before discussing the unsteady, one-dimensional open-channel flow equations and the numerical solution used to solve these equations as part of the hydraulic routing model. The applications of the watershed model and the hydraulic routing model are presented in the APPLICATION OF REAL-TIME RAINFALL-RUNOFF MODEL section. A discussion of the discharge hydrographs simulated for two large rainfall events that occurred in the basin during 1992 and 1993 is presented in the SIMULATION RESULTS section. Using rainfall data, topsoil capacity to absorb water, river channel geometry and roughness coefficients, and streamflow data, this model provides the PRASA with an algorithm that improves estimates of discharge at the Carraízo reservoir.

Purpose and Scope

The purpose of this report is to present the methodology used to develop a real-time rainfall-runoff model for the Carraízo-reservoir basin in Puerto Rico using Green-Ampt infiltration equations, the GUH algorithm, and the computer program HYDRAUX. The real-time capability of this model allows the estimation of water volumes at the reservoir from the rainfall and discharge data that is being obtained from the network stations inside the basin. The model estimates what the recession curve of the discharge hydrograph would be if no further rainfall were recorded after the time corresponding to the last available rainfall data for the event being simulated. The estimated water volumes at the reservoir can be used to simulate how the reservoir stage changes in time by tying these volumes with reservoir bathymetric data, storage capacity, and discharges through the reservoir gates. These real-time mode estimates could allow the PRASA to make appropriate management decisions on the opening and closing of the reservoir gates.

DESCRIPTION OF STUDY AREA

Located about 13.5 miles upstream from the Río Grande de Loíza delta and about 10 miles southeast of the San Juan metropolitan area, the Carraízo reservoir had an estimated storage capacity of 12,300 acre-feet in 1990 and of 11,500 acre-feet in 1994 (Richard M.T. Webb, USGS, written commun., 1995). The Carraízo-reservoir basin is characterized by steep mountainous areas separated by narrow valleys. The Sierra de Luquillo to the northeast and the Sierra de Cayey to the southwest are chains of mountains that delineate some of the boundaries of this mountainous upper basin. An alluvial valley surrounds the city of Caguas (fig. 1). Alluvial valleys, smaller than the Caguas valley, surround the towns of Gurabo and Juncos. Elevations within the basin range from 60 feet at the base of the Carraízo reservoir to 3,524 feet at El Toro mountain peak in the Sierra de Luquillo (fig. 1). The land uses within the basin can be generally classified as grazing (66 percent of the land), forest (23 percent), urban development (8 percent), and cropland (3 percent) according to Quiñones and others (1989). About 50 percent of the basin is underlain by the San Lorenzo batholith, a large mass of plutonic rock, which consists predominantly of granodiorite and quartz diorite (Briggs and Akers, 1965). Volcanic breccia and tuff, with a few thin lava flows and rare layers of siltstone and sandstone, as well as extensive terrace and alluvial deposits, are also present in the basin (Rogers, 1979; Pease, 1968).

The basin is characterized by the small range in average temperature variations throughout the year typical of a tropical climate. The wind circulation is dominated by the trade winds from the east-northeast. Mean annual rainfall over the basin varies both geographically and seasonally. Annual rainfall averages about 120 inches in the Sierra de Luquillo area (northeast of the basin), compared to 67 inches in the Juncos area. Due to the strong orographic effects present in the basin, there are no predominant rainfall patterns. Moisture-laden air from the ocean is carried by the trade winds inland and the cooling effect as the air ascends over the mountains causes condensation in the form of

rainfall. Rainfall in Puerto Rico is generally produced by either easterly waves or by cold fronts. Easterly waves occur during the period from May to November, and cold fronts are common from November to April. Rainfall over the basin is generally light from January to April and tends to be heavier from August to October.

Carraízo-Reservoir Basin Delineation

The raingage and streamgage network in the Carraízo-reservoir basin consists of 14 streamgages with a raingage installed at the same location and another 14 raingages areally distributed throughout the basin. Numbers 1 through 14 in figure 2 show the location of the streamgages with their respective raingages, and numbers 15 through 28 indicate the location of the additional raingages not located at streamgage sites. The USGS identification numbers, names, station type, figure 2 numbers, and longitude and latitude for each of these stations are listed in table 1.

The division of the Carraízo-reservoir basin into subbasins was performed taking into account the location of the streamgages. The drainage area of each subbasin is the entire watershed area contributing discharge to the streamgage at the outlet of each subbasin. These drainage areas are listed in table 2. The term "independent subbasin" is used in this report to make reference to subbasins I to X, which are the watersheds contributing discharge to streamgages 1 through 10 in figure 2. The discharge measured at the streamgage of each of the Carraízo-reservoir independent subbasins does not depend on the discharge measured at any other streamgage. Dependent subbasins XI to XIV are the watershed areas contributing discharge to streamgages 11 through 14 (fig. 2), respectively. The watershed area of subbasins XI to XIV lying outside the independent or other dependent subbasins is referred to as the intervening subbasin. For example, the drainage area of intervening subbasin XIII is 41.4 square miles as table 2 indicates. However, the drainage area of dependent subbasin XIII is 89.7 square miles, computed by adding the drainage areas of independent subbasins IV, VI, VII, VIII, and IX, and of intervening subbasins XI and XIII.

The discharge hydrograph measured at streamgage 11, from dependent subbasin XI, depends on the hydrographs measured at streamgages 4, 6, 7, and 8, from independent subbasins IV, VI, VII, and VIII, and the discharge generated within intervening subbasin XI. The discharge hydrograph measured at streamgage 12 (subbasin XII) is a function of the discharge measured at streamgages 5 and 10, and the discharge produced within intervening subbasin XII. The discharge recorded at streamgage 13 is a function of the hydrographs recorded at streamgages 9 and 11, and the discharge contribution from within intervening subbasin XIII. Analogously, the discharge measured at streamgage 2 and the discharge produced within intervening subbasin XIV are the two contributions to the discharge hydrograph measured at streamgage 14. Hydrographs measured at streamgages 1, 3, 12, 13, and 14 as well as the discharge produced within intervening subbasin XV, an ungaged subbasin, are the discharge contributions to the Carraízo reservoir.

The main tributaries to the Río Grande de Loíza, upstream from the Carraízo reservoir, are shown in figure 3. These tributaries are Quebrada Blanca (channel 2), Quebrada Salvatierra (channel 4), Río Cayaguas (channel 6), Río Turabo (channel 9), Río Cagüitas (channel 12), Río Bairoa (channel 15), Río Gurabo (channels 17, 19, and 20), and Río Cañas (river connecting subbasin III with channel 21 in figure 3). The main tributary of the Río Gurabo is the Río Valenciano (channel 18), also shown in figure 3. Channel 21 shows the extent of the Carraízo reservoir. A hydraulic routing model, discussed in the HYDRAUX - Hydraulic Routing Model section of this report, is performed along the 21 channels labeled in figure 3.

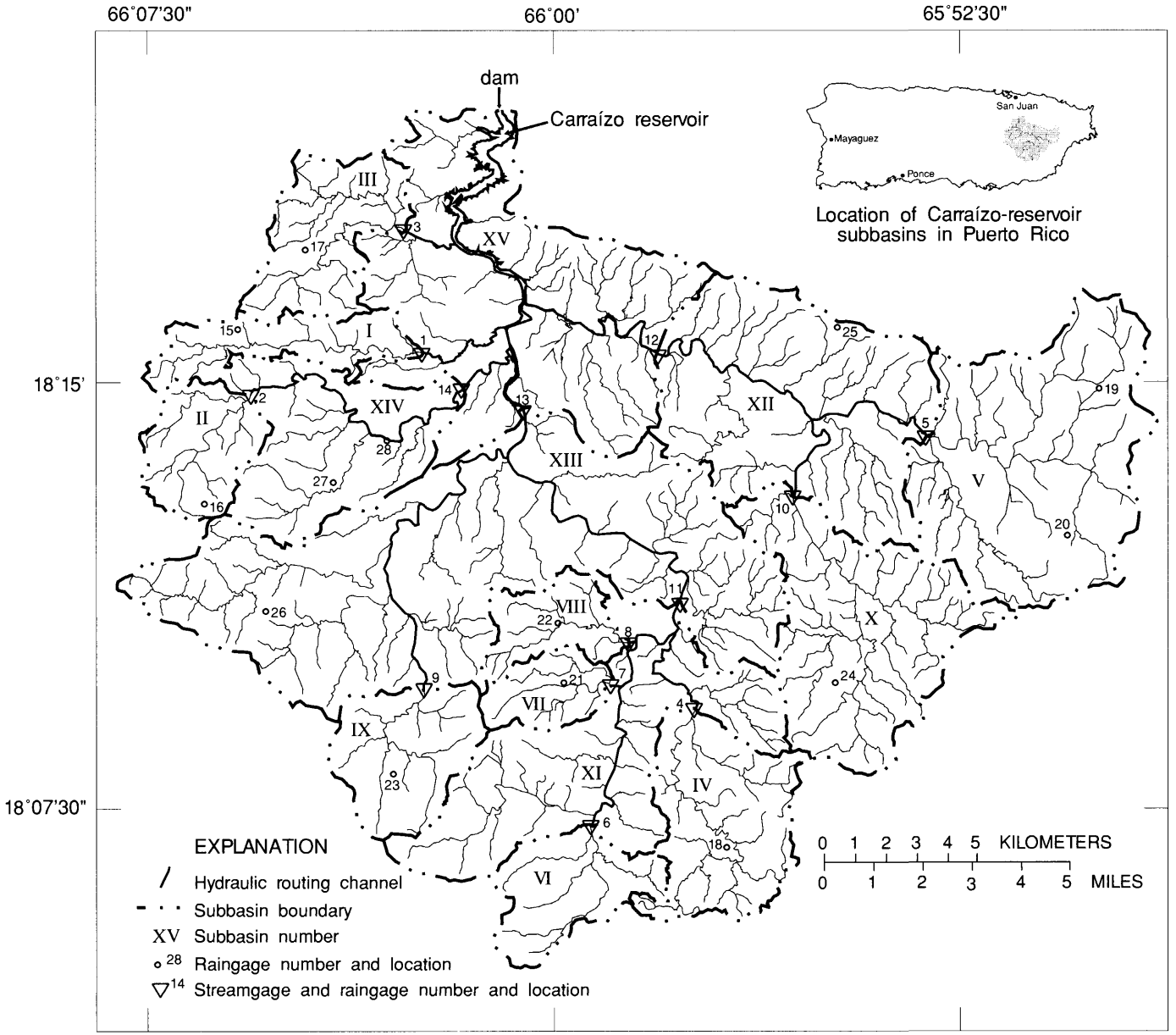

Figure 2. Carraízo-reservoir subbasins and station locations.

Table 1. USGS station names and identification numbers

[SIN, USGS station identification number; T, station type used in this report: 1, raingage only; 2, streamgage and raingage; NF2, station number in figure 2; °, degree; ′, minute; ″, second; RGDL, Río Grande de Loíza]

SIN	Station Name	T	NF2	Longitude	Latutude
50055390	Río Bairoa at Bairoa	2	1	66°02′25″	18°15′32″
50055100	Río Cagüitas	2	2	66°05′36″	18°14′48″
50058350	Río Cañas	2	3	66°02′44″	18°17′41″
50051310	Río Cayaguas	2	4	65°57′25″	18°09′13″
50055750	Río Gurabo below El Mangó	2	5	65°53′06″	18°14′02″
50050900	RGDL at Quebrada Arenas	2	6	65°59′19″	18°07′11″
50051150	Quebrada Blanca	2	7	65°58′59″	18°09′40″
50051180	Quebrada Salvatierra	2	8	65°58′38″	18°10′24″
50053025	Río Turabo above Borinquen	2	9	66°02′25″	18°09′35″
50056400	Río Valenciano near Juncos	2	10	65°55′33″	18°12′58″
50051800	RGDL at San Lorenzo	2	11	65°57′41″	18°11′09″
50057000	Río Gurabo at Gurabo	2	12	65°58′05″	18°15′31″
50055000	RGDL at Caguas	2	13	66°00′34″	18°14′33″
50055225	Río Cagüitas at Villa Blanca	2	14	66°01′40″	18°14′55″
50999964	Bairoa Arriba	1	15	66°05′45″	18°15′58″
50999962	Cañaboncito	1	16	66°06′25″	18°12′53″
50999963	Jagüeyes Abajo	1	17	66°04′34″	18°17′21″
50999960	Quebrada Arenas	1	18	65°56′49″	18°06′50″
50999958	Pueblito del Río	1	19	65°49′56″	18°14′54″
50999968	Las Piedras Construction	1	20	65°50′27″	18°12′16″
50999956	Quebrada Blanca	1	21	65°59′47″	18°09′43″
50999954	Quebrada Salvatierra	1	22	65°59′54″	18°10′46″
50999961	La Plaza	1	23	66°03′00″	18°08′08″
50999967	Barrio Montones	1	24	65°54′39″	18°09′48″
50999959	Gurabo Abajo	1	25	65°54′45″	18°16′02″
50999966	Barrio Beatriz	1	26	66°05′22″	18°11′00″
50999965	Vaquería El Mimo	1	27	66°04′03″	18°13′11″
50055170	Río Cagüitas near Caguas	1	28	66°02′53″	18°13′59″

Table 2. Subbasin drainage areas

[I to X are independent subbasins; XI to XV are intervening subbasins; TOT, total drainage area of the basin, in square miles]

Subbasin identification	Drainage area, in square miles
I	5.08
II	5.23
III	7.53
IV	10.1
V	22.3
VI	6.0
VII	3.23
VIII	3.78
IX	7.16
X	16.4
XI	18.0
XII	21.5
XIII	41.4
XIV	11.7
XV	28.3
TOT	207.7

Generalized Soil Categories

Topsoil types present in the Carraízo-reservoir basin were obtained from the Natural Resources Conservation Service (formerly the Soil Conservation Service, 1978). These soil types were re-grouped into 11 main categories. Urban areas where a soil classification survey had not been conducted were grouped under the *impermeable areas* category. Areas where rainfall becomes a direct runoff contribution with practically no water infiltration into the soil were classified under the *waterbodies* category. Areas having slopes greater than 60 percent with little or no soil cover were grouped in the category of *steep stony land.* The remaining eight soil categories used under this classification scheme are: *silty clay loam*, *silty clay*, *sandy loam*, *gravelly clay loam*, *clay*, *clay loam*, *loam*, and *alluvial deposits.* The areal distribution of these soil categories in the Carraízo-reservoir basin is shown in figure 4. Each of these soil categories is characterized by different hydraulic properties. The hydraulic conductivity values of these soil categories generally decrease in the following order: *alluvial deposits*, *sandy loam*, *loam*, *gravelly clay loam*, *clay loam*, *silty clay loam*, *silty clay*, *clay*, and *impermeable areas.* The fraction of the total energy possessed by the water in the soil-water mixture due to the soil suction forces tends to increase in the same order listed above (Rawls and others, 1983). Topsoil porosity varies from one category to another. These hydraulic parameters, in addition to the soil-moisture content at the beginning of a rainfall event, determine the amount of excess rainfall that a watershed yields from total rainfall volumes.

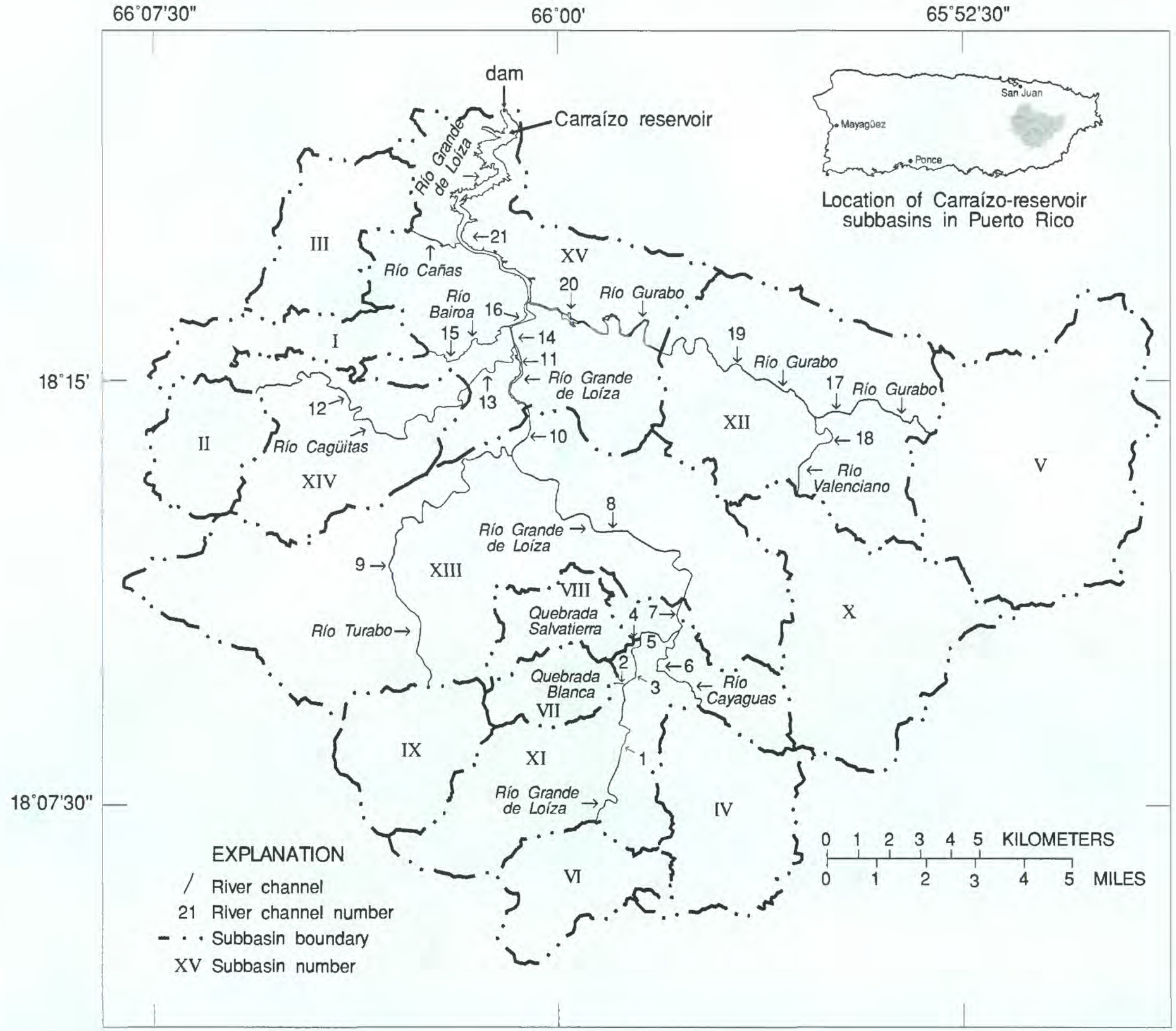

Figure 3. River channels in the Carraízo-reservoir basin where hydraulic routing is performed.

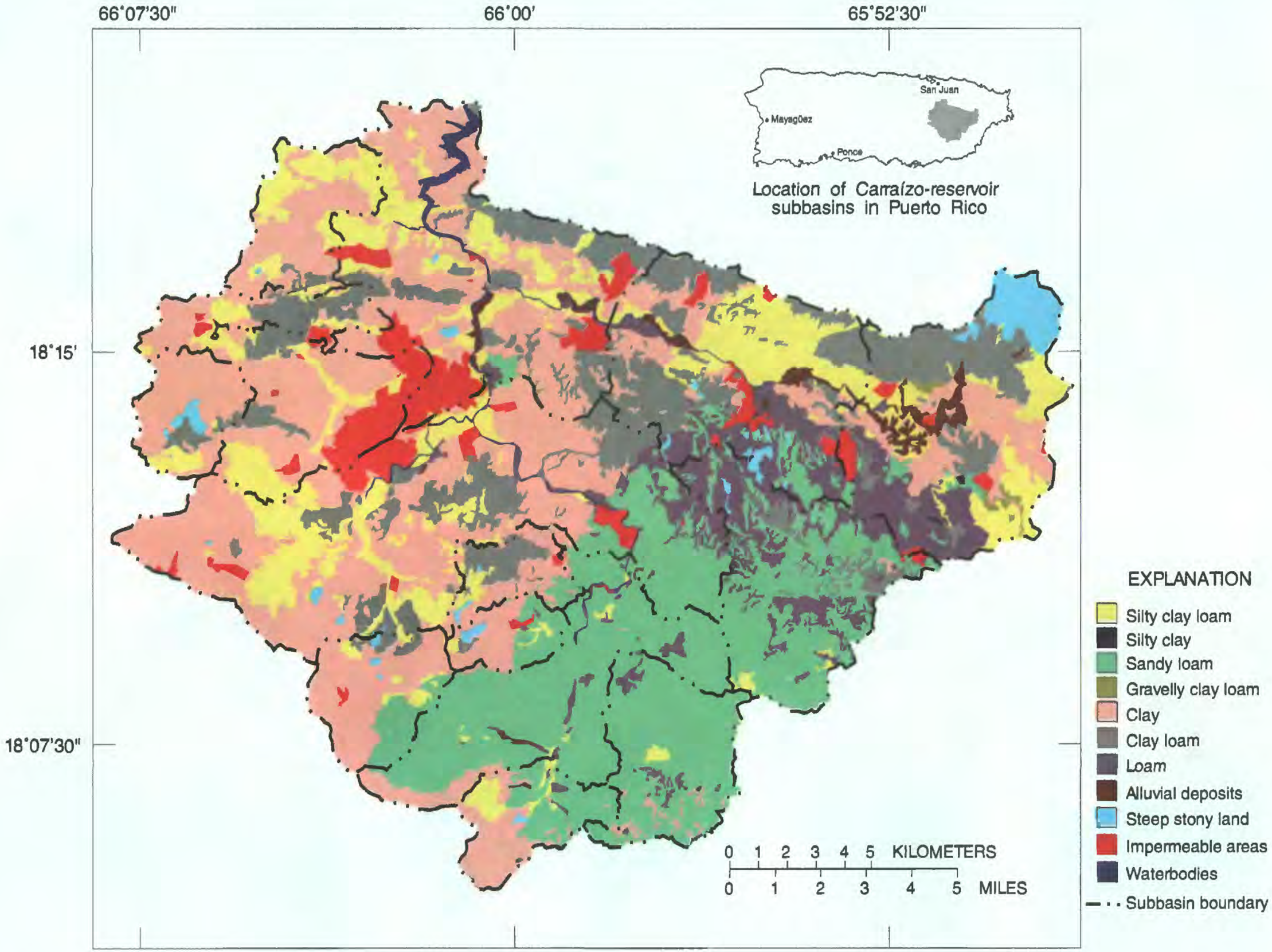

Figure 4. Generalized soil categories for each subbasin in the Carraízo-reservoir basin (Modified from the Soil Conservation Service, 1978).

REAL-TIME RAINFALL-RUNOFF MODEL

The two components of the real-time rainfall-runoff model, the watershed and the hydraulic routing models, are presented in this section. An overview of the methodology employed in the watershed model includes the computation of excess rainfall from the rainfall hyetograph through the application of Green-Ampt infiltration equations and the use of the GUH technique to generate the direct runoff hydrograph is discussed. The discharge hydrograph, obtained from the GUH algorithm by adding an estimated base flow component to the direct runoff hydrograph, is used as an upstream boundary condition in the hydraulic routing model whenever the streamgage of an independent subbasin is not operational prior to, or during, a rainfall event. HYDRAUX, the hydraulic routing model, presented after the watershed model, is used to route flow through the main river channels of the intervening subbasins XI to XV (fig. 3).

Watershed Model

The watershed model used in this study consists of the Green-Ampt infiltration equations to compute the excess rainfall unit values from the rainfall hyetograph associated with each subbasin, a hydrograph separation technique to calculate the direct runoff for each discharge hydrograph, and a GUH algorithm to estimate direct runoff through its convolution with the excess rainfall hyetograph. The rainfall hyetograph associated with each subbasin is the average rainfall volume as a function of time computed from the raingages within each subbasin (table 3). In addition, the computed excess rainfall hyetograph is used to derive the lateral inflow unit values needed for the hydraulic routing model. The computation of the GUH ordinates is derived in recursive form following the stochastic approach presented by Rodríguez-Iturbe and Valdés (1979). The theoretical aspects of these algorithms are explained in detail in the following sections.

Table 3. Raingage stations used to compute average rainfall volumes for each subbasin

Subbasin identification	Raingage station number (shown in figure 2)
I	1, 15
II	2, 16
III	3, 17
IV	4, 18
V	5, 19, 20
VI	6
VII	7, 21
VIII	8, 22
IX	9, 23
X	10, 24
XI	4, 6, 7, 8, 11, 18, 21, 22
XII	5, 10, 12, 19, 20, 24, 25
XIII	4, 6, 7, 8, 9, 11, 13, 18, 21, 22, 23, 26
XIV	2, 14, 16, 27, 28
XV	1, 3, 12, 13, 14

Green-Ampt Infiltration Equations

The Green-Ampt infiltration equations used to compute excess rainfall unit values from rainfall hyetographs are briefly discussed in this section. The rainfall unit values determined from this method are used to compute the watershed contribution to the hydraulic routing model and the direct runoff through the GUH algorithm. The reader i referred to Chow and others (1988) for a more detailed discussion and derivation of these equations. The parameters associated with the Green-Ampt infiltration equations are soil porosity η (dimensionless), effective soil porosity η_e (dimensionless), wetting front soil suction head ψ (in inches), hydraulic conductivity of the topsoil K (in inches per hour), and initial soil moisture content θ_i (dimensionless). The effective soil porosity η_e is defined as the difference between porosity η and residual moisture content of the soil after it has been completely drained, denoted by η_r; that is, $\eta_e = \eta - \eta_r$ (Chow and others, 1988). By definition, the value of θ_i is generally greater than η_r and smaller than η. The parameter ψ is defined as the total potential energy, expressed in units of height, that the water column acquires due to soil suction forces. As the size of the soil particles decreases, ψ increases and K decreases.

Although the Morel-Seytoux infiltration equations (Morel-Seytoux, 1988) were also programmed and analyzed for this study, the Green-Ampt infiltration equations were chosen over the Morel-Seytoux infiltration equations because the Green-Ampt infiltration equations produced better results in the estimation of excess rainfall generated from rainfall events. The computation of the excess rainfall from rainfall hyetographs obtained for each raingage in a subbasin using the Green-Ampt infiltration equations requires an estimate of the initial soil moisture content θ_i. The highest attainable value of θ_i is assumed to be η_e, whereas the lowest is $\eta - \eta_e$. If the highest and lowest base flow recorded at the streamgage are denoted by B_h and B_l, then the soil moisture content immediately preceding a rainfall event is assumed to be given by

$$\theta_i = (\eta - \eta_e)\left(\frac{\eta_e}{\eta - \eta_e}\right)^{\left(\frac{B_i - B_l}{B_h - B_l}\right)}, \qquad (1$$

where B_i is the base flow recorded at the streamgage at the time the rainfall begins. Equation (1) is obtained from the assumption that the values θ_i vary from its lowest value $\eta - \eta_e$ to its highest value η_e, and that θ_i is directly proportional to b^{ζ}, where the exponent ζ varies from 0 to 1 and the base b is determined from the boundary conditions $\theta_i(B_l) = \eta - \eta_e$ and $\theta_i(B_h) = \eta_e$. The exponent ζ can only assume values in the range of 0 to 1 because values larger than 1 may cause the value of θ_i to be lower than η_e under some conditions. Equation (1) associates the lowest base flow B_l to the lowest attainable value of θ_i and the highest base flow B_h to the highest attainable value of θ_i. Equation (1) establishes that the ability of the subbasin to drain water increases for greater values of initial soil moisture content.

The rainfall intensity unit values i_t, expressed in inches per hour, are defined in terms of the ratio $r_t/\Delta t$, where the rainfall unit values r_t are in inches and time is discretized in intervals Δt of 0.25 hour. Rainfall r_t and rainfall intensity i_t unit values are assumed to be piecewise constant functions defined in the time domain because their range values change only every multiple value of Δt. The infiltration rate f_t, in inches per hour, at time t is obtained from

$$f_t = K\left(\frac{\psi(\eta - \theta_i)}{F_t} + 1\right), \qquad (2$$

where F_t, in inches, is the cumulative infiltration at time t. The chosen F_t value at time $t = 0$, just before the rainfall begins, must preclude division by zero in equation (2). A nonzero initial value for F_t of 0.01 inch was assumed. Notice that equation (2) implies that the infiltration rate is always greater than the hydraulic conductivity K of the topsoil. The resulting f_t value computed from equation (2) is then compared with the value i_t for the same time t to determine if and when water begins to pond. Water begins to pond on the soil surface at the beginning of the time interval $(t, t + \Delta t)$ if $f_t \leq i_t$. If this is the case, then the cumulative infiltration value at the end of this time interval, $F_{t+\Delta t}$, is computed from the equation

$$F_{t+\Delta t} = F_t + \psi(\eta - \theta_i) \ln\left(\frac{F_{t+\Delta t} + \psi(\eta - \theta_i)}{F_t + \psi(\eta - \theta_i)}\right) + K\Delta t. \tag{3}$$

The application of Newton's iterative method to numerically solve nonlinear equation (3) (Conte and de Boor, 1980) results in the following iteration process

$$F^{n+1}_{t+\Delta t} = F^{n}_{t+\Delta t} + \frac{F_t + \psi(\eta - \theta_i) \ln\left[\frac{F^{n}_{t+\Delta t} + \psi(\eta - \theta_i)}{F_t + \psi(\eta - \theta_i)}\right] + K\Delta t - F^{n}_{t+\Delta t}}{\frac{F^{n}_{t+\Delta t}}{F^{n}_{t+\Delta t} + \psi(\eta - \theta_i)}}, \tag{4}$$

where

$F^{n}_{t+\Delta t}$ is the n^{th} iteration value for the cumulative infiltration at time $t + \Delta t$, and

$F^{n+1}_{t+\Delta t}$ is the $n^{\text{th}} + 1$ iteration value for the cumulative infiltration computed from $F^{n}_{t+\Delta t}$.

These two iterative values are generated at every iteration step. Convergence is achieved when the difference between $F^{n}_{t+\Delta t}$ and $F^{n+1}_{t+\Delta t}$ is less than or equal to one thousandth of one inch for some positive integer n, then the solution $F_{t+\Delta t}$ to equation (3) is taken to be $F^{n+1}_{t+\Delta t}$.

When the infiltration rate f_t is greater than the rainfall intensity i_t, water does not begin to pond on the soil surface at the beginning of time interval $(t, t + \Delta t)$. However, water may begin to pond during this time interval or may not pond at all throughout the interval. To determine which one of these two possibilities actually occurs, the value $F'_{t+\Delta t} = F_t + i_t\Delta t$ is used to compute $f'_{t+\Delta t}$ from the right-hand side of equation (2), replacing F_t by $F'_{t+\Delta t}$. If $f'_{t+\Delta t}$ is greater than i_t, then no ponding occurs throughout the interval $(t, t + \Delta t)$ and the cumulative infiltration $F_{t+\Delta t}$ up to time $t + \Delta t$ is set equal to $F'_{t+\Delta t}$. However, if $f'_{t+\Delta t}$ is less than or equal to i_t, then water ponding begins at time $t_p = t + \Delta t'$, where

$$\Delta t' = \frac{F_p - F_t}{i_t} = \frac{K\psi(\eta - \theta_i)}{i_t(i_t - K)} - \frac{F_t}{i_t}, \tag{5}$$

and F_p denotes the cumulative infiltration at time $t = t_p$. The cumulative infiltration $F_{t+\Delta t}$ when $f'_{t+\Delta t}$ is less than or equal to i_t is computed from equation (3) replacing F_t by F_p and using the computed value $\Delta t'$ from equation (5) instead of Δt. The excess rainfall at time $t + \Delta t$, denoted by $E_{t+\Delta t}$, is computed from the equation

$$E_{t+\Delta t} = r_{t+\Delta t} - (F_{t+\Delta t} - F_t), \tag{6}$$

where

$r_{t+\Delta t}$ is the rainfall unit value at time $t + \Delta t$,

F_t is the cumulative infiltration at time t, and

$F_{t+\Delta t}$ is the cumulative infiltration at time $t + \Delta t$.

The water infiltrated into the soil for every time step is computed following the computational progression of equations (2) through (5). As a result, all excess rainfall unit values: $E_{t+\Delta t}, E_{t+2\Delta t}, \ldots, E_{t+H\Delta t}$ can be computed following the steps of equations (2) through (6). The duration of the rainfall event is herein denoted by TD $= H\Delta t$. The total excess rainfall for the duration of the rainfall event is computed from the sum

$$\text{ER} = \sum_{k=1}^{H} E_{t+k\Delta t}, \tag{7}$$

where

k is the summation index running from 1 to H, and

$E_{t+k\Delta t}$ is the excess rainfall unit value at time $t + k\Delta t$.

Analogously, the total rainfall for the duration of the rainfall event is computed from the sum

$$\text{TR} = \sum_{k=1}^{H} r_{t+k\Delta t}, \tag{8}$$

where $r_{t+k\Delta t}$ is the rainfall unit value at time $t + k\Delta t$. From now on, to simplify the notation, it is assumed that rainfall begins at time $t = 0$ and therefore, the excess rainfall unit values become simply $E_{\Delta t}, E_{2\Delta t}, \ldots, E_{H\Delta t}$. It should be noted that the end of the rainfall event occurs prior to the end of the direct runoff contribution.

Hydrograph Separation Technique

The hydrograph separation technique used to calculate the direct runoff from discharge hydrographs measured at streamgages 1 to 14 of subbasins I to XIV (fig. 2) is described below. This hydrograph separation technique was applied to the several rainfall events used to calibrate the Green-Ampt infiltration parameters in each of these subbasins. The technique was also used to verify the calibration of the Green-Ampt infiltration parameters.

In this report, a discharge hydrograph is specified by the coordinate pairs (t_u, Q_u) for the index values $u = 1, 2, \ldots, G$. The hydrograph peak, denoted by index p, is (t_p, Q_p), expressed in units of hour and cubic feet per second, respectively. The point in the hydrograph immediately preceding direct runoff, identified by the coordinate pair (t_s, Q_s), is defined as the point just before an increase in discharge is measured. The point in the hydrograph where the direct runoff contribution is estimated to finish is identified by the coordinate pair (t_f, Q_f). The approach to estimate this index f is explained next.

A linear regression between the measured depletion curve (also known as recession curve) of the hydrograph ordinates $Q(t)$ and their computed slope $dQ(t)/dt$ was used to obtain the values for the slope b_1 and intercept b_2 in the equation

$$\frac{dQ_d(t)}{dt} = b_1 Q_d(t) + b_2. \tag{9}$$

The solution of this linear differential equation, with $Q_d(t_u) = Q_u$ as the initial condition for an index u in the depletion curve satisfying the condition $u > p$, is given by

$$Q_d(t; t_u) = \left(Q_u + \frac{b_2}{b_1}\right) exp\left(b_1 (t - t_u)\right) - \frac{b_2}{b_1}, \tag{10}$$

where the subscript d is used to denote the approximation of the depletion curve to the discharge hydrograph based on the linear regression coefficients b_1 and b_2. The semicolon in equation (10) implies t_u is a fixed parameter upon which the function Q_d depends. The index u in equation (10) is taken to be larger than index p and smaller than index $G - 3$ to allow the linear regression to be performed over at least three points. The expression $Q_d(t; t_u)$ of equation (10) is evaluated at times t greater or equal to t_u. The point in the hydrograph closest to the end of the direct runoff contribution is identified by the index that minimizes the following sum of squared errors

$$\sum_{w=u+1}^{G} \left(Q(t_w) - Q_d(t_w; t_u)\right)^2, \tag{11}$$

where the index u in equation (11) is the same index of the initial condition used to obtain equation (10). The index u in equation (11) is varied from $p + 1$ to $G - 4$ and such index that minimizes the sum in equation (11), denoted by f, identifies the point where direct runoff is estimated to finish. The base flow values at times t_s and t_f, denoted by B_s and B_f and expressed in units of cubic feet per second, are by definition, equal to the discharge values Q_s and Q_f, respectively. Now that the start and the finish of the direct runoff contribution have been identified with indices s and f in the discharge hydrograph, the approximation made to establish the separation between direct runoff and base flow at time t_u for $t_s < t_u < t_f$ can be presented.

A first linear regression is taken over points $(t_p, Q_p), (t_{p+1}, Q_{p+1}), \ldots, (t_{p+y}, Q_{p+y})$ where $y < f - p + 1$. The resulting slope is denoted by s_p. A second linear regression is taken over points $(t_f, Q_f), (t_{f+1}, Q_{f+1}), \ldots, (t_G, Q_G)$ and its resulting slope is denoted by s_f. The base flow at times t_u for $t_s < t_u < t_f$ is computed from

$$B_u = \begin{cases} Q_f + s_f\left(\dfrac{Q_p - Q_f}{s_p}\right) & \text{if} \quad u = p; \\ B_s + (Q_u - Q_s)\left(\dfrac{B_p - B_s}{Q_p - Q_s}\right) & \text{if} \quad s < u < p; \\ B_f + (Q_u - Q_f)\left(\dfrac{B_p - B_f}{Q_p - Q_f}\right) & \text{if} \quad p < u < f. \end{cases} \tag{12}$$

The direct runoff at time t_u, denoted by D_u and expressed in cubic feet per second, is computed from the equation $D_u = Q_u - B_u$. The empirical nature of equation (12) gives us some assurance that the shapes of the base flow and discharge hydrographs are proportional to each other by using the ratios $(Q_u - Q_s) / (Q_p - Q_s)$ and $(Q_u - Q_f) / (Q_p - Q_f)$ to compute base flow unit values for hydrograph indices $s < u < p$ and $p < u < f$, respectively. The results after the application of the hydrograph separation technique presented here are shown for the discharge hydrograph recorded at streamgage 9 on November 7, 1991 (fig. 5).

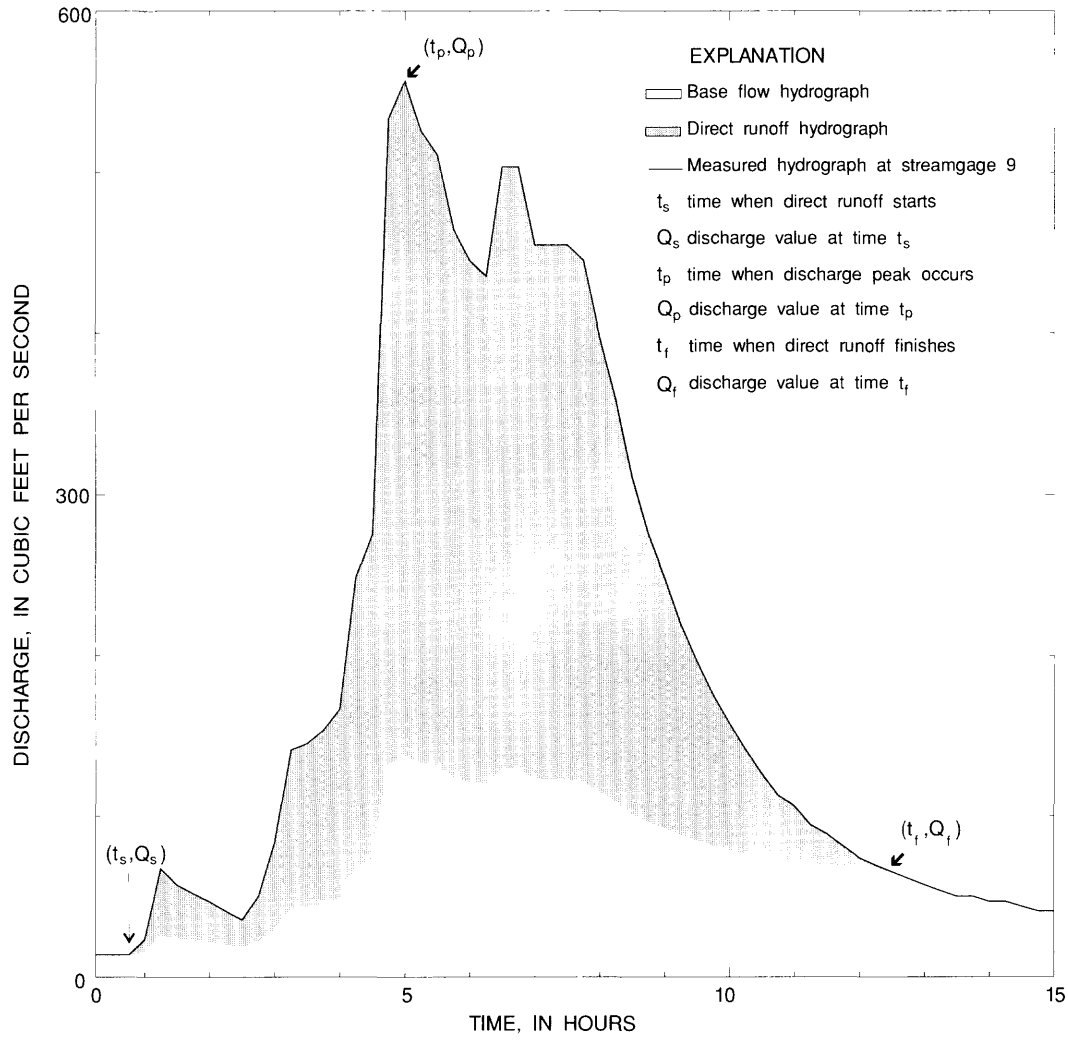

Figure 5. Application of hydrograph separation technique to measured discharge hydrograph at streamgage 9 on November 7, 1991.

Geomorphic Unit Hydrograph Method

The derivation of the GUH equations presented in this section is based on several variations to the statistical approach proposed by Rodríguez-Iturbe and Valdés (1979). The reader is referred to Rodríguez-Iturbe and Valdés (1979) for a more detailed analysis of the background theory on their statistical approach and to Smart (1972) for a review on channel network geomorphology. Some background theory on unit hydrographs is briefly reviewed in this section before presenting the derivation of the GUH equations.

In the present model, Laplace transforms are not used to compute the elements of the interval transition probability matrix for every different order of a basin, as Rodríguez-Iturbe and Valdés (1979) did. Instead, the exponential representation of the transition rate matrix for each independent subbasin was computed. Recursive-form equations were generated for the computation of the interval transition probability matrix from which the GUH equations are derived. Another variation to the approach presented by Rodríguez-Iturbe and Valdés (1979) is the equations used in this GUH representation to express the transition probabilities. Instead of using Horton's bifurcation, length, and area ratios (Smart, 1972), the transition probabilities are expressed in terms of the computed catchment area values. A third variation to the statistical approach presented earlier by Rodríguez-Iturbe and Valdés (1979) is the method used to compute the mean streamflow velocity value, a fundamental parameter that determines the shape of the GUH. In this GUH derivation, the mean streamflow velocity is determined from the excess rainfall unit values.

The instantaneous unit hydrograph (IUH), or equivalently, the unit impulse response function of a linearized hydrologic system, is the hydrograph resulting from the instantaneous application of a unit amount of excess rainfall during an infinitesimally small period of time. The direct runoff $D(t)$, which represents the hydrologic response to excess rainfall, is obtained from the convolution integral

$$D(t) = \int_0^t I(\tau)\, U(t-\tau)\, d\tau \quad , \tag{13}$$

where

$I(t)$ is the excess rainfall intensity, and

$U(t-\tau)$ is the hydrologic response of the basin at a later time t due to an input of a unit amount of excess rainfall at time τ. The term $t-\tau$ represents the time lag between the application of the unit excess rainfall and the direct runoff.

The discretization of the unit pulse response function over the time interval $[(m-1)\,\Delta t,\, m\Delta t]$ can be represented by (Chow and others, 1988)

$$U_m = \frac{1}{\Delta t} \int_{(m-1)\,\Delta t}^{m\Delta t} U(t)\, dt, \tag{14}$$

where

m is the unit hydrograph index running from 1 to M, and

t is the variable of integration over time.

The set of M nonzero values $\{U_m\}$ of equation (14) is the discrete representation of the unit hydrograph, also known as the discrete time-domain representation of the unit pulse response function. These unit hydrograph ordinate values satisfy the condition

$$\frac{12\,(3600)\,\Delta t}{5280^2\,A}\sum_{m=1}^{M} U_m = 1, \tag{15}$$

where

Δt is equal to 0.25 hour,

A is the basin drainage area, in square miles, and

U_m is in cubic feet per second per inch.

Assuming there are L nonzero direct runoff pulses $\{D_1, D_2, \ldots, D_L\}$ associated with $L-M+1$ excess rainfall unit values $\{E_{\Delta t}, E_{2\Delta t}, \ldots, E_{(L-M+1)\Delta t}\}$, then the discrete representation of equation (13) becomes (Mays and Taur, 1982)

$$D_n = D(n\Delta t) = \begin{cases} \displaystyle\sum_{k=1}^{min\{n,\,L-M+1\}} E_{k\Delta t}U_{n-k+1} & \text{if} \quad n \le M \\ \text{or} & \\ \displaystyle\sum_{k=1}^{min\{M,\,L-n+1\}} E_{(k+n-M)\Delta t}U_{M-k+1} & \text{if} \quad n > M, \end{cases} \tag{16}$$

where the index n used here denotes any one of the indices $\{1, 2, \ldots, L\}$. The total direct runoff, in inches, induced by the rainfall event is computed using the equation

$$\mathrm{DR} = \frac{12\,(3600)\,\Delta t}{5280^2 A}\sum_{n=1}^{L} D_n. \tag{17}$$

The GUH algorithm to be derived next makes use of four geomorphic parameters for the computation of the unit hydrograph ordinates. These parameters, required to represent the response of a basin during a rainfall event, are the geometric mean streamflow velocity $\bar{v}$, the average length $\bar{l}_i$ of rivers of order i, the sum of watershed areas A_i of rivers of order i, and the number n_i of rivers for order $1, 2, \ldots, N-1$. Rivers in a basin are ordered following Strahler's ordering procedure (Strahler, 1957). The basin is assumed to be of order N because the simulation of the outlet of the basin as a trapping state makes the basin increase its order by one, from $N-1$ to N.

A simple algorithm is used to estimate the geometric mean streamflow velocity $\bar{v}$, expressed in feet per second, at the basin outlet for each period of sequential nonzero rainfall unit values, that is, for each excess rainfall burst. Dimensionless slope and intercept constants c_1 and c_2 are obtained from a linear regression between the natural logarithm of the discharge, ln Q, and the natural logarithm of the streamflow velocity, ln v. Streamflow velocity measurements made for several low discharge values at the streamgage location of the basin were grouped together

with streamflow velocities for high-stage flows obtained from the step-backwater analysis performed at the same streamgage location to gather the data set needed for the linear regression between ln Q and ln v. The excess rainfall rate $E_{k\Delta t}$ computed from equation (6) for a given rainfall unit value is multiplied by the basin area A to obtain the estimated direct runoff associated with that excess rainfall unit value. This direct runoff estimate value is added to a base flow value estimated from the basin drainage area A to get the discharge value Q_k that is substituted in the linear approximation

$$\ln v_k = c_1 \ln Q_k + c_2 \tag{18}$$

to obtain an estimate for the streamflow velocity v_k for the time interval $[(k-1)\Delta t,\ k\Delta t]$. Derived values of slope c_1 and intercept c_2 in equation (18) for subbasins I to X are listed in table 4. A geometric mean streamflow velocity value $\bar{v}$ is computed from the resulting streamflow velocity values obtained from equation (18) for each excess rainfall burst. Multiple excess rainfall bursts within a single rainfall event require multiple applications of equation (16) because multiple sets of $\{U_m\}$ values are computed from equation (14) for each excess rainfall burst. Computing a single value of $\bar{v}$ for the several excess rainfall bursts that might occur in the same rainfall event results in estimating a hydrograph peak of smaller magnitude and delayed in time, particularly when excess rainfall hyetograph peaks are separated by large periods of no rainfall. Conversely, all isolated excess rainfall unit values were grouped together with the preceding rainfall burst to avoid overestimating the geometric mean streamflow velocity $\bar{v}$.

Table 4. Slope and intercept values of linear regression between river discharge and streamflow velocity for subbasins I to X

[c_1, slope (-); c_2, intercept (-)]

Subbasin identification	c_1	c_2
I	0.3043	-0.5626
II	0.2881	-0.7499
III	0.4246	-1.3206
IV	0.3956	-1.1752
V	0.3350	-1.3417
VI	0.3588	-1.1137
VII	0.3652	-1.0670
VIII	0.3233	-0.5079
IX	0.3722	-1.1428
X	0.3866	-1.7323

If the mean waiting time for the excess rainfall in a river of order i is defined by $\lambda_i^{-1} = \bar{l}_i/\bar{v}$, where $\bar{l}_i$ is the average length of rivers of order i and $\bar{v}$ is the geometric mean streamflow velocity, then the inverse waiting time matrix Λ is strictly diagonal and given by $\Lambda = diag\{\lambda_1, \lambda_2, \ldots, \lambda_{N-1}, 0\}$. The assumption of an artificial trapping state of order N with no river associated with it, $\bar{l}_N = 0$, implies that λ_N has to be set to zero. This waiting time,

computed for independent subbasins I to X, includes both overland flow and routing through river channels. The streamflow velocity v is assumed to be a function of time and space, but the streamflow velocity value used by the GUH to define the λ_i values is the geometric mean streamflow velocity $\bar{v}$ at the outlet of the basin, which is constant in space for every time interval.

The transition probability from a river of order i, referred to as state i, to a river of higher order j, or state j, is defined as p_{ij}. The matrix formed with these p_{ij} elements is denoted by P. These elements have the property that $p_{ij} = 0$ if $N > i \geq j$ or if $i - 1 < j = N$. The addition of an artificial trapping state implies that $p_{N-1,N} = p_{N,N} = 1$. The equations generalized by Gupta and others (1980) expressed the probabilities p_{ij} in terms of Horton's bifurcation, length, and area ratios. However, Allam and Balkhair (1987) demonstrated that the use of Gupta's equations can lead to major round-off errors associated with the linear regression approximation made computing Horton's bifurcation, length, and area ratios. In this study, the equation used to compute the transition probabilities is defined in terms of the computed catchment area values. The p_{ij} values were calculated from the ratio

$$p_{ij} = \frac{A_j}{\sum_{h=i+1}^{N-1} A_h}, \tag{19}$$

where A_j and A_h are the sum of watershed areas of all rivers of order j and h, respectively.

The transition rate matrix, with elements expressed in inverse units of time, is defined by $\mathbf{T} = \Lambda(\mathbf{P} - \mathbf{1})$, where $\mathbf{1}$ is used to denote the identity matrix. The interval transition probability matrix is given by $\Phi(t) = e^{\mathbf{T}t}$ with matrix elements denoted by $\phi_{ij}(t)$. The state probability vector is a function of the state at time $t = 0$, that is,

$$\Omega(t) = \Omega(0) \cdot \Phi(t) = \left(\sum_{i=1}^{N-1} \omega_i(0)\, \phi_{ij}(t) \right), \tag{20}$$

where the values $\omega_i(0) = A_i/A$ can be readily computed from the sum of watershed areas of rivers of order i, denoted by A_i, and from the total watershed area, that is, the total basin drainage area defined by

$$A = \sum_{i=1}^{N-1} A_i. \tag{21}$$

The probability that a volume of excess rain chosen at random reaches the basin outlet at time t or before is represented by the last component of $\Omega(t)$. The IUH for the basin of order N, including the trapping state, is given by

$$U(t) = \frac{d\omega_N(t)}{dt} = \sum_{i=1}^{N-1} \omega_i(0) \frac{d\phi_{iN}(t)}{dt}. \tag{22}$$

The GUH can now be calculated by substituting equation (22) in equation (14), to obtain

$$U_m = \sum_{i=1}^{N-1} \frac{\omega_i(0)}{\Delta t} \left(\phi_{iN}(m\Delta t) - \phi_{iN}((m-1)\Delta t)\right) . \tag{23}$$

The elements $\phi_{ij}(t)$ of matrix $\mathbf{\Phi}(t)$ need to be derived to obtain an analytical expression for the GUH. To accomplish this, the transition rate matrix $\mathbf{T} = \Lambda \cdot (\mathbf{P} - \mathbf{1})$ is diagonalized with a matrix $\mathbf{D}$ such that $\mathbf{T} = \mathbf{D}^{-1} \cdot (-\Lambda) \cdot \mathbf{D}$, where the columns of $\mathbf{D}^{-1}$ are the eigenvectors corresponding to the eigenvalues $\lambda = -\lambda_i$ of $\mathbf{T}$ for $i = 1, 2, \ldots, N$ (Hirsch and Smale, 1974). Solving the linear system $(\mathbf{T} + \lambda_i \mathbf{1}) \cdot \mathbf{x}_i = \mathbf{0}$ for each eigenvector $\mathbf{x}_i$ yields the upper diagonal matrix $\mathbf{D}^{-1}$ formed by the elements d_{ij}. These elements d_{ij} are computed from

$$d_{ij} = \begin{cases} \displaystyle\sum_{o=i+1}^{j} \frac{\lambda_i p_{io} d_{oj}}{(\lambda_i - \lambda_j)} & \text{if } i < j < N; \\ 1 & \text{if } i = j; \\ 1 & \text{if } j = N; \\ 0 & \text{if } i > j. \end{cases} \tag{24}$$

Algebraic computations lead to the computation of the inverse of $\mathbf{D}^{-1}$, given by elements a_{ij} of matrix $\mathbf{D}$. These elements a_{ij} are given by

$$a_{ij} = \begin{cases} \displaystyle -\sum_{o=i}^{j-1} a_{io} d_{oj} & \text{if } i < j \\ 1 & \text{if } i = j; \\ 0 & \text{if } i > j. \end{cases} \tag{25}$$

The elements ϕ_{ij} of the interval transition probability matrix $\mathbf{\Phi}(t) = e^{\mathbf{T}t} = \mathbf{D}^{-1} e^{-\Lambda t} \mathbf{D}$ are computed from the equation

$$\phi_{ij}(t) = \begin{cases} \displaystyle\sum_{o=i}^{j} d_{io} a_{oj} exp(-\lambda_o t) & \text{if } i < j; \\ exp(-\lambda_i t) & \text{if } i = j; \\ 0 & \text{if } i > j. \end{cases} \tag{26}$$

Equations (24) to (26) are used to compute the elements

$$\phi_{iN}(t) = \sum_{o=i}^{N} d_{io} a_{oN} \, exp(-\lambda_o t) = \sum_{o=i}^{N} d_{io} a_{oN} \, exp\left(-\frac{\bar{v}t}{\bar{l}_o}\right), \tag{27}$$

needed to evaluate the GUH ordinates given by equation (23). The elements d_{ij} and a_{ij} given by equations (24) and (25) indicate the recursive nature of this GUH representation.

HYDRAUX - Hydraulic Routing Model

HYDRAUX is a computer program written in FORTRAN 77 (American National Standards Institute, 1978) using FORTRAN 77 modules (DeLong and others, 1992; Thompson and others, 1992) in a data-encapsulation programming paradigm. HYDRAUX is capable of simulating unsteady one-dimensional flow in networks of open channels. HYDRAUX can also simulate storage in off-channel one-dimensional reservoirs as well as explicit point or laterally-distributed contribution of flow from watersheds.

Previous Applications

An earlier version of HYDRAUX (DeLong and Schoellhamer, 1989) has been used to simulate the extremely abrupt floods and debris flows associated with volcanic activity (Laenen and Hansen, 1988) and potential moraine-dam failures (Laenen and others, 1987; Laenen and others, 1988). The HYDRAUX version used to develop the rainfall-runoff model presented in this report (version 95.1) resulted from the addition of numerical algorithms employed in the earlier version of HYDRAUX to a modified version of FOURPT (DeLong and others, 1995). FOURPT is a flow model based on the four-point-implicit finite-difference numerical scheme (Preissmann, 1961).

Governing Equations

The governing equations describing one-dimensional, unsteady, open-channel flow may be written in differential form as (Cunge and others, 1980; DeLong, 1986)

$$\frac{\partial A}{\partial t} + \frac{\partial Q}{\partial x} - q = 0 \tag{28}$$

and

$$\frac{\partial Q}{\partial t} + \frac{\partial}{\partial x}\left(\beta \frac{Q^2}{A}\right) + gA\left(\frac{\partial Z}{\partial x} + \frac{Q|Q|}{K^2}\right) = 0, \tag{29}$$

where

Q is the volumetric discharge,

A is the cross-sectional area,

Z is the water-surface elevation,

K is the channel conveyance,

x is the downstream reference distance,

t is time,

q is lateral inflow,

β is the momentum coefficient, and

g is the acceleration due to gravity.

The momentum coefficient, β, is defined by

$$\beta = \frac{1}{V^2 A} \int_A v^2 dA \,, \tag{30}$$

where v is the velocity through a small element of area dA in the channel cross section and V is the mean velocity in the cross section.

Equations (28) and (29) assume that the flow is one dimensional and that the momentum coefficient can sufficiently account for nonuniform velocity distribution. Streamline curvature and accelerations in directions other than the x direction are not significant. The effects of turbulence and friction are adequately described by the resistance laws used for steady flow, and the channel slope is sufficiently mild so that the cosine of its angle with the horizontal is close to unity. Water density is constant, and momentum associated with lateral inflow q in equation (29) is not significant.

Watershed Contribution

Volumetric rate of flow contributed by watersheds, Q_w, is explicitly computed from $Q_w = A_d E$ where A_d is the contributing drainage area in units of length squared and E is the excess rainfall rate. This time-dependent excess rainfall rate, E, in inches per hour, is obtained from the application of equation (6). Flow from a watershed, Q_w, may be contributed directly as a point source, or distributed along a channel. If flow is distributed along a channel, lateral inflow to a unit length of channel is directly proportional to the amount of drainage area contributing exclusively to that unit length of channel as expressed by

$$q_w \, dx = E \, da, \tag{31}$$

where q_w is the lateral volumetric inflow per unit length of channel, and da is an increment of drainage area contributing exclusively to an increment of channel, dx. The total flow, Q_w, distributed along a channel of length l is then expressed by

$$Q_w = \int_0^l q_w \, dx \,. \tag{32}$$

Because, in this application, only watersheds contribute to lateral inflow, the volumetric inflow per unit length of channel contributed by the watershed, q_w, is equal to the lateral inflow term, q, shown in equation (28).

Numerical Solution

Equations (28) and (29), in general, cannot be solved analytically. The numerical scheme employed in this application is finite-element collocation with hermitian interpolation in space and finite difference in time. The numerical solution technique used for the application discussed in this report was found to be more robust than the four-point-implicit finite-difference scheme.

Finite-Element Collocation Formulation

A general description of the finite-element collocation method may be found in texts such as Lapidus and Pinder (1982) and was previously described in Pinder and Shapiro (1979) and DeLong and Schoellhamer (1989). Each channel is divided longitudinally into discrete reaches referred to as elements. Dependent variables are approximated within each element using Hermite polynomials in terms of dependent variables and their gradients located at the extremities of the elements. Dependent variables are discharge Q, discharge gradient $\partial Q/\partial x$, water-surface elevation Z, and water-surface slope or gradient $\partial Z/\partial x$. Equations (28) and (29) are each approximated at two Gaussian quadrature points within each element.

Boundary Conditions

Equations (28) and (29), written at two quadrature points within each element, in a channel of n elements, result in $2 \cdot 2 \cdot n = 4n$ equations. The number of dependent variables is $4 \cdot (n + 1) = 4n + 4$, which is 4 degrees of freedom more than the number of equations. Two known boundary values or constraining equations (one at each channel end) account for two of the remaining 4 degrees of freedom. Two additional equations, either equation (28) or (29), written at each channel end account for the final 2 degrees of freedom.

Several constraining boundary conditions can be imposed in HYDRAUX. Two of these constraining boundary conditions is to force either the water-surface elevation or the flow to be equal to a known value. Another possible boundary condition is to set the water surface of a channel equal to that of an adjacent connecting channel. Other boundary conditions HYDRAUX can simulate include forcing the algebraic sum of all flows into a junction of channels to zero, setting the water-surface slope equal to a known value, satisfying a specified relation between flow and water-surface elevation, or satisfying a three-parameter relation among water-surface elevations and flow in adjacent connecting channels.

Simultaneous Solution

Equations (28) and (29) described above are solved simultaneously in terms of incremental change in dependent variables Q, $\partial Q/\partial x$, Z, and $\partial Z/\partial x$ using Gaussian elimination (Carnahan and others, 1969; DeLong and others, 1995). Because the resulting coefficient matrix is very sparse (very few locations in the coefficient matrix contain nonzero terms), a technique is used to avoid unnecessary computer storage and computation. The virtual two-dimensional coefficient matrix is transformed into a one-dimensional array. This one-dimensional array stores only coefficients actually computed from the equations and coefficients potentially computed during Gaussian elimination. Gaussian elimination is performed only on coefficients stored in the one-dimensional array, thereby avoiding unnecessary computation on void locations in the sparse two-dimensional coefficient matrix.

APPLICATION OF REAL-TIME RAINFALL-RUNOFF MODEL

The application of the two components of the real-time rainfall-runoff model, the watershed and the hydraulic routing models, are presented in this section. The watershed model application includes the calibration and verification of the Green-Ampt infiltration equations and the application of the GUH technique to compute the direct runoff hydrographs. Results of the application of the watershed model to rainfall events in independent subbasins I to X (fig. 3) are presented in this section. The application of the hydraulic routing model to the Carraízo-reservoir basin river network is performed on intervening subbasins XI to XV (fig. 3) and results are presented for events of minimal lateral inflow to assess the accuracy of HYDRAUX. Simulation results obtained from the application of the real-time

rainfall-runoff model to large rainfall events used for verification purposes are presented in this section. These simulation results are compared with measured values to determine the accuracy and reliability of the integration of the watershed and the hydraulic routing models.

Watershed Model Application

The section Hydrograph Separation Technique presented earlier was used to compute the direct runoff of each discharge hydrograph measured at streamgages 1 to 14 (fig. 2) for all calibration and verification events corresponding to subbasins I to XIV. Five rainfall events were used to calibrate the Green-Ampt infiltration parameters for each subbasin. The dates of these rainfall events used for calibration, the events used to verify this calibration, and the magnitude and duration of each event are listed in table 5.

The convolution between the excess rainfall, obtained from the application of the calibrated Green-Ampt infiltration parameters to the rainfall hyetograph, and the GUH, obtained from equation (23), is computed from equation (16) for each of the verification events listed in table 5 for subbasins I to X. The resulting hydrograph is compared with the measured direct runoff to assess the capability of the GUH technique to accurately estimate direct runoff hydrographs. The measured direct runoff hydrograph is obtained by applying the hydrograph separation technique, developed for this study, to the measured discharge hydrograph.

Calibration of Green-Ampt Infiltration Parameters

The Green-Ampt infiltration parameters were calibrated by minimizing the sum of absolute differences between the excess rainfall and the direct runoff over five rainfall events. The calibrated Green-Ampt infiltration parameters η, η_e, ψ, and K for subbasins I through XIV were obtained after computing θ_i from equation (1) for the events listed in table 5 and applying the optimization program listed in Appendix 2. This optimization program, written in Fortran 77, contains in the subroutine VALGA, the Green-Ampt infiltration equations and solves for excess rainfall at every time step. In this subroutine, small corrections are made to the excess rainfall unit values when they are equal to zero and the corresponding rainfall unit value is nonzero. These corrections assume that the fraction of rainfall that falls directly into river areas is excess rainfall. These river areas were computed for each subbasin using a Geographical Information System (GIS). The calibrated parameter values for each subbasin are listed in table 6.

The calibrated Green-Ampt infiltration parameter values listed in table 6 indicate that the values for hydraulic conductivity K for all subbasins fall within the range of 0.125 to 0.617 inch per hour and the wetting front soil suction head values ψ vary from 2.770 to 6.250 inches. The Green-Ampt parameters for subbasin XV were obtained by taking the average over calibrated values for subbasins I, III, XII, XIII, and XIV. The lowest hydraulic conductivity value listed in table 6 is 0.125 inch per hour and corresponds to subbasin XIV. Figure 4 shows that subbasin XIV has the highest ratio of the *impermeable areas* category to other soil categories. The highest hydraulic conductivity value corresponds to subbasin III, where the predominant soil categories are *clay* and *silty clay loam*.

Verification of Green-Ampt Infiltration Parameters

The calibrated Green-Ampt infiltration parameters were verified using large rainfall events which had not been used in the calibration process for which rainfall and discharge data were available. These events were selected to examine the reliability of the calibrated Green-Ampt parameters in estimating the excess rainfall volumes produced during potentially flood-causing events. The calibrated parameters shown in table 6 were applied to the verification events listed in table 5. Results of this verification are listed in table 7. A comparison between the total excess rainfall volumes, ER, computed from equation (7), and the total direct runoff, DR, obtained after applying the hydrograph

Table 5. Rainfall events used for calibration of Green-Ampt infiltration parameters and events used for verification

[DC, dates of rainfall events used for calibration; DV, dates of rainfall events, also in YYMMDD-DD format, used for verification; TR, average of total rainfall recorded at raingages in the subbasin, in inches; TD, duration of rainfall event, in hours]

Subbasin identification	Date of rainfall events used for calibration										DV	
I	910205-05		910718-18		920805-06		921006-06		930711-12		930918-18	
I -TR TD	1.20	4	1.66	3.25	1.87	4	1.50	3	3.76	11.5	1.69	4.25
II	901015-15		921226-26		930415-16		930514-14		930711-12		920105-06	
II-TR TD	1.65	3.75	2.86	3.75	2.57	4	2.92	6.75	4.10	12	5.5	22.5
III	920105-06		920526-26		921010-11		921127-27		921129-30		940828-28	
III-TR TD	5.57	20.5	1.25	2.5	1.55	4.25	2.93	9.75	1.35	4.5	3.53	6.5
IV	911108-09		920105-06		920523-24		920525-26		930711-12		940919-20	
IV-TR TD	6.29	6.25	8.88	27	5.36	19.5	5.62	7.25	6.04	15.75	6.06	17.75
V	901020-21		911107-08		920105-06		920523-24		921130-30		930711-12	
V-TR TD	3.08	16.75	4.48	18.25	4.61	19.75	3.37	14.25	1.30	13	4.73	14.25
VI	901024-25		910630-30		910917-17		930514-14		930615-16		940920-20	
VI-TR TD	2.02	4.75	3.83	7.5	3.18	8.75	1.87	6.25	0.92	3	3.26	7.25
VII	901020-21		910917-17		920920-20		930711-11		930816-16		940920-20	
VII-TR TD	2.32	5.5	2.24	6.75	2.18	3.25	5.81	12.25	2.75	7	3.81	11.5
VIII	910917-17		920919-19		920920-20		921128-28		930711-12		920105-06	
VIII-TR TD	2.03	6.5	1.80	2	2.14	1.75	2.02	3.5	5.48	10	7.04	14.5
IX	910716-16		911107-07		911108-09		920526-26		920920-20		930514-14	
IX-TR TD	2.72	8	2.26	8.5	2.41	6.25	0.96	6.75	1.68	2.25	2.51	10.25
X	911107-08		920525-26		921129-30		930618-19		930711-12		920105-06	
X-TR TD	4.43	13.5	3.38	6.25	3.10	8.25	4.46	18.75	5.41	12.25	5.76	21.75
XI	901020-21		910630-30		911108-09		930711-12		940920-20		920105-06	
XI-TR TD	2.69	4.25	2.81	7.75	4.54	8	5.83	14	3.23	6.5	9.51	27.5
XII	911107-08		920105-06		920523-24		921129-30		940919-20		930711-12	
XII-TR TD	3.20	13.75	5.37	21.25	2.71	14	1.92	13.25	3.05	14.75	5.30	20
XIII	911108-09		920525-26		920920-21		930711-12		940919-20		920105-06	
XIII-TR TD	3.64	21.5	1.92	15.0	3.15	17.5	5.36	15.75	3.73	14.5	9.08	25
XIV	920805-06		921226-27		930415-16		930514-14		930711-12		920105-06	
XIV-TR TD	2.90	4.25	2.34	4	2.06	4	2.01	7	3.12	12.25	7.34	21

Table 6. Calibrated Green-Ampt infiltration parameter values and performance on calibration events

[η, soil porosity (-); η_e, effective soil porosity (-); ψ, wetting front soil suction head, in inches; K, hydraulic conductivity, in inches per hour; P1, P2, P3, P4, and P5, percentage error of difference between computed excess rainfall and direct runoff for each calibration event using calibrated parameters with positive numbers indicating excess rainfall was larger than direct runoff]

Subbasin Identification	η	η_e	ψ	K	P1	P2	P3	P4	P5
I	0.432	0.370	2.775	0.523	-30.2	-4.1	-31.0	+9.3	+4.8
II	0.470	0.381	5.512	0.366	-40.2	-6.6	+26.8	+34.8	-0.1
III	0.453	0.375	2.816	0.617	+4.1	+14.7	-20.2	-0.1	-23.4
IV	0.480	0.410	6.250	0.329	-2.9	+21.1	-5.8	+0.1	-19.5
V	0.449	0.385	3.807	0.165	+0.1	-1.1	+23.2	+2.8	-21.5
VI	0.430	0.390	2.770	0.242	+16.1	-0.1	+41.9	-22.5	-13.5
VII	0.431	0.364	4.836	0.495	-48.6	+46.3	-0.7	-0.3	+39.8
VIII	0.449	0.360	3.720	0.306	+40.9	+40.4	+21.3	-19.1	-0.2
IX	0.443	0.360	4.914	0.356	+22.4	-30.3	+0.2	-40.2	-18.4
X	0.447	0.371	3.560	0.155	-10.1	+37.7	-9.8	+12.9	-0.1
XI	0.459	0.360	5.263	0.441	-26.7	+25.6	+0.7	-8.9	+0.1
XII	0.457	0.389	5.100	0.180	-36.1	+1.7	-35.1	-22.3	+20.9
XIII	0.461	0.350	6.123	0.192	-0.1	-14.1	+15.5	-15.9	+3.1
XIV	0.455	0.378	4.691	0.125	+24.9	-22.3	+26.7	+28.8	-0.1

separation technique to the measured discharge hydrograph to obtain the D_n values of equation (17), indicates that the largest error among the independent subbasins (I through X) was 27.9 percent while the largest error among the dependent subbasins (XI to XIV) was 13.5 percent (table 7). The fact that the dependent subbasins have a more extensive coverage of raingages than the independent subbasins may explain this difference. In addition to using the excess rainfall unit values to generate the GUH-estimated direct runoff hydrographs, they are used to compute the lateral inflow values in equation (28) represented by q.

Sensitivity Analysis of Green-Ampt Infiltration Parameters

A sensitivity analysis was conducted to determine how the verification results would change if the two main Green-Ampt infiltration parameters, the wetting front soil suction head ψ and the hydraulic conductivity K, were increased and decreased by 20 percent from the calibrated values. In general, as K increases, the total excess rainfall decreases and vice versa. As a result, spatial and temporal rainfall variations may confuse the analysis of the results of this sensitivity analysis. To avoid this confusion the sum taken over the rainfall events used for calibration of absolute differences between excess rainfall and direct runoff volumes was computed and listed in table 7 for each set of parameters. Although ER+ values for subbasins I, V, VI, and XIII as well as ER- values for subbasins II, VII, IX, X, and XII may indicate the calibrated Green-Ampt infiltration parameters were not optimal, corresponding results for SUM+ and SUM- indicate these ER+ and ER- values are a consequence of the spatial and temporal rainfall variations that occurred in the verification events. The calibration events were carefully chosen to have minimal spatial and temporal rainfall variations based on the data recorded from the raingages in the subbasin.

Table 7. Verification results and sensitivity analysis of calibrated Green-Ampt infiltration parameter values

[SBI, subbasin identification; DR, total direct runoff for verification event obtained from hydrograph separation technique, in inches; ER, total excess rainfall for verification event obtained from Green-Ampt infiltration parameters, in inches; ERROR, percentage error computed from 100(ER-DR)/DR; ER+, total excess rainfall obtained when calibrated parameters ψ and K are increased by 20 percent, in inches; ER-, total excess rainfall obtained when calibrated parameters ψ and K are decreased by 20 percent, in inches; SUM, sum over all calibration events of absolute differences between excess rainfall and direct runoff for calibrated Green-Ampt parameters, in inches; SUM+ and SUM-, corresponding SUM values when parameters ψ and K are increased and decreased by 20 percent, respectively]

SBI	DR	ER	ERROR	ER+	ER-	SUM	SUM+	SUM-
I	0.57	0.72	+27.9	0.59	0.86	0.36	0.75	0.69
II	1.79	1.39	-22.2	1.13	1.69	0.86	0.95	1.48
III	0.98	1.07	+8.5	0.74	1.43	0.31	0.94	0.93
IV	2.67	2.75	+2.9	2.26	3.26	1.23	2.04	2.13
V	2.25	2.44	+8.4	2.13	2.82	0.52	0.87	1.29
VI	1.80	2.09	+15.9	1.91	2.27	0.98	1.15	1.54
VII	1.85	1.58	-14.6	1.28	1.93	0.40	0.84	1.21
VIII	4.36	4.26	-2.2	3.86	4.66	0.84	1.05	1.49
IX	0.77	0.62	-18.9	0.44	0.84	0.53	0.86	0.64
X	3.18	2.87	-9.7	2.56	3.25	1.18	1.62	1.52
XI	3.63	3.60	-0.8	3.01	4.27	0.59	1.26	1.45
XII	2.69	2.33	-13.5	2.01	2.72	1.13	1.47	1.28
XIII	4.71	5.02	+6.5	4.56	5.58	0.72	1.33	0.93
XIV	3.99	4.08	+2.3	3.71	4.56	1.42	1.49	1.85

Performance of GUH Algorithm

The verification events listed in table 5 were also used to measure the accuracy of the GUH technique by computing direct runoff from equation (16). The computation of the GUH is based on the subbasin geomorphology and the excess rainfall unit values for the appropriate rainfall event. The geomorphology-based parameters needed to compute the GUH for subbasins I to X are listed in table 8. The resulting estimated direct runoff hydrograph from this convolution is compared to the direct runoff obtained from the application of the hydrograph separation technique to the measured hydrographs in all independent subbasins, I through X, to assess the accuracy of the GUH technique.

The peaks of the geomorphic unit hydrographs shown in figures 6a to 15a increase in magnitude as the geometric mean streamflow velocity increases. As the geometric mean streamflow velocity estimates decrease, the GUH shapes become more attenuated. This can be observed in equation (27) where smaller $\bar{v}$ values imply smaller $\phi_{iN}(t)$ values. Every GUH shape is associated with a specific excess rainfall burst within the rainfall event.

The GUH-estimated direct runoff hydrographs presented in this report are based on the perennial stream networks shown in figure 2 for subbasins I to X. Another stream network from which the GUH could be derived is the ephemeral and perennial stream network. This stream network was derived for subbasins V, VI, VII, and X (Sepúlveda, 1996). However, it was determined that there is no practical improvement in estimating direct runoff when the ephemeral and perennial stream network is used instead of the strictly perennial stream network (Sepúlveda, 1996). This finding means the generation of the ephemeral and perennial stream network of any subbasin from the digital elevation model for the purpose of computing its GUH is unnecessary.

Table 8. Geomorphology-based parameters for subbasins I to X

[n_i , number of perennial rivers of order i ; l_i , sum of river lengths of order i, in miles; A_i , sum of catchment areas of rivers of order i, in square miles]

Subbasin identification	Subbasin order						
I	2	n_1	10	l_1	7.36	A_1	2.30
		n_2	1	l_2	6.95	A_2	2.78
II	3	n_1	11	l_1	7.51	A_1	2.67
		n_2	4	l_2	4.26	A_2	1.75
		n_3	1	l_3	2.41	A_3	0.81
III	4	n_1	17	l_1	16.27	A_1	4.95
		n_2	4	l_2	3.34	A_2	0.96
		n_3	2	l_3	5.05	A_3	1.52
		n_4	1	l_4	0.29	A_4	0.10
IV	3	n_1	22	l_1	17.74	A_1	5.58
		n_2	4	l_2	7.20	A_2	2.23
		n_3	1	l_3	5.72	A_3	2.26
V	4	n_1	41	l_1	34.16	A_1	13.19
		n_2	12	l_2	13.95	A_2	6.25
		n_3	3	l_3	4.25	A_3	1.50
		n_4	1	l_4	2.98	A_4	1.39
VI	3	n_1	6	l_1	8.18	A_1	4.05
		n_2	2	l_2	3.97	A_2	1.65
		n_3	1	l_3	0.62	A_3	0.29
VII	3	n_1	8	l_1	6.55	A_1	2.40
		n_2	3	l_2	1.73	A_2	0.40
		n_3	1	l_3	1.49	A_3	0.43
VIII	3	n_1	9	l_1	6.26	A_1	2.11
		n_2	3	l_2	2.90	A_2	0.89
		n_3	1	l_3	2.00	A_3	0.78
IX	3	n_1	10	l_1	10.79	A_1	5.93
		n_2	2	l_2	3.23	A_2	1.00
		n_3	1	l_3	0.34	A_3	0.23
X	4	n_1	45	l_1	33.15	A_1	9.83
		n_2	13	l_2	12.11	A_2	3.47
		n_3	3	l_3	5.33	A_3	1.94
		n_4	1	l_4	2.51	A_4	1.16

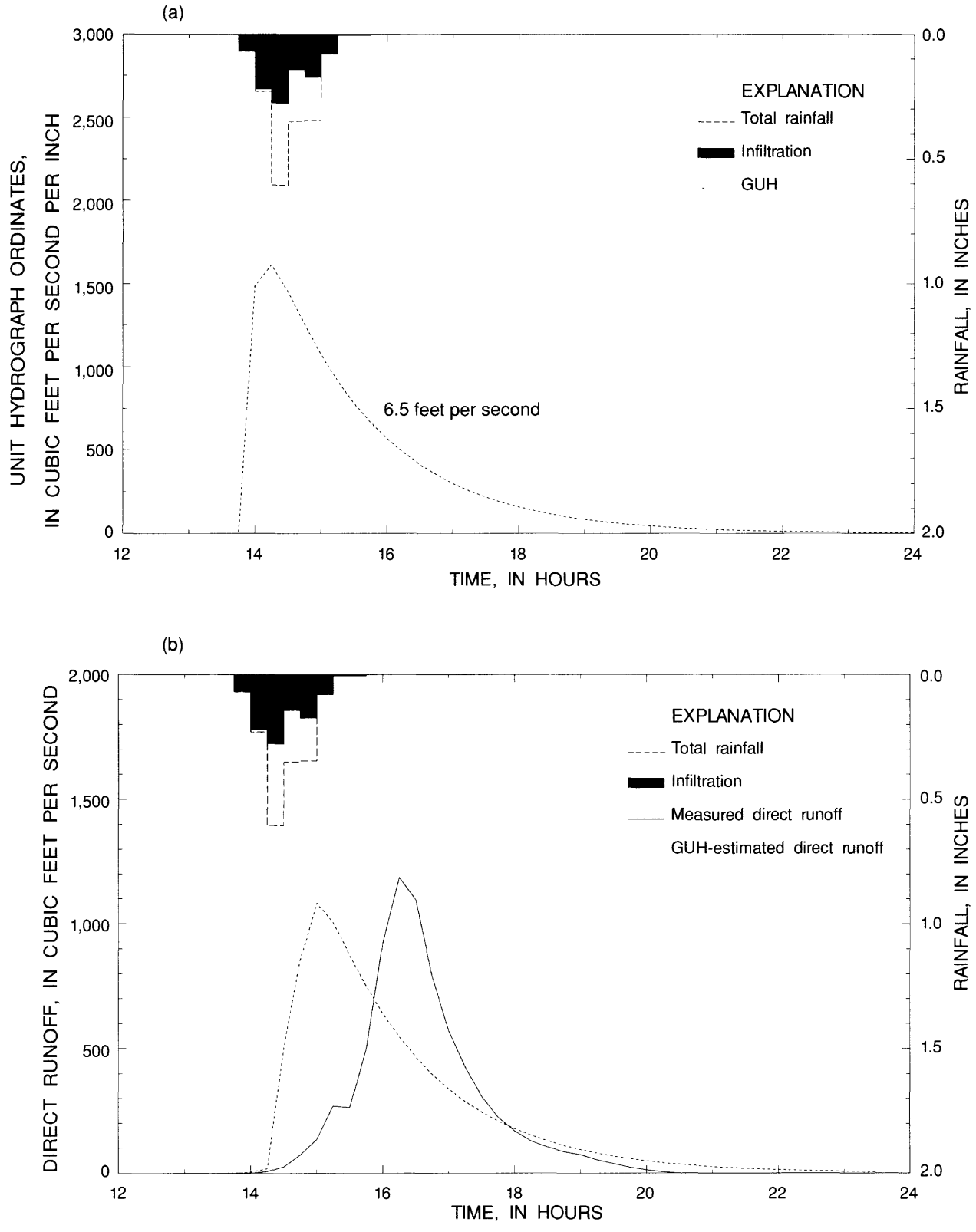

Figure 6. Rainfall hyetograph of September 18, 1993, for subbasin I with (a) GUH shape and geometric mean streamflow velocity and (b) measured and GUH-estimated direct runoff hydrographs.

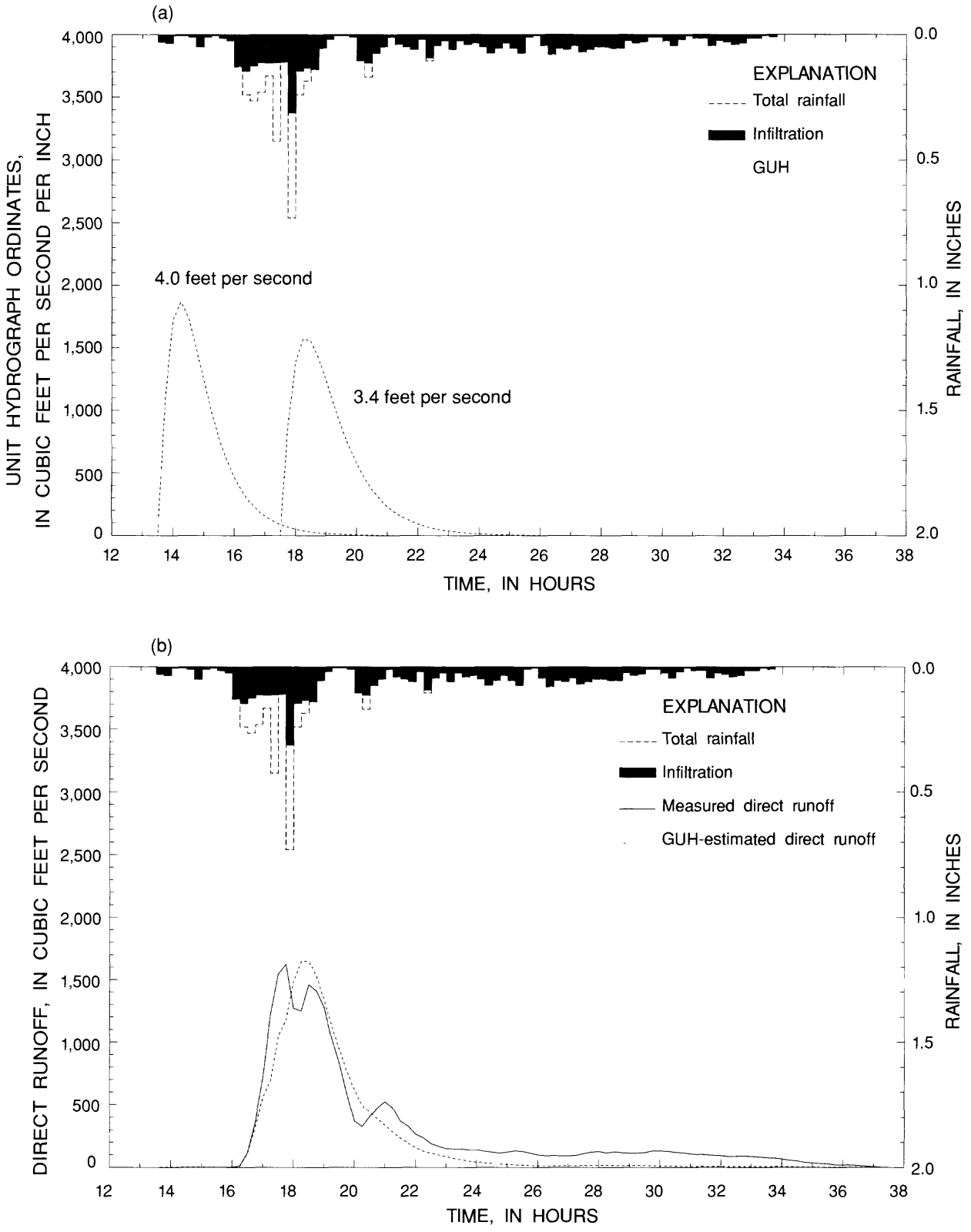

Figure 7. Rainfall hyetograph of January 5-6, 1992, for subbasin II with (a) GUH shape and geometric mean streamflow velocity and (b) measured and GUH-estimated direct runoff hydrographs.

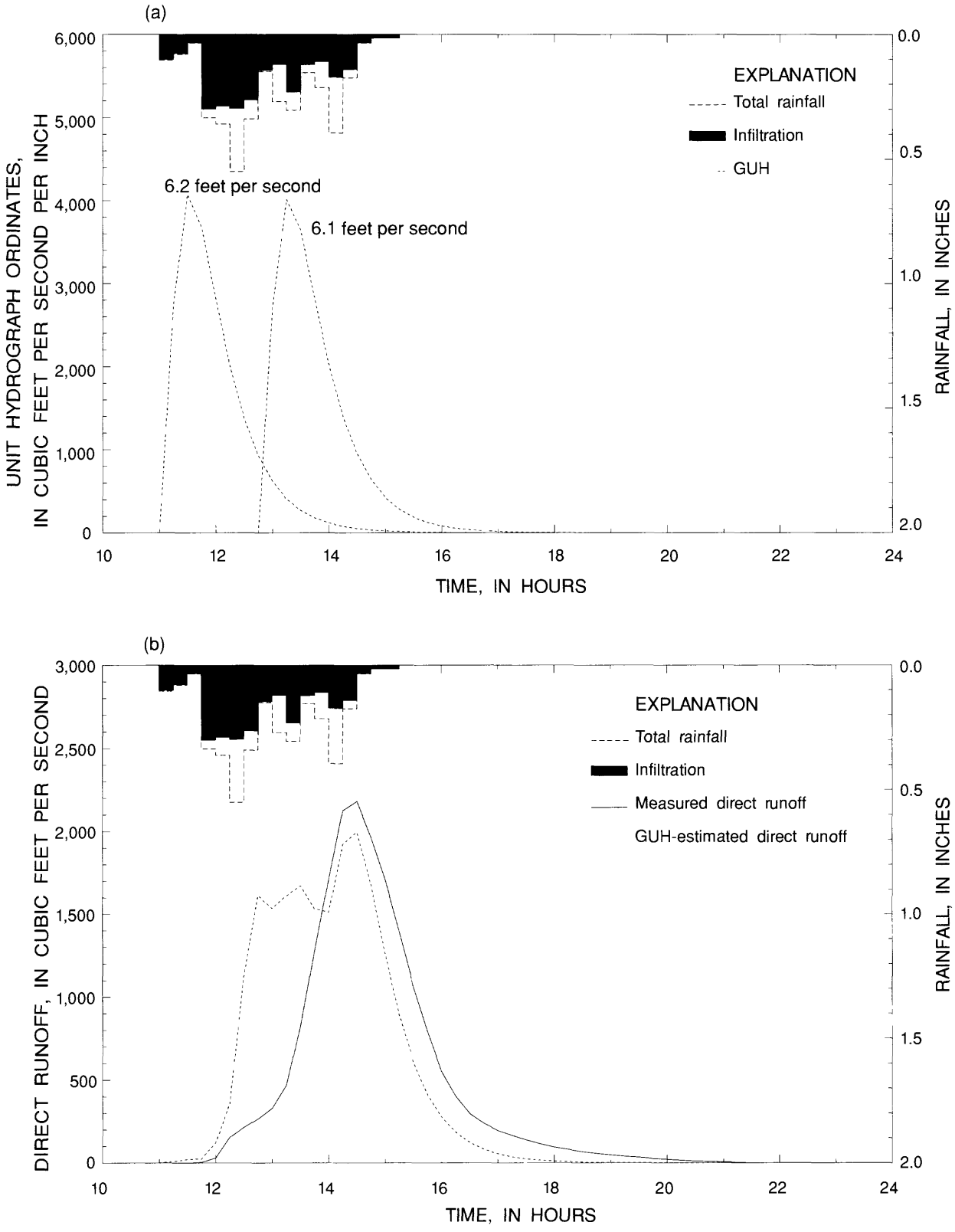

Figure 8. Rainfall hyetograph of August 28, 1994, for subbasin III with (a) GUH shapes and geometric mean streamflow velocities and (b) measured and GUH-estimated direct runoff hydrographs.

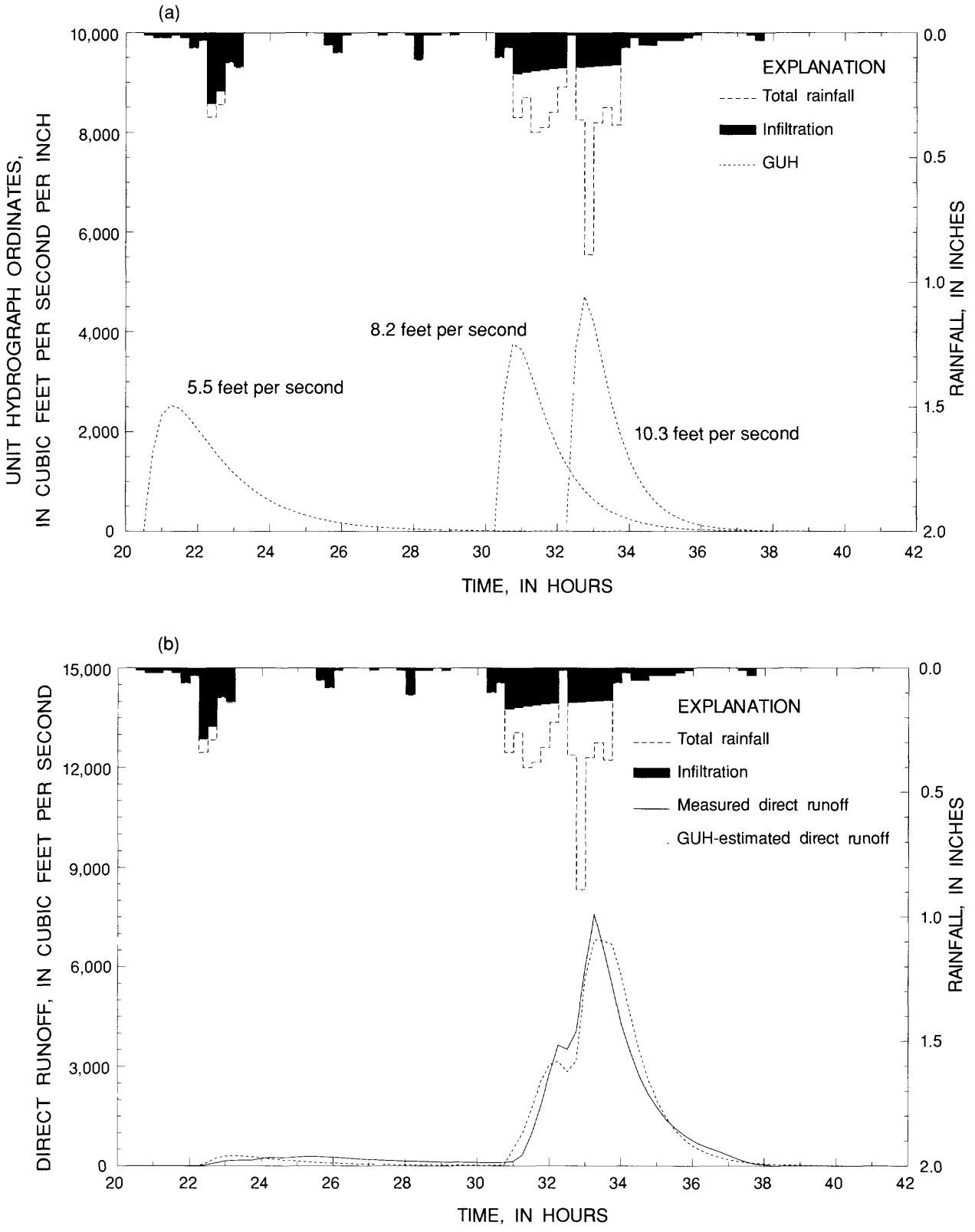

Figure 9. Rainfall hyetograph of September 19-20, 1994, for subbasin IV with (a) GUH shapes and geometric mean streamflow velocities and (b) measured and GUH-estimated direct runoff hydrographs.

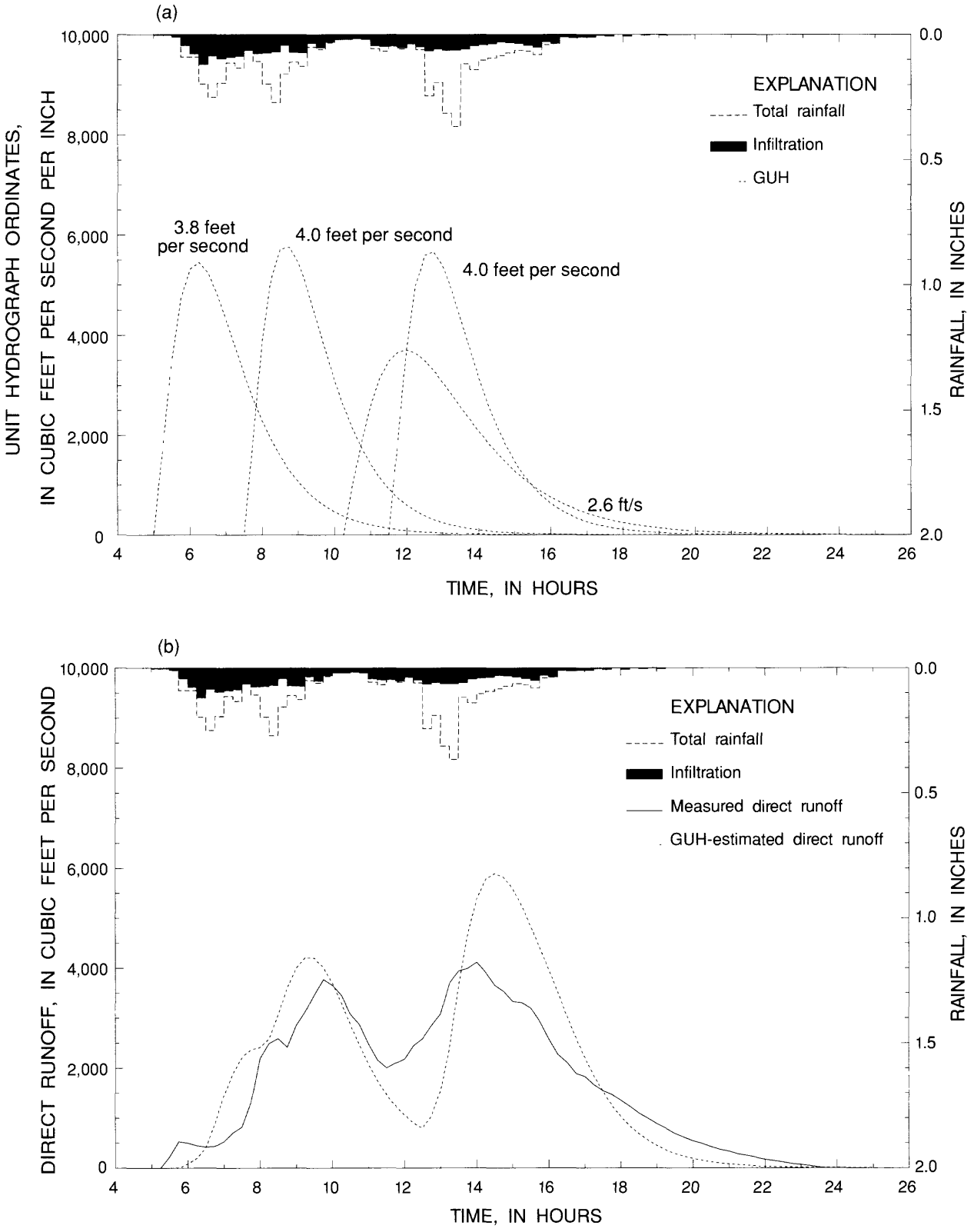

Figure 10. Rainfall hyetograph of July 11-12, 1993, for subbasin V with (a) GUH shapes and geometric mean streamflow velocities and (b) measured and GUH-estimated direct runoff hydrographs.

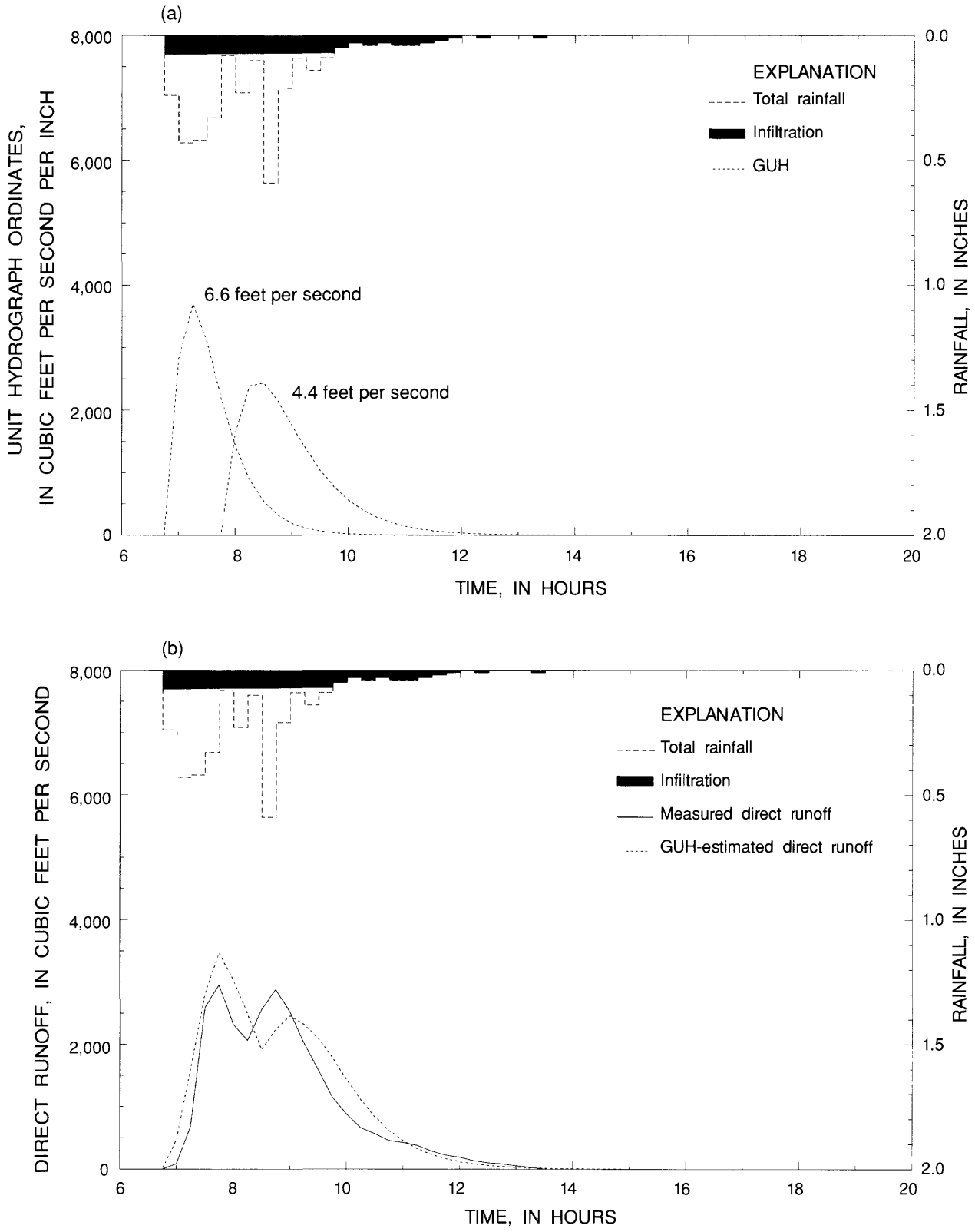

Figure 11. Rainfall hyetograph of September 20, 1994, for subbasin VI with (a) GUH shapes and geometric mean streamflow velocities and (b) measured and GUH-estimated direct runoff hydrographs.

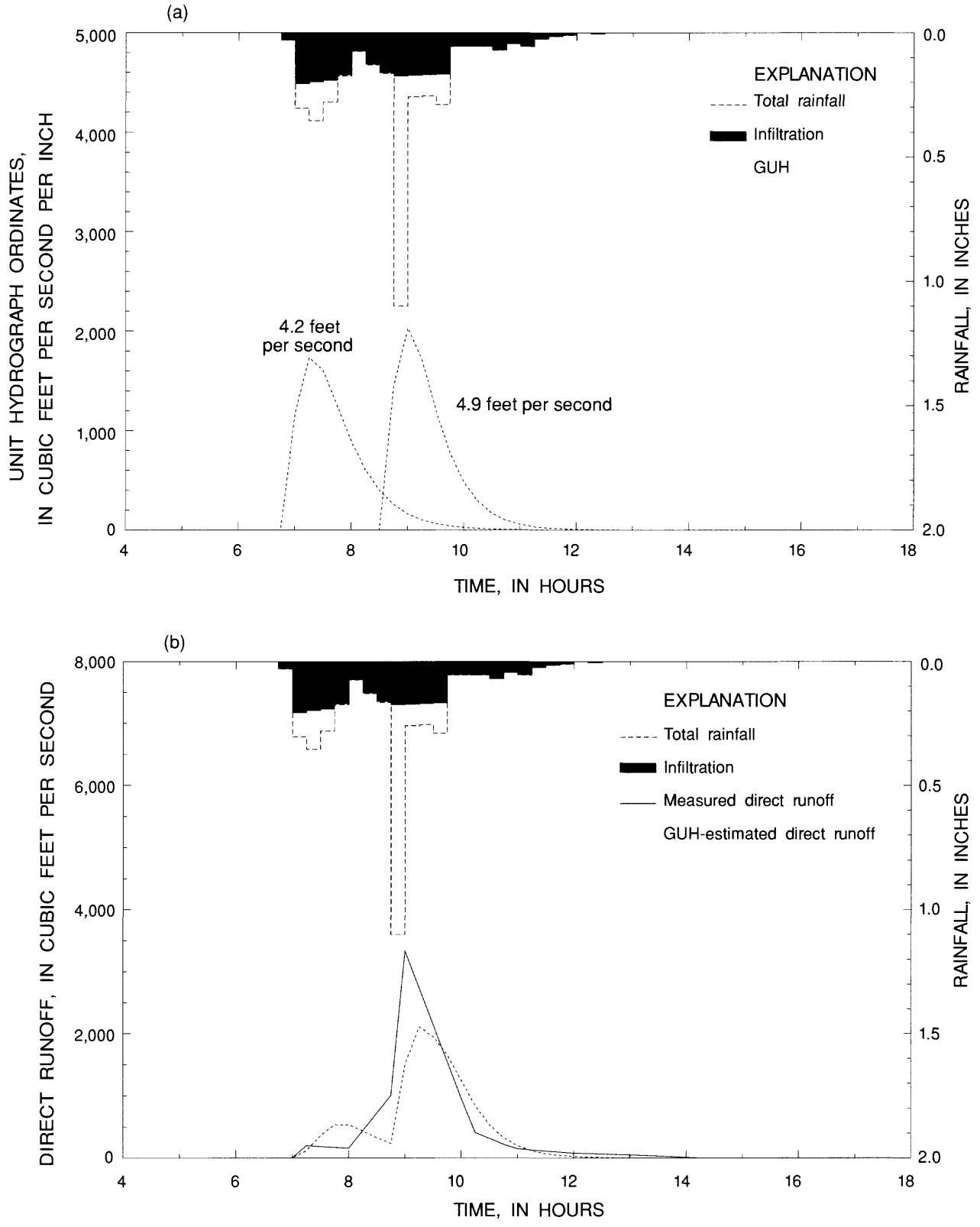

Figure 12. Rainfall hyetograph of September 20, 1994, for subbasin VII with (a) GUH shapes and geometric mean streamflow velocities and (b) measured and GUH-estimated direct runoff hydrographs.

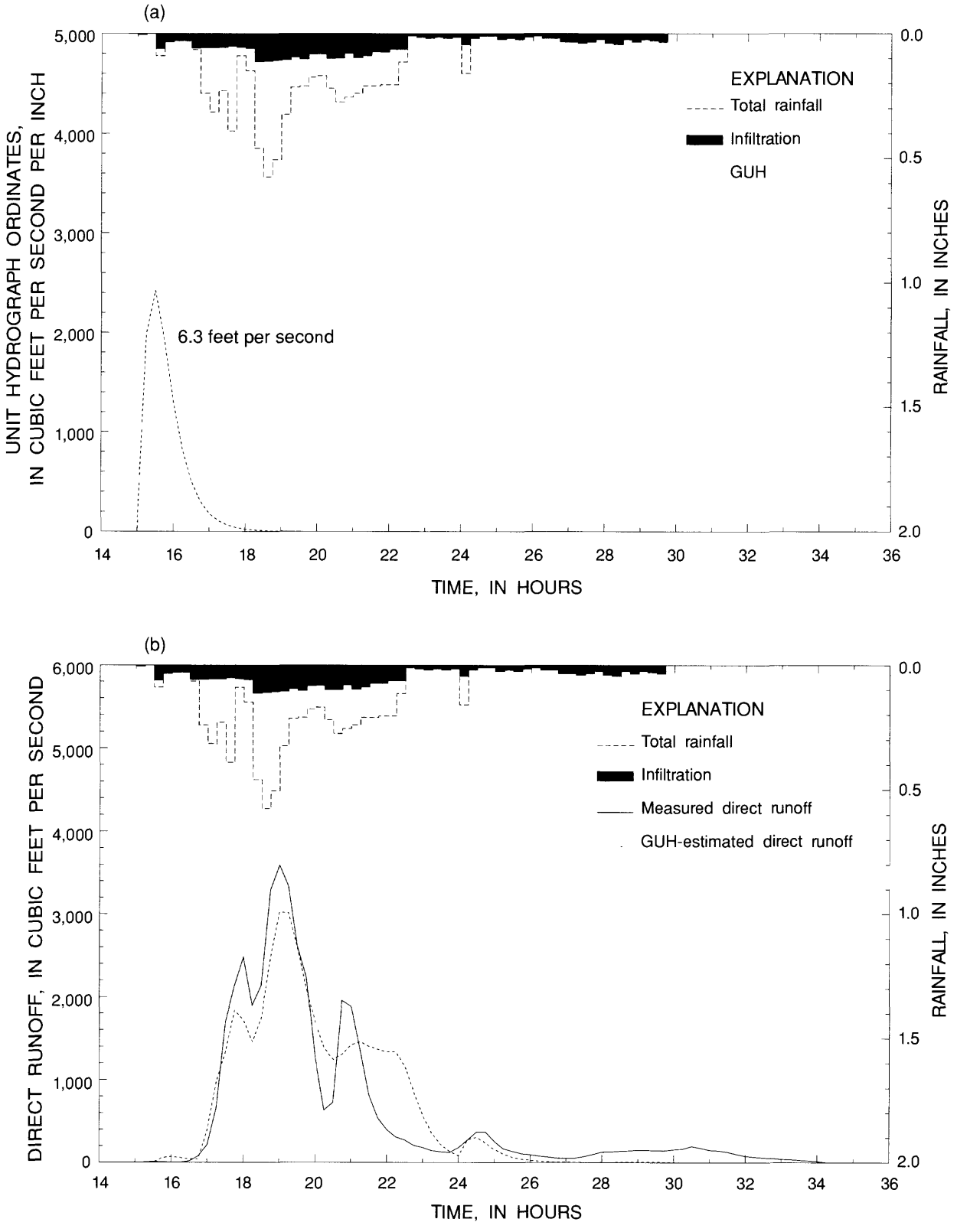

Figure 13. Rainfall hyetograph of January 5-6, 1992, for subbasin VIII with (a) GUH shape and geometric mean streamflow velocity and (b) measured and GUH-estimated direct runoff hydrographs.

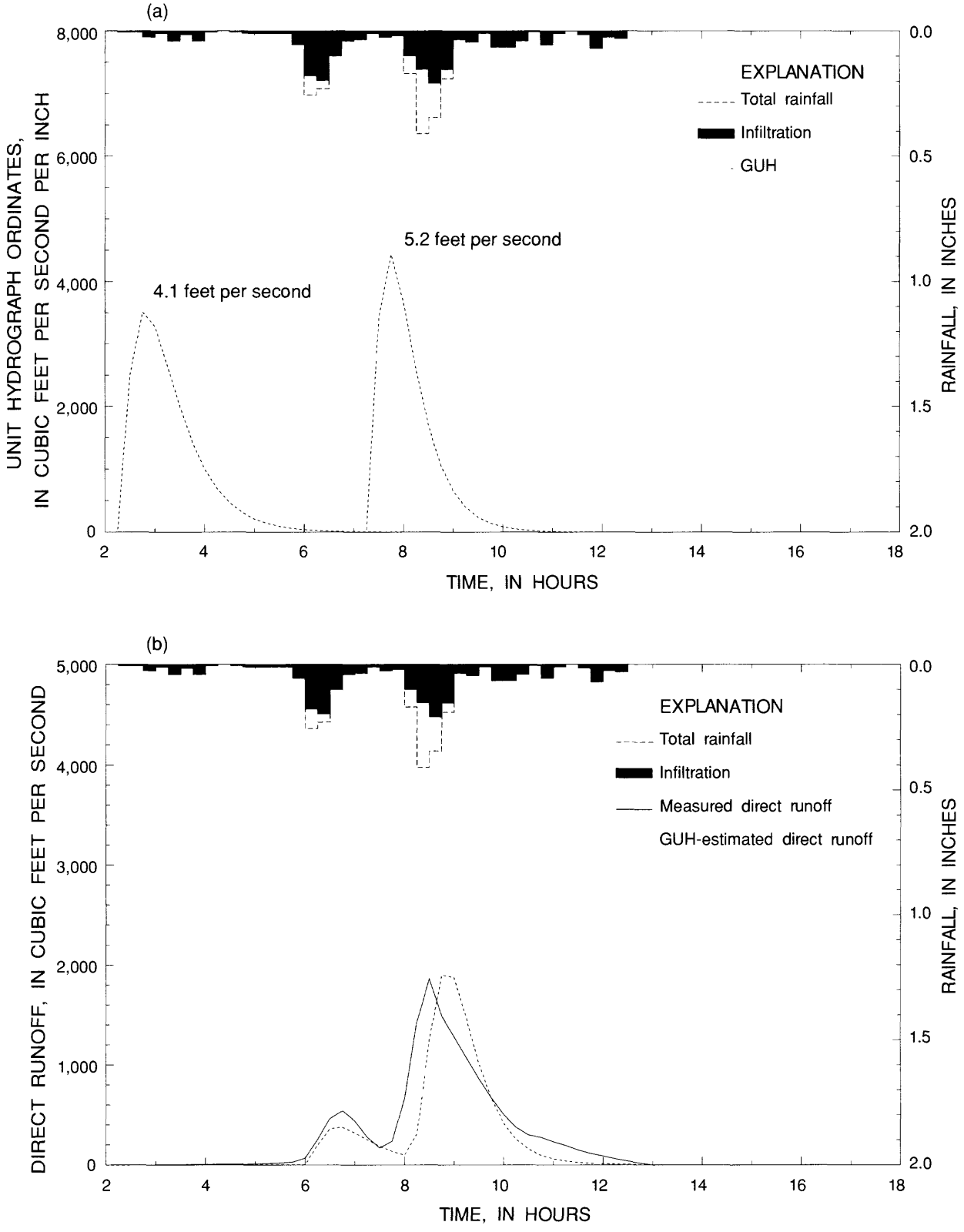

Figure 14. Rainfall hyetograph of May 14, 1993, for subbasin IX with (a) GUH shapes and geometric mean streamflow velocities and (b) measured and GUH-estimated direct runoff hydrographs.

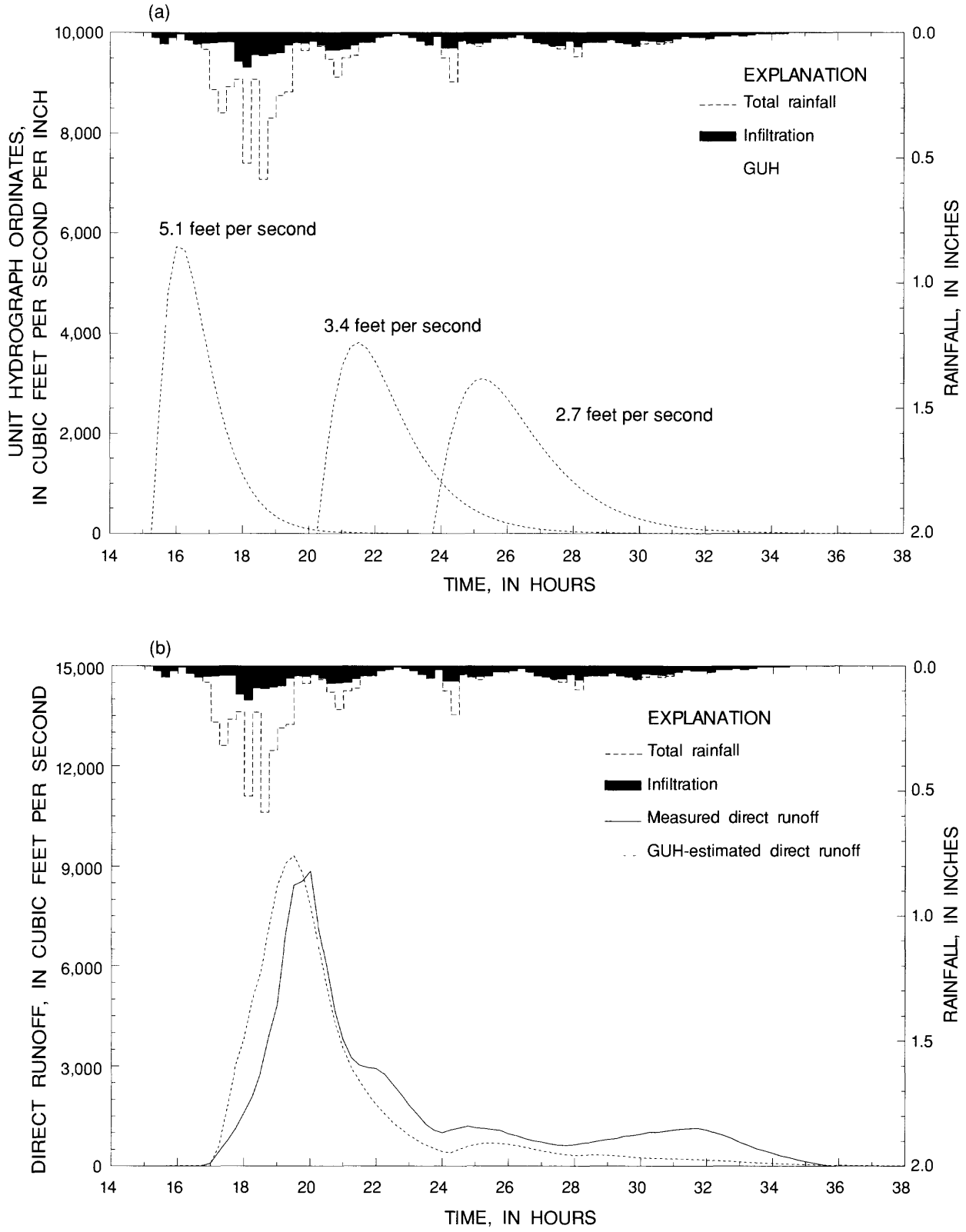

Figure 15. Rainfall hyetograph of January 5-6, 1992, for subbasin X with (a) GUH shapes and geometric mean streamflow velocities and (b) measured and GUH-estimated direct runoff hydrographs.

The rainfall and infiltration hyetographs shown in figures 6 to 15 are the result of applying the calibrated Green-Ampt infiltration parameters to individual rainfall hyetographs obtained from each raingage in the subbasin and then computing the resulting arithmetic average. If the excess rainfall, which is the area between the rainfall and the infiltration hyetographs, is computed from a single application of the calibrated Green-Ampt infiltration parameters to the average rainfall computed from all raingages in the subbasin, then runoff produced by isolated regional rainfall is artificially reduced because the Green-Ampt infiltration equations are nonlinear. Computing the excess rainfall as the resulting average from individual applications of the calibrated Green-Ampt parameters to each rainfall hyetograph reduces the effects that spatial and temporal rainfall variations cause to the timing and magnitude estimation of the direct runoff hydrograph peaks. Orographic effects could be strong during isolated rainfall events. Among all ten infiltration hyetographs shown in figures 6 to 15, only figure 11 shows the exponentially decreasing function expected from a single application of the Green-Ampt infiltration equations. This is explained by the fact that subbasin VI has only one raingage. The monotone decreasing property of the infiltration hyetograph is not observed in any one of the remaining subbasins because the averaging process explained earlier makes these infiltration hyetographs non-monotonic functions.

Spatial and temporal variations in rainfall intensity from one raingage to another within the same subbasin may cause hydrograph peaks to occur earlier or later with respect to the measured peak, depending upon the rainfall intensity around each raingage location. On September 18, 1993, in subbasin I, rainfall volumes recorded at raingage 15 in figure 2 were more intense than the ones recorded at raingage 1. Figure 6b shows the peak of the measured direct runoff occurred 1.25 hours earlier than the measured peak. Equation (13) assumes that the excess rainfall instantaneously stresses the basin uniformly. Orographic effects, in general, do not satisfy this criterion. If rainfall volumes recorded at raingage 1 were greater than volumes recorded at raingage 15, then the estimated hydrograph peak would be delayed in time with respect to the peak that would be measured in this scenario. This is what occurred in subbasin II during the January 5-6, 1992, rainfall event and in subbasin IX during the May 14, 1993, event, as shown in figures 7b and 14b, respectively. However, the time discrepancies between the measured and simulated peaks are less significant in these two events than for the September 18, 1993, event in subbasin I.

The computed initial soil moisture content for the August 28, 1994, rainfall event in subbasin III was 0.14. If instead, this value is assumed to be 0.07, then the total excess rainfall decreases to 0.96 inch from the 1.07 inch value listed in table 7. However, the simulated hydrograph peaks occurring at 12.75 and 13.5 hours only decrease from 1,614 and 1,672 cubic feet per second to 1,255 and 1,494 cubic feet per second, respectively. This supports the hypothesis that the estimated peaks at 12.75 and 13.5 hours are due to orographic effects. These effects are also causing the measured peak at 14.5 hours to be underestimated by the simulation.

Figures 9b and 15b show very good agreement between the GUH-estimated and measured hydrographs. The area under the excess rainfall hyetographs in figures 6 to 15 multiplied by the subbasin area equals the area under the GUH-estimated direct runoff hydrograph. These estimated hydrographs mimic the shape of the excess rainfall hyetographs. This observation can be readily verified by examining equation (13), where the kernel of the convolution integral is the excess rainfall hyetograph. This property is particularly noticeable in figure 10b where the first two excess rainfall bursts are not as large in magnitude as the fourth one and thus, the GUH-estimated direct runoff peak around 14.5 hours is larger than the measured peak at 14 hours. The first measured peak has a shorter recession curve than the estimated hydrograph. The fact that the second measured hydrograph peak occurs closer to the fourth excess rainfall burst than the first measured peak relative to the first two excess rainfall bursts is indicative of orographic effects. The area under the estimated hydrograph, proportional to the total excess rainfall listed in table 7 for subbasin V, is larger than the area under the measured hydrograph. This is also the case for the September 20, 1994, event in subbasin VI,

shown in figure 11b with the contrasting note that larger rainfall volumes are measured in the first hyetograph peak rather than in the second one. Figure 12b shows, for the September 20, 1994, event in subbasin VII, a discrepancy between the simulated and measured hydrographs proportional to the difference between DR and ER values for subbasin VII listed in table 7.

The measured hydrograph peak at 21 hours during the January 5-6, 1992, event in subbasin VIII, shown in figure 13b, has a shorter duration and larger magnitude than the estimated peak. The computed excess rainfall for the time period from 20 to 23 hours demonstrates why the estimated hydrographs had wider peaks. The hydrograph estimation based on only one GUH for a rainfall event causes the hydrograph peak to be underestimated because the geometric mean streamflow velocity estimate decreases as smaller hyetograph peaks are grouped together in the calculation. The GUH algorithm implemented in this report to estimate direct runoff hydrographs gives reliable results as long as a good calculation of the Green-Ampt infiltration parameters is achieved. With the exception of rainfall events with strong orographic effects, the timing and magnitude of the measured hydrograph peaks were simulated reasonably accurately.

Representation of the Basin River Network - Application of HYDRAUX

The river channels in the Carraízo-reservoir basin where HYDRAUX is used to perform hydraulic routing are shown in figure 3. These 21 river channels are located in intervening subbasins XI to XV. The length of these channels are listed in table 9. River cross sections defining the geometry of the channel in the vicinity of each streamgage station are plotted in Appendix 4. The elevations shown in all these cross sections are referenced to the mean sea level datum. The first 21 cross sections shown in Appendix 4 refer to sections along the Río Grande de Loíza main channel in an upstream to downstream sequential order; the following 20 cross sections show sections of tributaries to the Río Grande de Loíza also in an upstream to downstream sequential order. Two of these cross sections were extrapolated; section RG37 was extrapolated from section RG29 and section RB28 was extrapolated from section RC20. A confluence, an intersection of two rivers, is represented in the hydraulic routing model by three cross sections: one upstream from the confluence along the main channel, another downstream from the confluence along the main channel, and a third upstream from the confluence along the river channel of the tributary. Cross sections RES4, RES3, RES2, and RES1, shown in Appendix 4 in an upstream to downstream sequential order, define the geometry of the Carraízo reservoir. The Manning's roughness coefficient values assigned to these cross sections were weighted considering the obstacles to streamflow, the vegetation, the channel geometry, and the river bank geometry for the purpose of assigning values that would apply to high-stage flows. These Manning's roughness coefficients varied from 0.030 to 0.140.

River channels 1 to 7 in figure 3 lie within intervening subbasin XI. A routed hydrograph is computed at the downstream end of river channel 7, where streamgage 11 (fig. 2) is located. This routed hydrograph has the additional six-hour predictive component because the upstream boundary conditions for streamgages 4, 6, 7, and 8 (fig. 2) were provided with this additional six-hour predictive component from the GUH algorithm. The lateral inflow unit values corresponding to this six-hour predictive component were computed strictly from base flow because no rainfall-prediction component is herein developed. HYDRAUX uses two upstream boundary conditions to route flow through channels 8, 9, and 10 in intervening subbasin XIII. One upstream boundary condition supplied as input for subbasin XIII is the resulting composition of the measured hydrograph (if available) and the routed hydrograph. If streamgage 11 is not operational, then all of the routed hydrograph at streamgage 11 is supplied as upstream boundary to HYDRAUX to obtain the routed hydrograph at streamgage 13. If streamgage 11 is operational, then the measured hydrograph is used and the six-hour prediction component of the routed hydrograph is joined to the measured

Table 9. Lengths of river channels where hydraulic routing is performed

River channel number (shown in figure 3)	Length of river channel, in feet
1	19,004
2	1,400
3	6,185
4	869
5	5,636
6	14,124
7	3,919
8	33,344
9	43,239
10	6,056
11	10,196
12	39,015
13	9,444
14	2,117
15	14,287
16	4,076
17	16,382
18	12,811
19	26,257
20	32,780
21	31,101

hydrograph. A five-point moving average approximation is used to smooth the section where the measured hydrograph is joined with the six-hour predictive component of the routed hydrograph. The resulting composition of the measured hydrograph at streamgage 9 (fig. 2) and the GUH-estimated hydrograph at subbasin IX is another upstream boundary condition used by HYDRAUX to route flow within intervening subbasin XIII.

Flow is routed through river channels 17, 18, and 19 (fig. 3) for intervening subbasin XII and through river channel 12 for intervening subbasin XIV. The routed hydrographs at subbasins XII and XIV are computed at the downstream end of channels 19 and 12, respectively. Routing in the intervening subbasin XV is performed on river channels 11, 13, 14, 15, 16, 20, and 21. The confluence of river channels 16 and 20, representing the most upstream point of the Carraízo reservoir, is the point at which the simulated hydrographs are presented.

Schematic Representation

The application of routing model HYDRAUX requires a schematic representation of the channels where routing is to be performed. This schematic representation is established by defining the channel cross sections, the number of cross sections needed to define a channel, and the boundary conditions that apply to the upstream and downstream ends of each channel. This information is supplied to the model in an input file named schmat.dat. An example of the format of this input file is shown in Appendix 5.

For the HYDRAUX application presented in this report, each channel where flow is routed is represented using two or more cross sections. Each of channels 1 through 20 have one cross section located at the upstream end and another one at the downstream end of the channel. Channel 21 has five cross sections taken along the Carraízo reservoir. Table 10 identifies the cross sections used to define the geometry of each of these 21 channels and describes their locations.

Table 10. Location and descriptions of cross sections in each river channel where hydraulic routing is performed

[RCN, river channel number shown in figure 3; CSI, cross section identification; CSLD, cross section location description; RGDL, Río Grande de Loíza]

RCN	CSI	CSLD
1	QA1	RGDL at streamgage number 6 in figure 2
	QB2	Quebrada Blanca and RGDL confluence, upstream RGDL from confluence
2	QB3	Quebrada Blanca at streamgage number 7 in figure 2
	QB4	Quebrada Blanca and RGDL confluence, upstream Quebrada Blanca from confluence
3	QB5	Quebrada Blanca and RGDL confluence, downstream RGDL from confluence
	QST6	Quebrada Salvatierra and RGDL confluence, upstream RGDL from confluence
4	QST7	Quebrada Salvatierra, at streamgage number 8 in figure 2
	QST8	Quebrada Salvatierra and RGDL confluence, upstream Quebrada Salvatierra from confluence
5	QST9	Quebrada Salvatierra and RGDL confluence, downstream RGDL from confluence
	RC10	Río Cayaguas and RGDL confluence, upstream RGDL from confluence
6	RC11	Río Cayaguas at streamgage number 4 in figure 2
	RC12	Río Cayaguas and RGDL confluence, upstream from confluence
7	RC13	Río Cayaguas and RGDL confluence, downstream RGDL from confluence
	RGL14	RGDL at streamgage number 11 in figure 2
8	RGL14	RGDL at streamgage number 11 in figure 2
	RT15	Río Turabo and RGDL confluence, upstream RGDL from confluence
9	RT16	Río Turabo at streamgage number 9 in figure 2
	RT17	Río Turabo and RGDL confluence, upstream Río Turabo from confluence
10	RT18	Río Turabo and RGDL confluence, downstream RGDL from confluence
	RGL19	RGDL at streamgage number 13 in figure 2
11	RGL19	RGDL at streamgage number 13 in figure 2
	RC24	Río Cagüitas and RGDL confluence, upstream RGDL from confluence
12	RC21	Río Cagüitas at streamgage number 2 in figure 2
	RC22	Río Cagüitas at streamgage number 14 in figure 2

Table 10. Location and descriptions of cross sections in each river channel where hydraulic routing is performed--Continued

RCN	CSI	CSLD
13	RC22	Río Cagüitas at streamgage number 14 in figure 2
	RC23	Río Cagüitas and RGDL confluence, upstream Río Cagüitas from confluence
14	RC20	Río Cagüitas and RGDL confluence, downstream RGDL from confluence
	RB28	Río Bairoa and RGDL confluence, upstream RGDL from confluence
15	RB26	Río Bairoa at streamgage number 1 in figure 2
	RB27	Río Bairoa and RGDL confluence, upstream Río Bairoa from confluence
16	RB25	Río Bairoa and RGDL confluence, downstream RGDL from confluence
	RG29	Río Gurabo and RGDL confluence, upstream RGDL from confluence
17	RG30	Río Gurabo at streamgage number 5 in figure 2
	RV31	Río Valenciano and Río Gurabo confluence, upstream Río Gurabo from confluence
18	RV32	Río Valenciano at streamgage number 10 in figure 2
	RV33	Río Valenciano and Río Gurabo confluence, upstream Río Valenciano from confluence
19	RV34	Río Valenciano and Río Gurabo confluence, downstream Río Gurabo from confluence
	RG35	Río Gurabo at streamgage number 12 in figure 2
20	RG35	Río Gurabo at streamgage number 12 in figure 2
	RG36	Río Gurabo and RGDL confluence, upstream Río Gurabo from confluence
21	RG37	Río Gurabo and RGDL confluence, downstream RGDL from confluence
	RES4	At Carraízo reservoir, 29,028 feet upstream from dam
	RES3	At Carraízo reservoir, 13,448 feet upstream from dam
	RES2	At Carraízo reservoir, 6,560 feet upstream from dam
	RES1	At Carraízo reservoir, 164 feet upstream from dam

Initial Conditions

The initial conditions assumed for each river channel in this application are summarized in table 11. Initial conditions are supplied to the model in the input file schmat.dat. Normal depth computations, steady state approximations, and linear interpolations are used to compute the initially supplied stage and its corresponding discharge value for initial conditions in this application. The initial water levels assumed for the river channels in subbasin XV were obtained from steady-state conditions at various stages of the Carraízo dam. Once the stage at the dam is entered for the beginning of the runoff simulation, the appropriate water levels for the river channels in subbasin XV are entered in the schmat.dat file. The effects of the initial conditions normally disappear with time because they are damped by friction. After some time, the specified boundary conditions become dominant. HYDRAUX has the flexibility to accept user-supplied initial values. The reader is referred to HYDRAUX supporting documentation (DeLong, 1995) for all possible initial conditions the model can simulate.

Table 11. Initial conditions assumed at each river channel where hydraulic routing is performed

River channel number (shown in figure 3)	Initial condition assumed
1	normal depth computations, channel filled to remove adverse slope
2	normal depth computations, channel filled to remove adverse slope
3	normal depth computations, channel filled to remove adverse slope
4	normal depth computations, channel filled to remove adverse slope
5	normal depth computations, channel filled to remove adverse slope
6	normal depth computations, channel filled to remove adverse slope
7	normal depth computations, channel filled to remove adverse slope
8	normal depth computations, channel filled to remove adverse slope
9	normal depth computations, channel filled to remove adverse slope
10	normal depth computations, channel filled to remove adverse slope
11	steady state approximation
12	normal depth computations, channel filled to remove adverse slope
13	normal depth computations, channel filled to remove adverse slope
14	linear interpolation of discharge and stage
15	normal depth computations, channel filled to remove adverse slope
16	linear interpolation of discharge and stage
17	normal depth computations, channel filled to remove adverse slope
18	normal depth computations, channel filled to remove adverse slope
19	normal depth computations, channel filled to remove adverse slope
20	steady state approximation
21	steady state approximation

Lateral Inflows

Watershed areas were computed along 12 of the 21 river channels where hydraulic routing is performed. Based on GIS-developed topographic contours for the Carraízo-reservoir basin, contributing areas were computed along channel numbers 1, 3, 5, 6, 7, 8, 9, 10, 12, 17, 18, and 19 shown in figure 3. These contributing areas were not computed for very short river channels, as is the case for channel numbers 2, 4, 14, and 16, or for those river channels having cumulative catchment areas nearly proportional to the corresponding cumulative distances, as is the case for channel numbers 11, 13, 15, 20, and 21. Lengths of several channel segments and the corresponding watershed areas were measured for these river channels using GIS. These data are input to HYDRAUX for the purpose of providing spatial discretization of the lateral inflow term q in equation (28). HYDRAUX accepts these values as cumulative percentages of total channel distance and total watershed area corresponding to the channel. Table 12 shows the cumulative percentages for the channels where cumulative values for distance and watershed area measurements were made.

Boundary Conditions

The documentation for HYDRAUX (DeLong, 1995) provides specific details on all boundary condition types that HYDRAUX is capable of simulating. Boundary condition types used in this application for the upstream and downstream ends of each channel, which must be specified for each channel, are listed in table 13. Whenever the inflow discharge hydrograph is known at the upstream end of a channel, the boundary condition reflects a known volumetric discharge. If the inflow discharge hydrograph is not known, and the upstream end is a confluence, a boundary condition is applied to require that the algebraic sum of discharges at the junction is set equal to zero. At the downstream end of each channel, a boundary condition is applied to reflect a known water-surface slope. At each downstream end of a channel where a back-water effect is observed to occur, a boundary condition is used to require that the water surface elevation be equal to that of the connecting channel. The boundary condition used at the dam reflects the usage of a rating curve.

The discharge hydrograph for the confluence of channels 16 and 20 entering the Carraízo reservoir (fig. 3) is estimated for a time period that begins when the sum of rainfall unit values, taken from all raingages in the Carraízo-reservoir basin, exceeds the threshold value of 0.30 inch and ends six hours after the most recently available rainfall data, which gives this rainfall-runoff model the real-time attribute. This additional six-hour time period, referred to as the predictive component of the hydrograph, does not involve rainfall forecasting. Thus, this predictive component is interpreted as the depletion curve the discharge hydrograph would assume if no rainfall occurred after the time of the most recent available rainfall data. The six-hour time period was chosen based on the fact that base flow, travelling at its HYDRAUX-estimated streamflow velocity from the streamgage of any of the independent subbasin, would take at most six hours to arrive at the confluence of channels 16 and 20 (fig. 3). The 24 discharge unit values corresponding to this time period are generated for each independent subbasin where the GUH technique is applied. A five-point moving average technique is employed to smooth the point of contact between the measured hydrograph and the six-hour predictive component of the hydrograph obtained from the GUH technique. The resulting discharge hydrograph at every independent subbasin is provided as an upstream boundary condition to HYDRAUX.

Calibration

The rating curves for high water at the 14 gaging stations in the Carraízo-reservoir basin were obtained from step-back water analysis. Direct measurements and slope-area indirect measurements were made to improve the definition of the rating curves for high water. The roughness coefficients assigned to the cross sections of the river reaches where the gaging stations are located were validated with the medium to high-stage discharge values computed at the same gaging stations. Roughness coefficients used for this application of HYDRAUX were not varied in the calibration process.

Table 12. Cumulative distance percentages and corresponding watershed area percentages along confluences of several river channels where hydraulic routing is performed

[RCN, river channel number shown in figure 3; CPTD, cumulative percentage of total distance of river channel; CPTW, cumulative percentage of total watershed area corresponding to CPTD]

RCN	CPTD	CPTW
1	0.0601	0.5190
	0.3557	0.6751
	0.4906	0.8438
	0.6656	0.9001
	0.7884	0.9628
	1.0000	1.0000
3	0.4642	0.3873
	0.6584	0.8060
	1.0000	1.0000
5	0.2688	0.5101
	0.6055	0.8891
	1.0000	1.0000
6	0.1721	0.6744
	0.4202	0.8211
	0.7071	0.8821
	0.8683	0.9867
	1.0000	1.0000
7	0.1454	0.1842
	1.0000	1.0000
8	0.0989	0.2914
	0.2993	0.4777
	0.5358	0.5938
	0.8015	0.6738
	0.8207	0.7773
	0.8494	0.8436
	1.0000	1.0000

RCN	CPTD	CPTW
9	0.2193	0.1672
	0.2839	0.4319
	0.4204	0.7700
	0.5968	0.8625
	0.7279	0.9736
	1.0000	1.0000
10	0.7598	0.9626
	1.0000	1.0000
12	0.1329	0.1141
	0.1873	0.1345
	0.4999	0.3725
	0.5757	0.7151
	0.8056	0.9352
	1.0000	1.0000
17	0.3302	0.1525
	0.4644	0.2022
	0.6071	0.3235
	0.9025	0.8633
	0.9485	0.9953
	1.0000	1.0000
18	0.2249	0.5686
	0.3657	0.8365
	1.0000	1.0000
19	0.1651	0.1950
	0.3583	0.3810
	0.4371	0.4598
	0.4629	0.6915
	0.8612	0.9267
	1.0000	1.0000

Table 13. Upstream and downstream boundary conditions for each river channel where hydraulic routing is performed

River channel number shown in figure 3	Upstream boundary condition	Downstream boundary condition
1	known volumetric discharge	known water surface slope
2	known volumetric discharge	known water surface slope
3	sum of discharges equals zero	known water surface slope
4	known volumetric discharge	known water surface slope
5	sum of discharges equals zero	known water surface slope
6	known volumetric discharge	known water surface slope
7	sum of discharges equals zero	known water surface slope
8	known volumetric discharge	known water surface slope
9	known volumetric discharge	known water surface slope
10	sum of discharges equals zero	known water surface slope
11	known volumetric discharge	known water surface slope
12	known volumetric discharge	known water surface slope
13	known volumetric discharge	known water surface slope
14	sum of discharges equals zero	water surface elevation equal to that of connecting channel
15	known volumetric discharge	known water surface slope
16	sum of discharges equals zero	water surface elevation equal to that of connecting channel
17	known volumetric discharge	known water surface slope
18	known volumetric discharge	known water surface slope
19	sum of discharges equals zero	known water surface slope
20	known volumetric discharge	water surface elevation equal to that of connecting channel
21	sum of discharges equals zero	rating curve at the dam

Performance of HYDRAUX

The rainfall events of June 18-19, 1993, December 26-27, 1992, November 27-28, 1992, and September 18, 1993, were used to analyze the performance of HYDRAUX in estimating discharge at subbasins XI, XII, XIII, and XIV, respectively. The rainfall rate obtained from the raingage stations located in the vicinity of the river channels where hydraulic routing is performed was generally lower than the corresponding calibrated hydraulic conductivity of the topsoil for each of these four subbasins. The lateral inflow q in equation (28) computed for these four events was mainly based on an estimated base flow component. Thus, the resulting routed discharge hydrographs are predominantly a function of the upstream boundaries input to HYDRAUX. Consequently, these are the best events with available data that can be used to assess the performance of HYDRAUX. There was no significant rainfall event for which all discharge computed at streamgages 11 through 14 could be strictly attributed to the discharge computed at the upstream boundaries and to the base flow of the tributaries. The discharge hydrographs generated during these four rainfall events were mainly a function of the upstream boundaries because the contribution from lateral inflow was small.

The routed hydrographs for subbasins XI, XII, XIII, and XIV for the June 18-19, 1993, December 26-27, 1992, November 27-28, 1992, and September 18, 1993, rainfall events (figs. 16-19) show that the routed and measured hydrographs reasonably agree on the magnitude of the peaks and the time at which these occur. The discrepancies between routed and measured hydrographs during early times of the simulation at subbasins XI through XIV is due to the effects of the assumed initial conditions. The effect of the initial conditions on the routed hydrograph vanishes during the initial 3 to 5 hours after which the boundary conditions become dominant. The magnitude of the hydrograph peaks shown in figures 16 through 19 is predominantly a function of the peaks recorded at the upstream boundaries because the discharge produced by the intervening subbasins was substantially lower than the discharge produced by the independent subbasins. The hydrograph peaks occurring at streamgages 11 through 14 have a small delay in time with respect to the hydrograph peaks occurring at the upstream boundaries, giving an idea to the reader of the streamflow velocities associated with these hydrograph peaks.

SIMULATION RESULTS

The events of January 5-6, 1992, and July 11-12, 1993, were used to test the performance of the real-time rainfall-runoff model of the Carraízo-reservoir basin. The routed hydrographs at subbasins XI to XIV are compared to the measured hydrographs at streamgages 11 to 14 to analyze the combined performance of both, the watershed and the hydraulic routing models. These two events are also used to study the effect of changing the spatial and temporal discretization on the routed hydrograph to the confluence of channels 16 and 20. Routed hydrographs at this confluence, which is the upstream end of the Carraízo reservoir, are computed for the rating curves at the dam spillway when all eight gates are open and when only four of these gates are open. The purpose of presenting these results is to study the effect the open gates have on the computed hydrograph at this confluence.

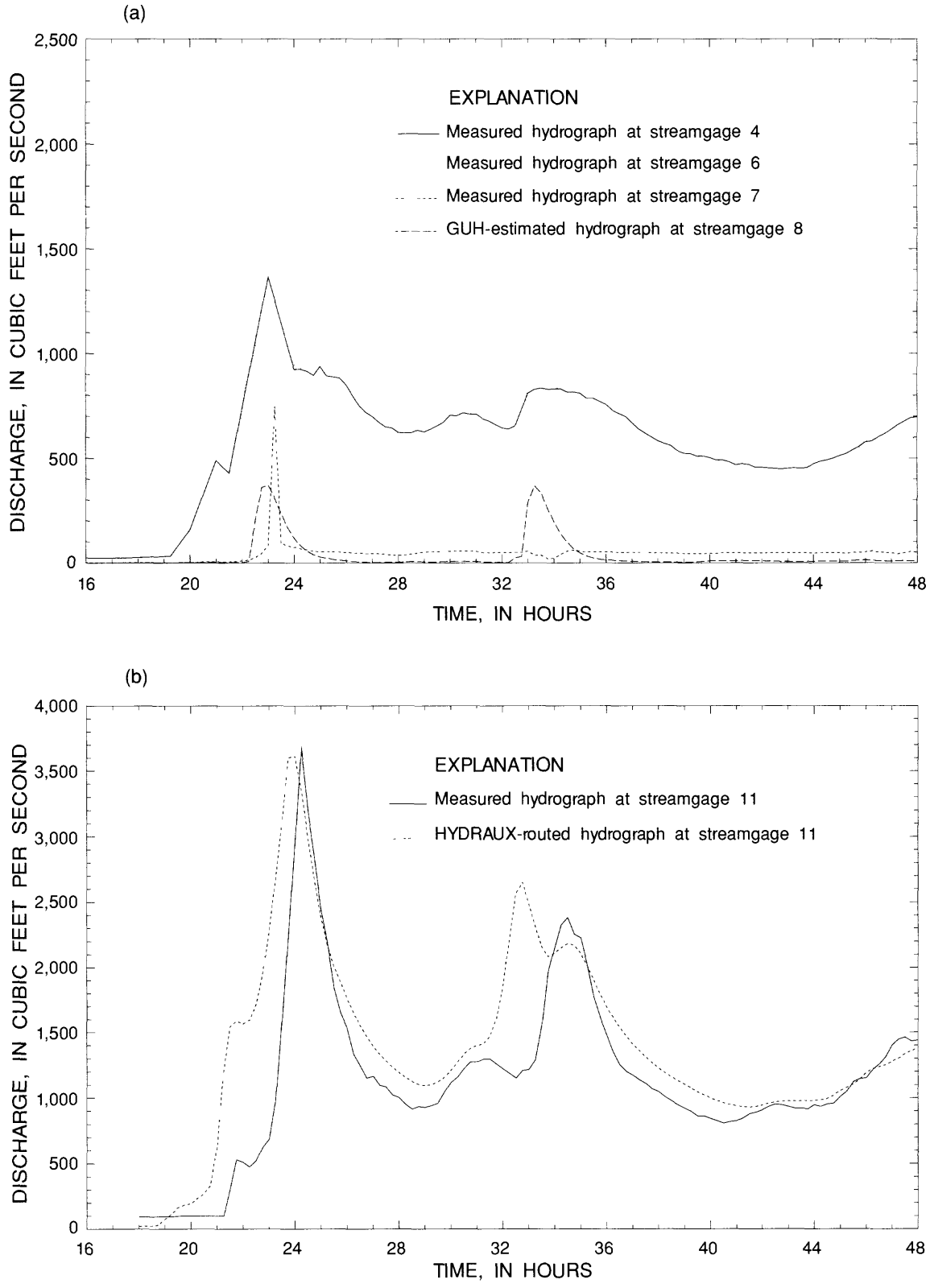

Figure 16. (a) Discharge hydrographs for streamgages 4, 6, 7, and 8 used as upstream boundaries to HYDRAUX and (b) measured and HYDRAUX-routed discharge hydrographs at subbasin XI during June 18-19, 1993.

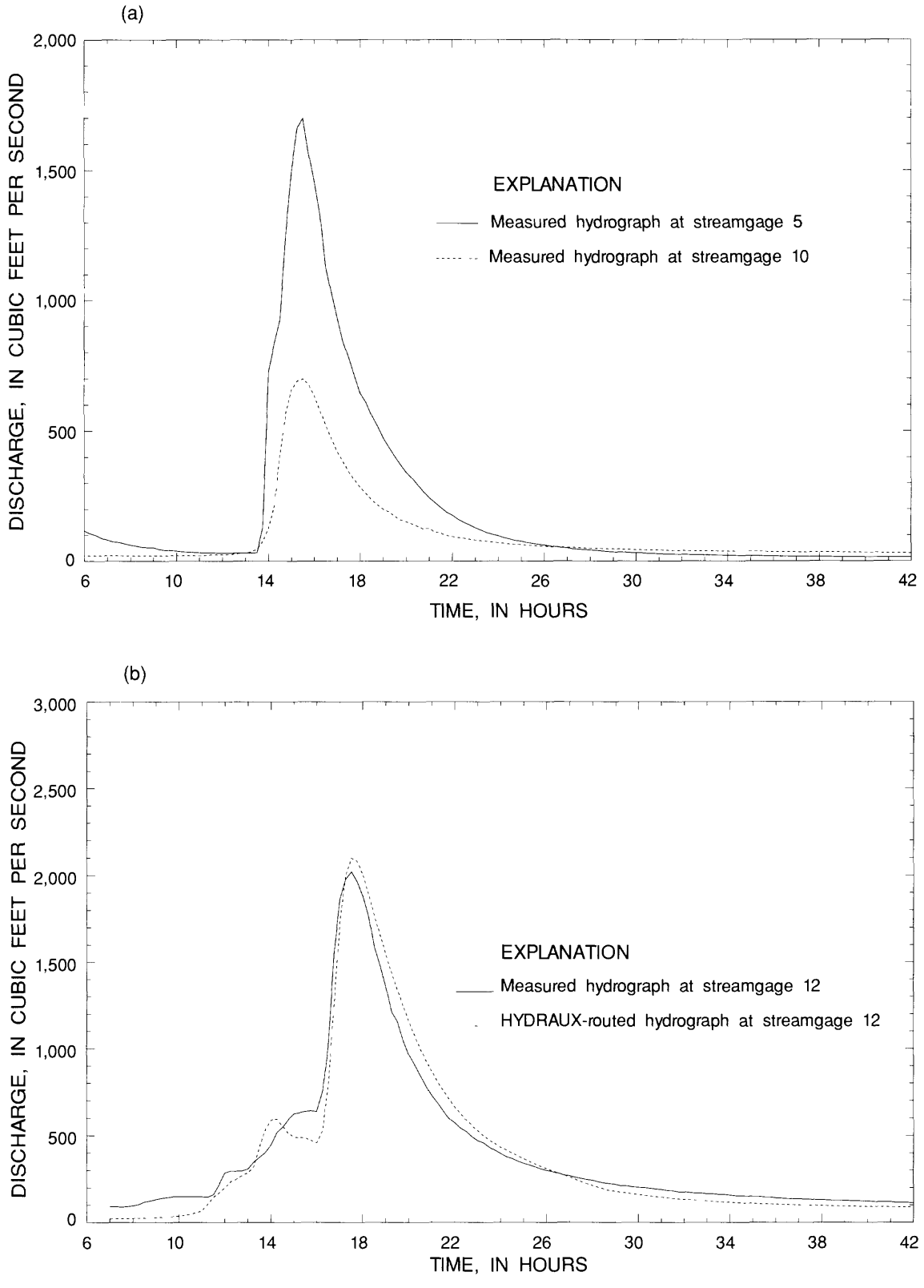

Figure 17. (a) Discharge hydrographs for streamgages 5 and 10 used as upstream boundaries to HYDRAUX and (b) measured and HYDRAUX-routed discharge hydrographs at subbasin XII during December 26-27, 1992.

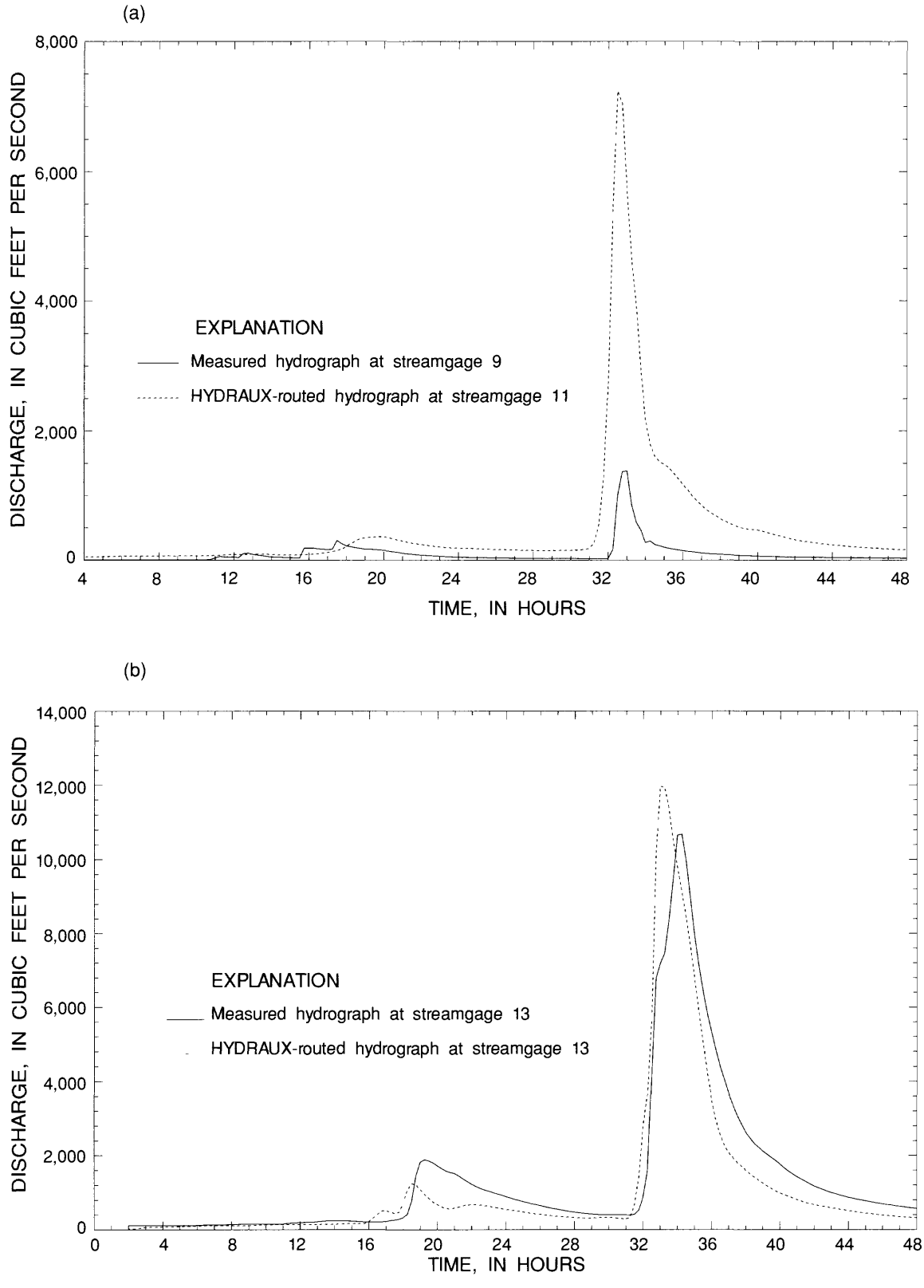

Figure 18. (a) Discharge hydrographs for streamgages 9 and 11 used as upstream boundaries to HYDRAUX and (b) measured and HYDRAUX-routed discharge hydrographs at subbasin XIII during November 27-28, 1992.

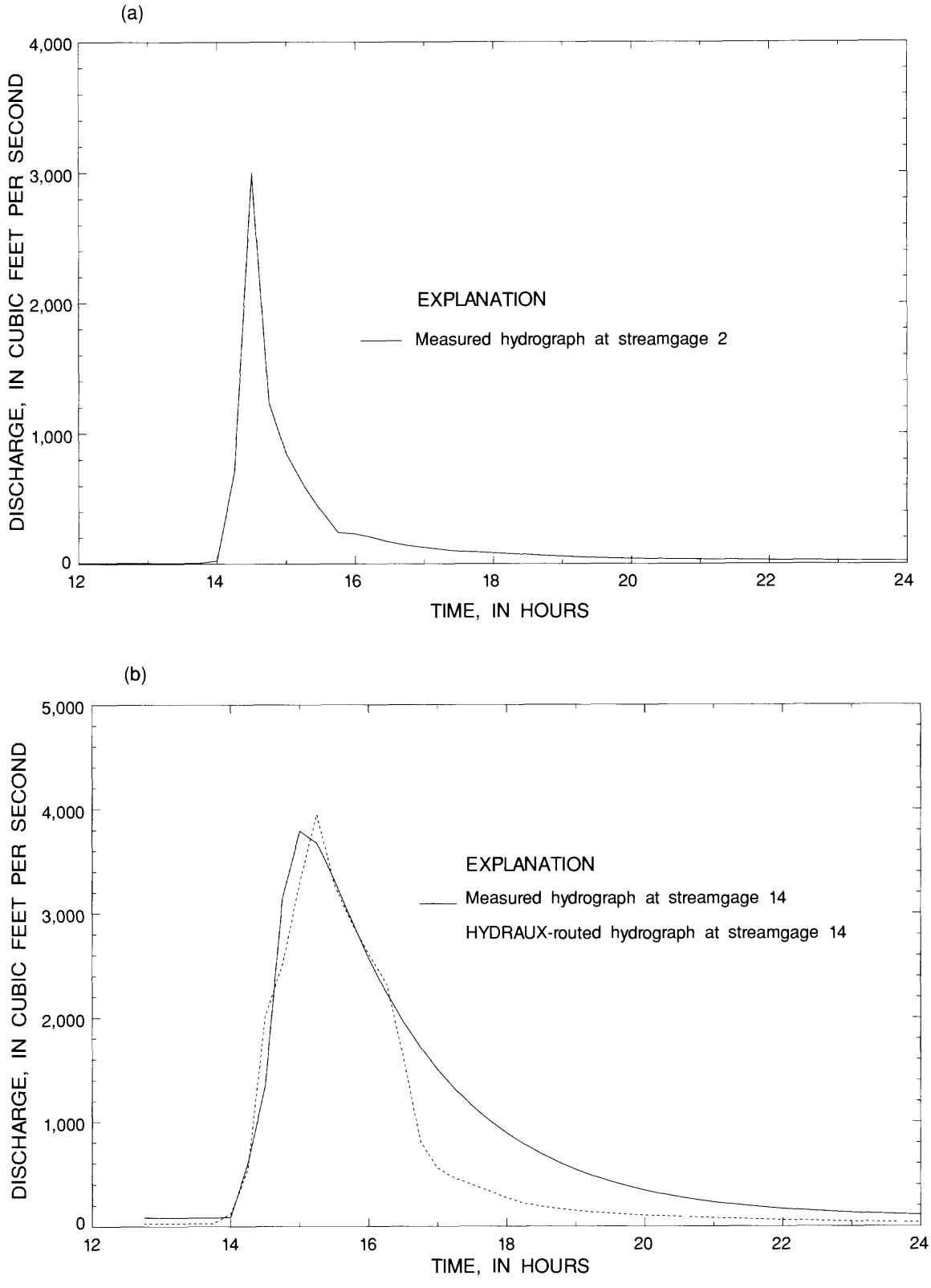

Figure 19. (a) Discharge hydrographs for streamgage 2 used as upstream boundary to HYDRAUX and (b) measured and HYDRAUX-routed discharge hydrographs at subbasin XIV during September 18, 1993.

Rainfall Event 1-- January 5-6, 1992

The rainfall event of January 5-6, 1992, caused extensive damage throughout Puerto Rico. Subbasins XI, XIII, and XIV used this event for calibration of the Green-Ampt infiltration parameters, as table 5 indicates, and because of its magnitude, it is used to test the overall performance of the model in subbasins XI, XIII, and XIV. Rainfall data from raingages 1, 6, 11, 16, and 28 (fig. 2) were substituted for data recorded at raingages 14, 23, 8, 26, and 27, respectively, because the latter gages were not operating correctly during this heavy rainfall event. The GUH-estimated hydrographs, computed from the direct runoff hydrograph derived from equation (16) and from the base flow hydrograph estimate, were used to provide discharge unit values at streamgages 1, 6, and 7. The measured and simulated hydrographs at streamgage 11 for this event are shown in figure 20b. The time difference between the simulated and the measured discharge main peak was 0.25 hour whereas the timing of the secondary peaks was excellent. The magnitude of the main peak of the simulated hydrograph was overestimated whereas the magnitude of the secondary peak was underestimated. This may indicate that the computed lateral inflow values needed a slight delay in time possibly explained by spatial rainfall variations.

An explanation of the simulated hydrograph peaks shown in figure 21b for subbasin XIII may rely on a difference in travel time between the discharge contributions of channels 8 and 9 (fig. 3). The difference between the recession curves shown in figure 21b is larger than that in figure 20b, even though measured peaks at streamgage 11 (fig. 2) at 25 and 31 hours were later measured at streamgage 13 at 26 and 32 hours. The difference between the measured and simulated recession curves at streamgage 13 may be explained by the fact that subbasin XI has a better raingage coverage than intervening subbasin XIII. Spatial and temporal variations in rainfall in a basin may result in an under- or overestimation of the computed lateral inflow values as it seems to have happened in the rainfall event of January 5-6, 1992, where lateral inflow values from 26 hours onward were underestimated (fig. 21b). The time difference between the upstream boundary peaks and the peaks occurring at streamgage 13 is less than 2 time-step intervals, that is, less than 30 minutes. The same observation applies to figure 20.

The area under the simulated hydrograph shown in figure 22b, corresponding to subbasin XIV, is smaller than the area under the measured hydrograph. However, table 7 indicates that the total excess rainfall computed from the calibrated Green-Ampt infiltration parameters is larger than the measured direct runoff. This excludes the possibility that the computed lateral inflow unit values were lower than the actual values. The simulated hydrograph may have been affected by low initial water storage values in channel 12 (fig. 3). The time difference between the upstream boundary peaks and the peaks occuring at streamgage 14 is about one hour. The application of the real-time rainfall-runoff model to the rainfall event of January 5-6, 1992, showed that the measured and the simulated hydrographs at streamgages 11, 13, and 14 had very good agreement in terms of the magnitude of the hydrograph peaks and in terms of the time at which these hydrograph peaks occurred.

Rainfall Event 2-- July 11-12, 1993

The rainfall event of July 11-12, 1993, generated larger runoff volumes in subbasin XII than the runoff generated by the rainfall event of January 5-6, 1992, as 2.05 inches of excess rainfall were computed for the latter event compared to the 2.33 inches of excess rainfall for the former. The calibration of the Green-Ampt infiltration parameters did not use the rainfall event of July 11-12, 1993, for subbasin XII (table 5), therefore this event was used to test the overall performance of the model in subbasin XII. As was the case for the previous event, some raingages and streamgages were not operating appropriately so data from raingages 7, 10, 12, 13, 18, and 20 (fig. 2) were substituted for data recorded at raingages 21, 25, 5, 14, 6, and 19, respectively. The measured hydrograph at streamgage 12, shown in figure 23b, was obtained from an A-35 graphical recorder. The underestimation of the measured peak by the simulated hydrograph may be explained by the fact that a high percent of the raingages operating in subbasin XII did not record reliable data, thus weakening the reliability of estimates of the lateral inflow unit values.

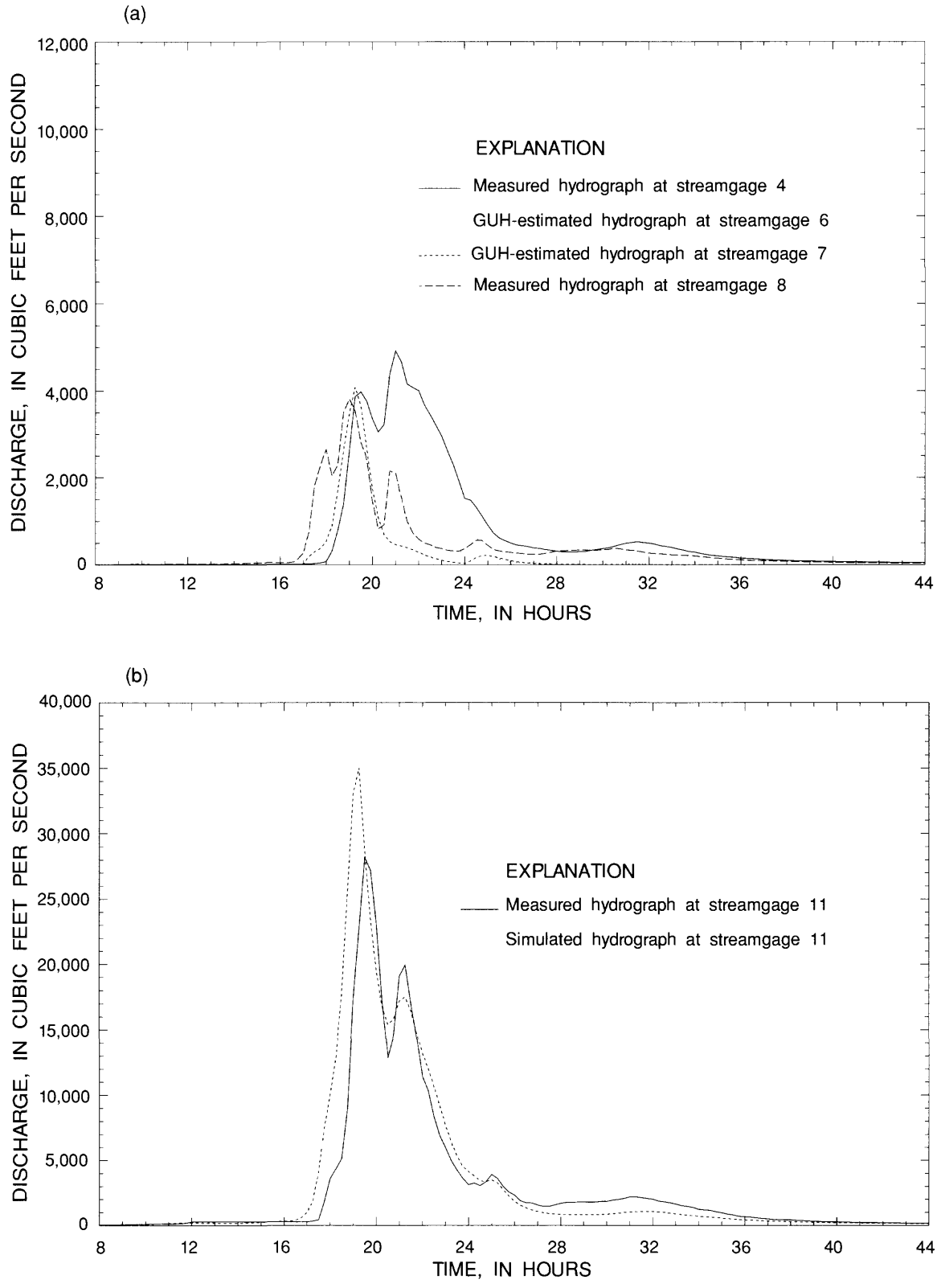

Figure 20. (a) Discharge hydrographs for streamgages 4, 6, 7, and 8 used as upstream boundaries to HYDRAUX and (b) measured and HYDRAUX-routed discharge hydrographs at subbasin XI during January 5-6, 1992.

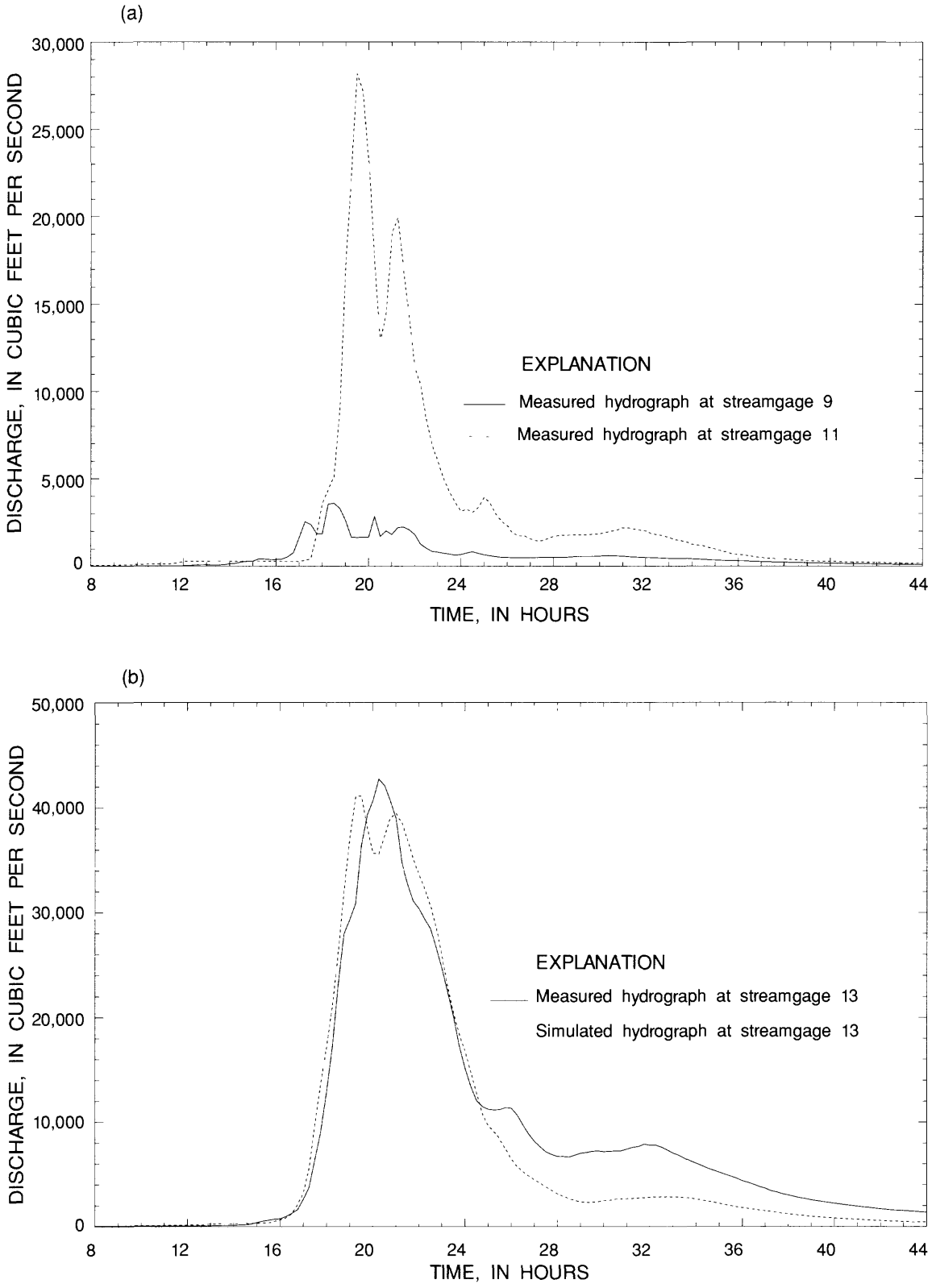

Figure 21. (a) Discharge hydrographs for streamgages 9 and 11 used as upstream boundaries to HYDRAUX and (b) measured and HYDRAUX-routed discharge hydrographs at subbasin XIII during January 5-6, 1992.

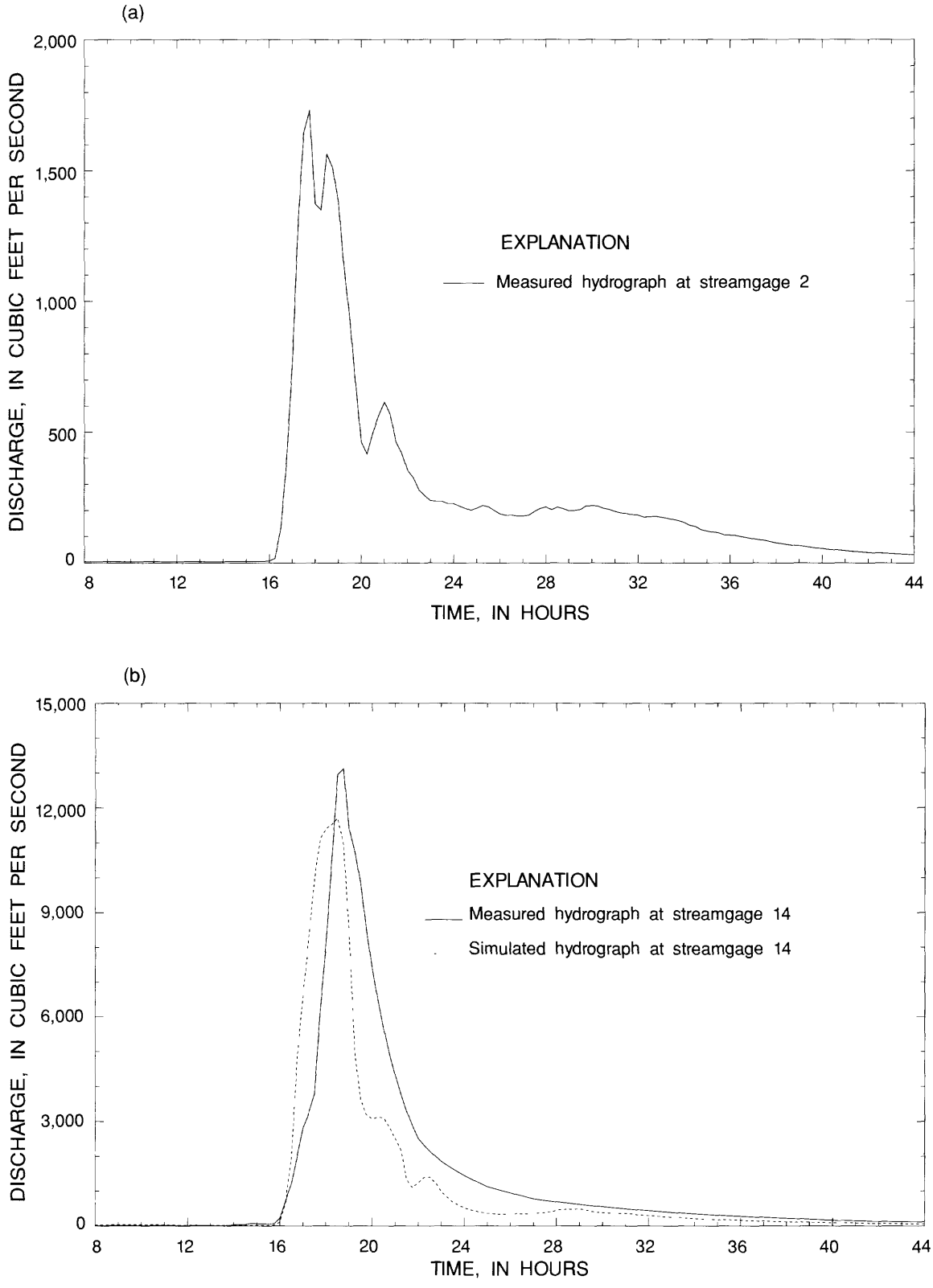

Figure 22. (a) Discharge hydrograph for streamgage 2 used as upstream boundary to HYDRAUX and (b) measured and HYDRAUX-routed discharge hydrographs at subbasin XIV during January 5-6, 1992.

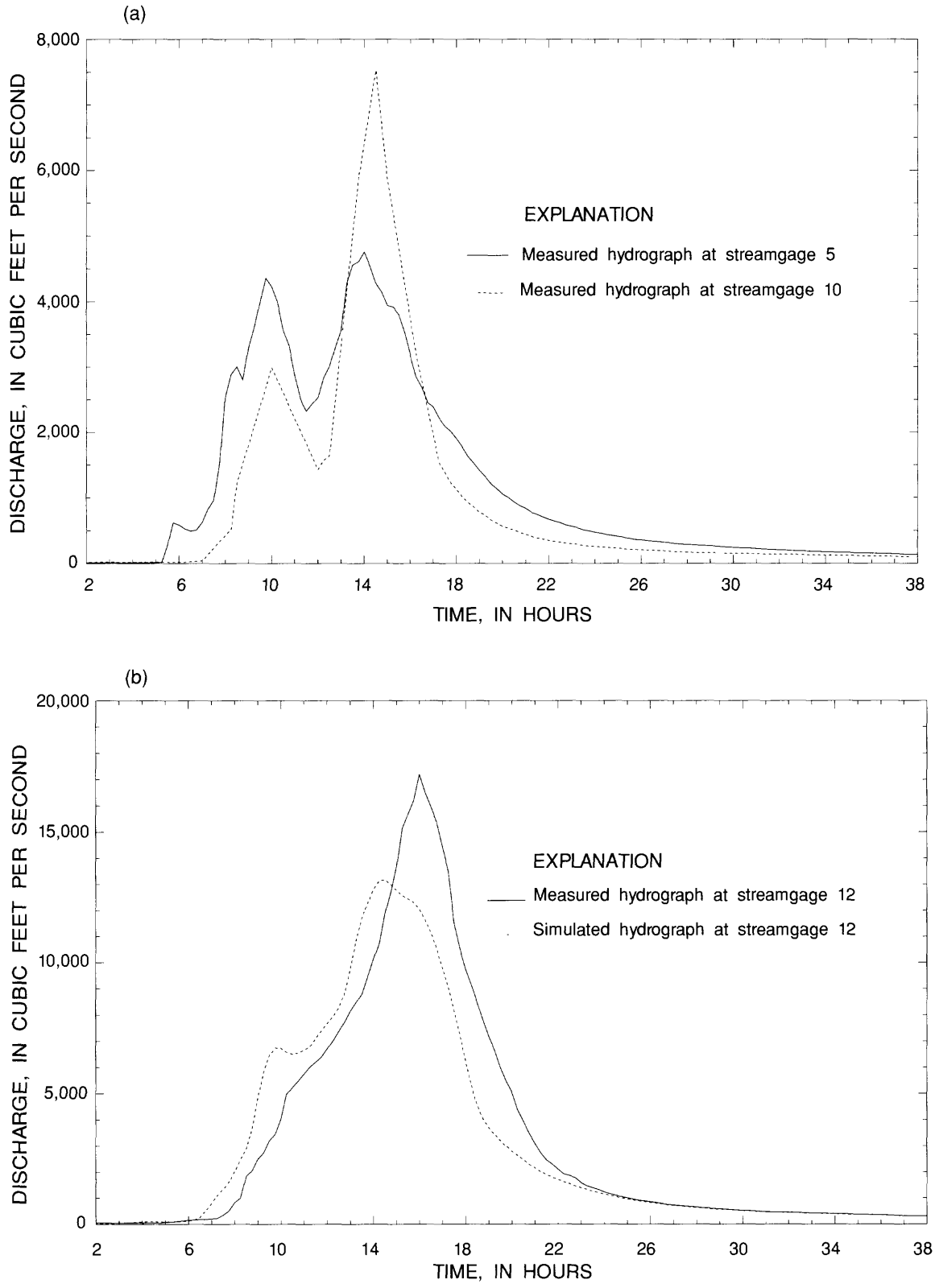

Figure 23. (a) Discharge hydrographs for streamgages 5 and 10 used as upstream boundaries to HYDRAUX and (b) measured and HYDRAUX-routed discharge hydrographs at subbasin XII during July 11-12, 1993.

Spatial and Temporal Discretization

Numerical convergence of the HYDRAUX application presented in this report was examined by running the events of January 5-6, 1992, and July 11-12, 1993. Three different channel-length interval values (DX) with a fixed time-step interval value (DT) of 180 seconds were used to examine the effect of varying spatial discretization. Four different DT values with a fixed DX value of 500 feet were used to examine the effect of varying temporal discretization. The results obtained for the simulated hydrographs at the confluence of channels 16 and 20 in subbasin XV for three different DX values and for DT equal to 180 seconds for these two events showed that all three hydrographs overlap each other. The simulated hydrographs for four different DT values and a fixed DX value showed all four hydrographs overlap each other for both events. These results indicate that HYDRAUX has numerically converged for the channel-length interval values of 400, 500, and 600 feet as well as for the time-step interval values of 60, 90, 150, and 180 seconds. Values for DX and DT finally chosen were 500 feet and 180 seconds, respectively.

Effects of Stage-Discharge Relation at the Dam

The rating curve at the Carraízo dam spillway is shown in figure 24. This curve estimates the flow through the dam when the stage is higher than a reference elevation denoted by Z_0. The value of Z_0 is 134.51 feet above mean sea level. The rating curve shown in figure 24 at the Carraízo dam spillway can be approximated by

$$Q(Z) = G\left(\frac{a}{8}\right)(Z - Z_0)^{\gamma}, \tag{33}$$

where

G is the number of open gates at the dam, from a total of eight,

Z is the stage at the spillway, in feet above mean sea level,

Q is the volumetric discharge, in cubic feet per second, and

a and γ are coefficients that can be obtained from a linear regression between $\log Q$ and $\log (Z - Z_0)$ taken over the measurement points (Quiñones and Associates, 1962) shown in figure 24. Figure 24 shows that $\log Q$ and $\log (Z - Z_0)$ are linearly correlated. The correlation coefficient of this line is 0.999. The approximation of the rating curve at the Carraízo dam spillway expressed by equation (33), after computing values a and γ of equation (33) from the linear regression, becomes

$$Q(Z) = \frac{G}{8} \cdot 637.59 \cdot (Z - Z_0)^{1.6988}. \tag{34}$$

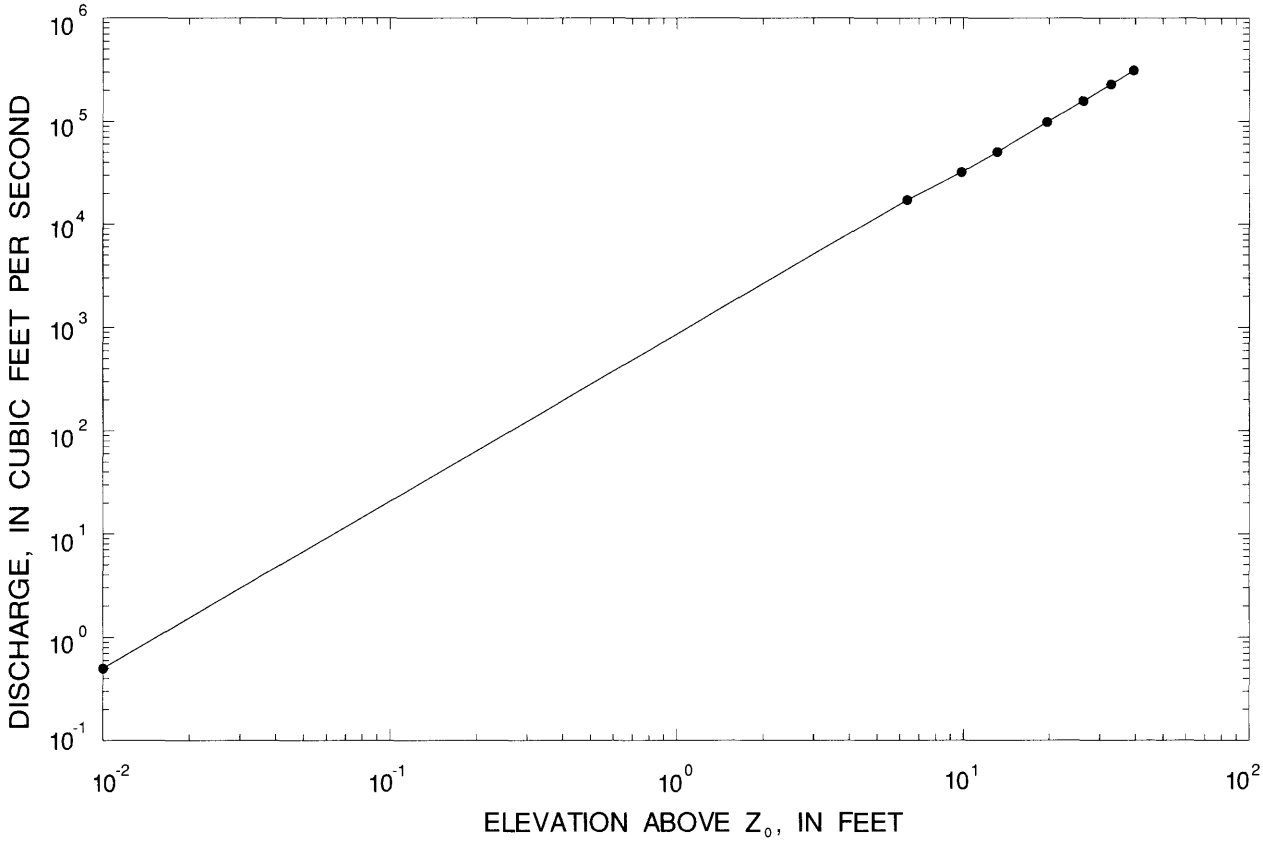

Figure 24. Linear regression performed over measurement points to form the rating curve at the Carraízo dam spillway.

The downstream boundary condition imposed at the Carraízo dam, given by equation (34), is a function of three parameters: G, a, and γ. Two of these three parameters are already provided in equation (34). Figures 25b and 26b show that the discharge hydrographs simulated at the confluence of channels 16 and 20 for the rainfall events of January 5-6, 1992, and July 11-12, 1993, using $G = 4$ and $G = 8$ in equation (34) barely differ from each other. Thus, the discharge hydrograph simulated at the confluence of channels 16 and 20 is not significantly changed if either four or all eight gates are open at the dam. The hydrograph peaks occurring at the upstream boundaries to the confluence of river channels 16 and 20 are delayed nearly 30 minutes with respect to the hydrograph peak simulated at this confluence.

The cumulative water volumes arriving at the confluence of river channels 16 and 20 are obtained by integrating the area under the discharge hydrograph at this confluence. A trapezoidal rule is used to calculate these cumulative water volumes. Figure 27 shows the results of applying a trapezoidal rule to the hydrographs shown in figures 25b and 26b. It can be deduced from figure 27a that the rainfall event of January 5-6, 1992, produced water volumes equivalent to approximately four times the storage capacity of the Carraízo reservoir. The rainfall event of July 11-12, 1993, produced nearly three times the storage capacity of the reservoir (fig. 27b).

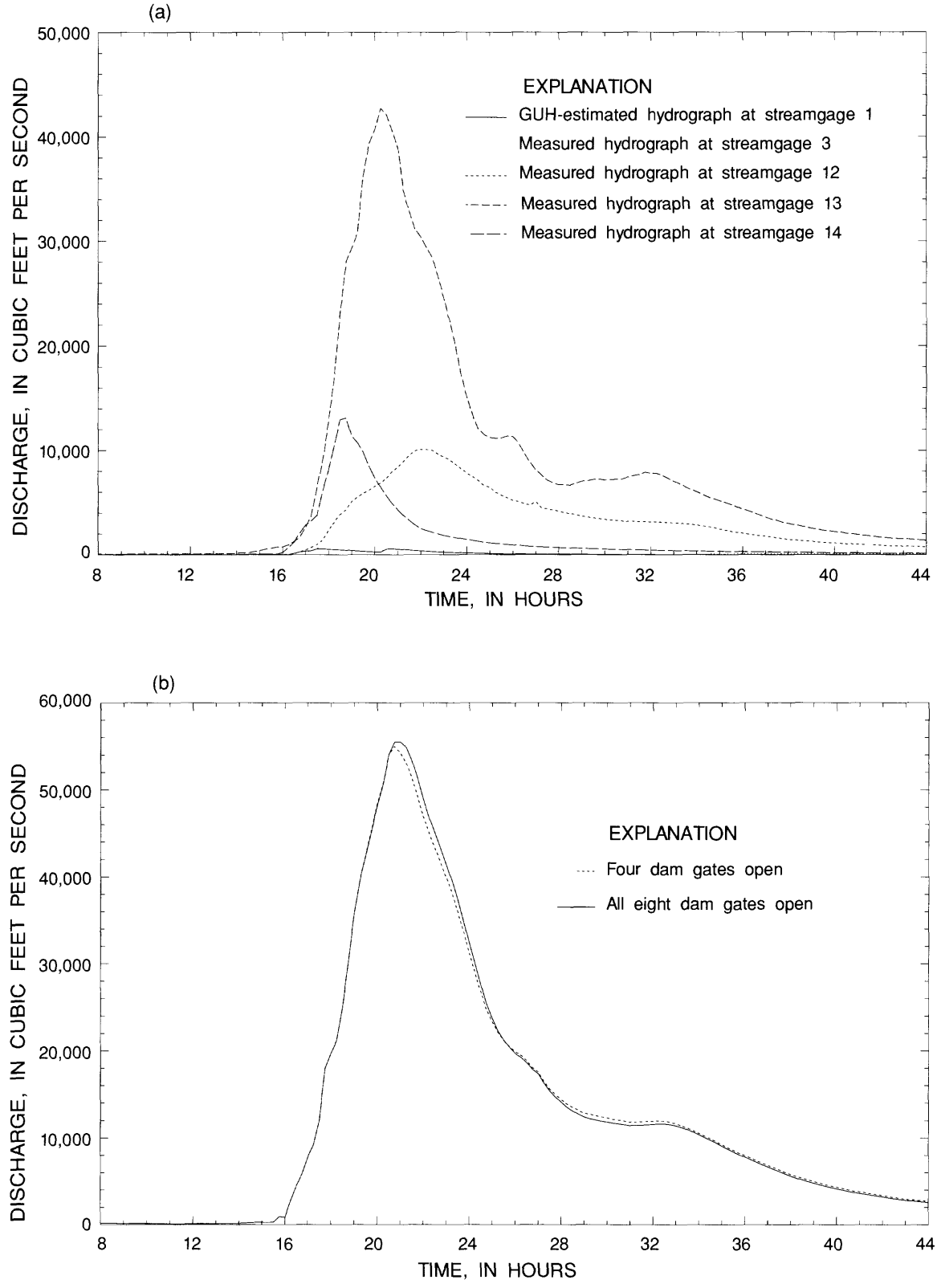

Figure 25. (a) Discharge hydrographs for streamgages 1, 3, 12, 13, and 14 used as upstream boundaries to HYDRAUX and (b) simulated discharge hydrograph at the confluence of river channels 16 and 20 in subbasin XV using rating curves with only four dam gates open and with all eight gates open during January 5-6, 1992.

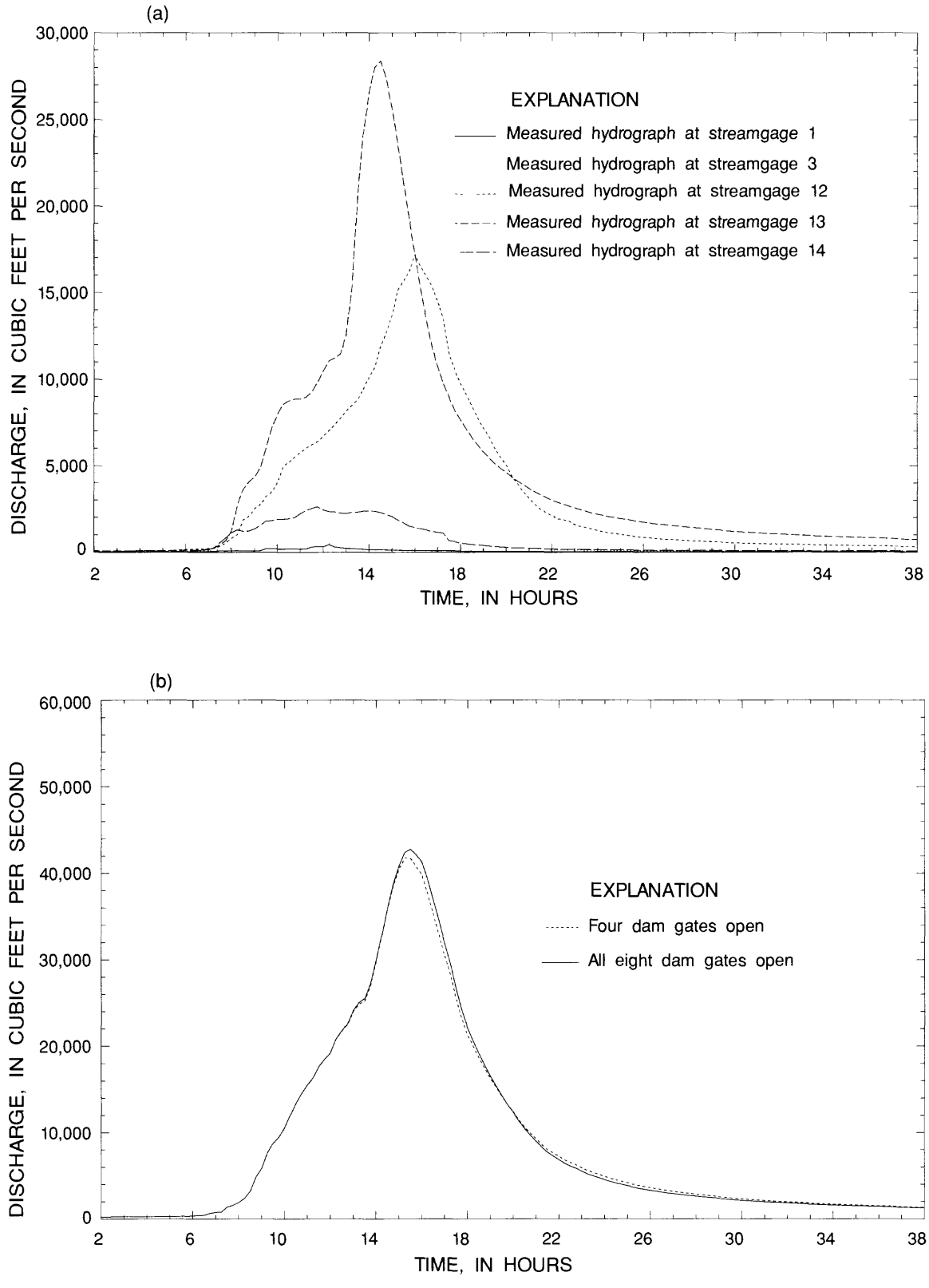

Figure 26. (a) Discharge hydrographs for streamgages 1, 3, 12, 13, and 14 used as upstream boundaries to HYDRAUX and (b) simulated discharge hydrograph at the confluence of river channels 16 and 20 in subbasin XV using rating curves with only four dam gates open and with all eight gates open during July 11-12, 1993.

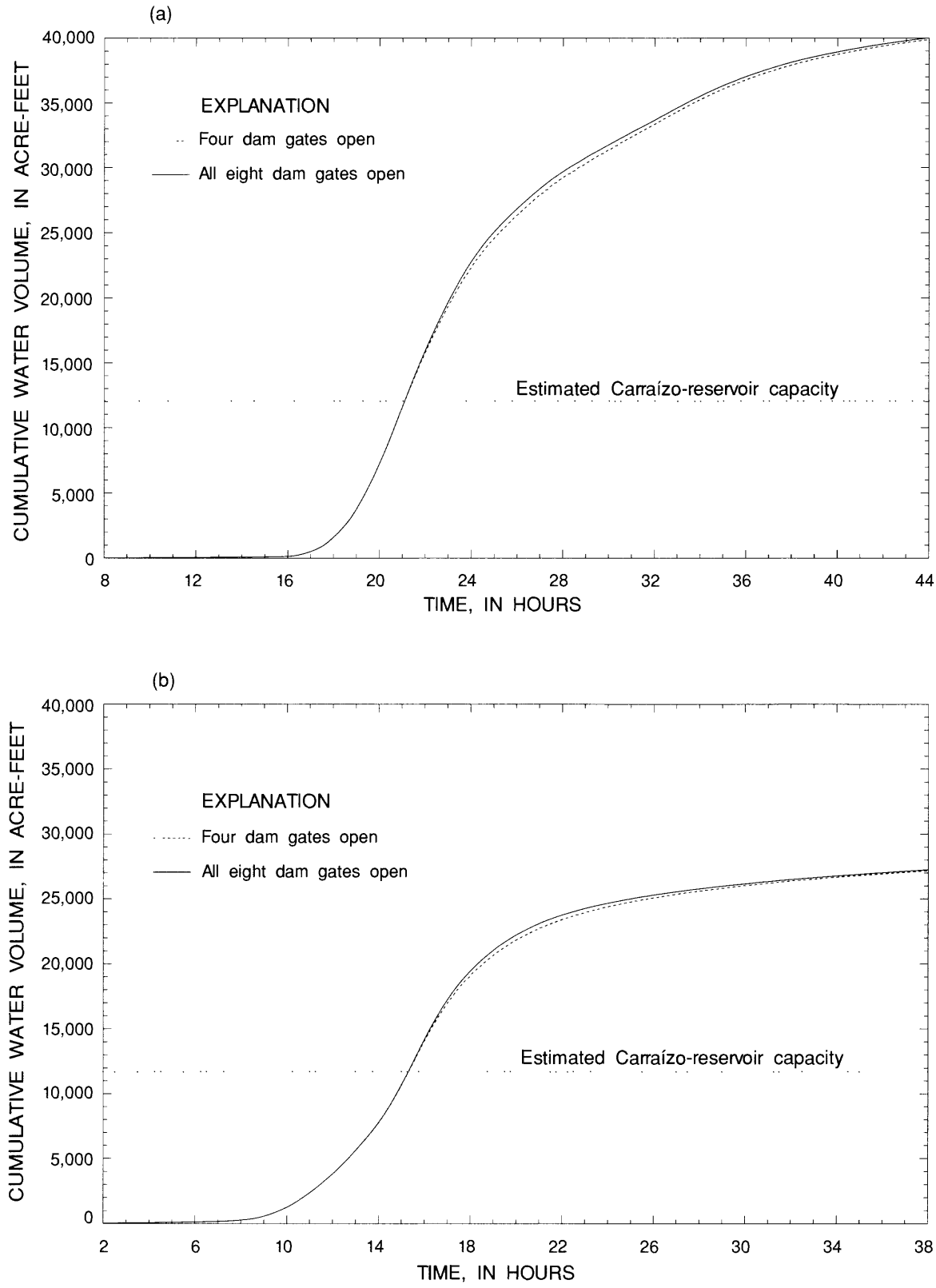

Figure 27. (a) Cumulative water volumes arriving at the confluence of river channels 16 and 20 in subbasin XV using rating curves with only four dam gates open and with all eight gates open during (a) January 5-6, 1992, and (b) July 11-12, 1993.

SUMMARY AND CONCLUSIONS

A real-time rainfall-runoff model for the Carraízo-reservoir basin in Puerto Rico has been developed by the U.S. Geological Survey, in cooperation with the PRASA. The Carraízo-reservoir basin was divided into 10 independent and 5 dependent subbasins. A hydrograph separation technique was developed to determine the direct runoff unit values from the measured discharge hydrograph computed at the outlet of each subbasin. The calibration of the Green-Ampt infiltration parameters for each subbasin was performed through an optimization program that minimized the sum of absolute differences between the total excess rainfall and the total direct runoff volumes for the five rainfall events used in the calibration process. The calibrated parameters were tested on verification events selected based on the magnitude of the recorded rainfall volumes. The verification process of these calibrated Green-Ampt infiltration parameters demonstrated that the small differences between the excess rainfall and direct runoff volumes were mainly attributed to spatial and temporal rainfall variations detected from rainfall hyetographs recorded at the raingage stations within the subbasin. The excess rainfall unit values obtained from the application of these calibrated Green-Ampt infiltration parameters are used to compute the GUH for each independent subbasin and the lateral inflow unit values needed by the hydraulic routing program HYDRAUX.

The GUH equations were derived based on variations to the statistical approach presented earlier by Rodríguez-Iturbe and Valdés (1979). The geomorphologic parameters for each subbasin were obtained from a GIS. A fundamental geomorphologic parameter, the mean streamflow velocity, is computed for every excess rainfall burst that occurs within a rainfall event. The GUH algorithm, used to estimate the direct runoff hydrograph through its convolution with the excess rainfall hyetograph, was tested on the independent subbasins for the events used to verify the calibration of the Green-Ampt infiltration equations. The direct runoff hydrograph estimated using the GUH algorithm mimics the shape of the excess rainfall hyetograph because the kernel of the convolution integral is the excess rainfall hyetograph itself. Thus, the accuracy of the GUH algorithm is directly tied with the reliability of the calibrated Green-Ampt infiltration parameters.

The performance of the hydraulic routing model HYDRAUX was assessed by simulating streamflow for rainfall events where the lateral inflow contributed to the river channels 1 to 21 was predominantly a function of the base flow component of the tributaries. The upstream boundaries for these events were the main variables determining the magnitude of the downstream hydrograph peaks. The effect of the initial conditions on the routed hydrograph diminishes quickly as the boundary conditions become dominant. It was shown in this report, through the routing of these special events, that HYDRAUX is a reliable computer code for estimating discharge values. The simulated discharge hydrographs generated by the overall real-time rainfall-runoff model presented in this report for the January 5-6, 1992, and July 11-12, 1993, rainfall events demonstrated that the water volumes generated at the confluence of river channels 16 and 20 were four and nearly three times larger, respectively, than the water storage capacity of the Carraízo reservoir. The overall performance of the model showed reliable accuracy in the simulated discharge hydrographs of the large rainfall events for which the model was tested.

REFERENCES

Allam, M.N., and Balkhair, K.S., 1987, Case study evaluation of the geomorphologic instantaneous unit hydrograph: Water Resources Management, v. 1, p. 267-291.

American National Standards Institute, 1978, American National Standard Programming Language FORTRAN: New York, N.Y., 400 p.

Briggs, R.P., and Akers, J.P., 1965, Hydrogeologic map of Puerto Rico and adjacent islands: U.S. Geological Survey Hydrologic Investigations Atlas HA-197, 1 sheet.

Carnahan, Brice, Luther, H.A., and Wilkes, J.O., 1969, Applied numerical methods: John Wiley and Sons, Inc., New York, N.Y., 604 p.

Chow, V.T., Maidment, D.R., and Mays, L.W., 1988, Applied hydrology: McGraw-Hill, New York, N.Y., 572 p.

Conte, S.D., and de Boor, Carl, 1980, Elementary numerical analysis, an algorithmic approach (3d ed.): McGraw-Hill, New York, N.Y., 432 p.

Cunge, J.A., Holly, F.M. Jr., and Verwey, A., 1980, Practical aspects of computational river hydraulics: Pitman Publishing, Inc., Marshfield, Massachusetts, 420 p.

DeLong, L.L., 1986, Extension of the unsteady one-dimensional open-channel flow equations for flow simulation in meandering channels with flood plains, *in* Selected Papers in the Hydrologic Sciences, S. Subitzky (ed.): U.S. Geological Survey Water-Supply Paper 2290, p. 101-105.

_____, 1995, Computer Program HYDRAUX 95.1 - a model for simulating one-dimensional, unsteady, open-channel flow: On file with U.S. Geological Survey at Stennis Space Center, Miss., 66 p.

DeLong, L.L., and Schoellhamer, D.H., 1989, Computer program HYDRAUX - a model for simulating one-dimensional, unsteady, open-channel flow: U.S. Geological Survey Water-Resources Investigations Report 88-4226, 57 p.

DeLong, L.L., Thompson, D.B., and Fulford, J.M., 1992, Data encapsulation using FORTRAN 77 modules: Fortran Forum, v. 11, n. 3, p. 11-19.

DeLong, L.L., Thompson, D.B., and Lee, J.K., 1995, *in review*, Computer program FOURPT - a model for simulating one-dimensional, unsteady, open-channel flow: On file with U.S. Geological Survey at Stennis Space Center, Miss.

Gupta, V.K., Waymire, Ed, and Wang, C.T., 1980, A representation of an instantaneous unit hydrograph from geomorphology: Water Resources Research, v. 16, n. 5, p. 855-862.

Hirsh, M.W., and Smale, Stephen, 1974, Differential equations, dynamical systems, and linear algebra: Academic Press, New York, N.Y., 358 p.

Kirshen, D.M., and Bras, R.L., 1983, The linear channel and its effect on the geomorphologic IUH: Journal of Hydrology, v. 65, p. 175-208.

Laenen, Antonius, and Hansen, R.P., 1988, Simulation of three lahars in the Mount St. Helens area, Washington, using a one-dimensional, unsteady state streamflow model: U.S. Geological Survey Water-Resources Investigations Report 88-4004, 20 p.

Laenen, Antonius, Scott, K.M., Costa, J.E., and Orzol, L.L., 1987, Hydrologic hazards along Squaw Creek from a hypothetical failure of the glacial moraine impounding Carver Lake near Sisters, Oregon: U.S. Geological Survey Open-File Report 87-41, 45 p.

_____, 1988, Modeling flood flows from a hypothetical failure of the glacial moraine impounding Carver Lake near Sisters, Oregon, *in* Selected Papers in the Hydrologic Sciences, S. Subitzky (ed.): U.S. Geological Survey Water-Supply Paper 2340, p. 151-164.

Lapidus, Leon, and Pinder, G.F., 1982, Numerical solution of partial differential equations in science and engineering: John Wiley and Sons, Inc., New York, N.Y., 677 p.

Mays, L.W., and Taur, C.-K., 1982, Unit hydrographs via nonlinear programming: Water Resources Research, v. 18, n. 4, p. 744-752.

Morel-Seytoux, H.J., 1988, Recipe for simple but physically based modeling of the infiltration and local runoff processes: Proc. 8th Annual Hydrology Days, Hydrology Days Publications, Ft. Collins, Colo., p. 226-247.

National Dam Safety Board, 1979, Loíza Dam, Trujillo Alto, Puerto Rico, Phase 1 - Inspection Report: Puerto Rico Water Resources Authority, San Juan, P.R., 55 p.

Pease, M.H., Jr., 1968, Geologic map of the Aguas Buenas quadrangle, Puerto Rico: U.S. Geological Survey Miscellaneous Geologic Investigations Map I-479, 1 sheet.

Pinder, G.F., and Shapiro, Allen, 1979, A new collocation technique for the solution of the convection-dominated transport equation: Water Resources Research, v. 15, n. 5, p. 1177-1182.

Preissmann, Alexandre, 1961, Propagation des intumescences dans les canaux et rivieres, *in* 1st Congress de l'Assoc. Française de Calcul, Grenoble, Fr., p. 433-442.

Quiñones, Ferdinand, Green, Bruce, and Santiago, Luis, 1989, Sedimentation survey of Lago Loíza, Puerto Rico, July 1985: U.S. Geological Survey Water-Resources Investigations Report 87-4019, 17 p.

Quiñones, M.A., and Associates, 1962, Loíza river flood control studies: prepared for the Puerto Rico Planning Board, Commonwealth of Puerto Rico, San Juan, P.R., 112 p.

Rawls, W.J., Brakensiek, D.L., and Miller, Norman, 1983, Green-Ampt infiltration parameters from soils data: Journal of Hydraulic Engineering, ASCE, v. 109, n. 1, p. 62-70.

Rodríguez-Iturbe, Ignacio, and Valdés, J.B., 1979, The geomorphologic structure of hydrologic response: Water Resources Research, v. 15, n. 6, p. 1409-1420.

Rogers, C.L., 1979, Geologic map of the Caguas quadrangle, Puerto Rico: U.S. Geological Survey Miscellaneous Investigations Series Map I-1152, 1 sheet.

Sepúlveda, Nicasio, 1996, *in review*, Application of two direct runoff prediction methods in Puerto Rico: On file with U.S. Geological Survey at Altamonte Springs, Florida.

Soil Conservation Service, 1978, Soil Survey of San Juan Area of Puerto Rico: U. S. Department of Agriculture, Soil Conservation Service, 141 p.

Strahler, A.N., 1957, Quantitative analysis of watershed geomorphology: American Geophysical Union Trans., v. 38, n. 6, p. 913-920.

Thompson, D.B., DeLong, L.L., and Fulford, J.M., 1992, Data Encapsulation Using Fortran-77 Modules -- a first step toward object-oriented programming: U.S. Geological Survey Water-Resources Investigations Report 92-4123, 73 p.

APPENDIXES

APPENDIX 1. UNIX System V Bourne Shell Executable Program

Shell program hyd

```
#
#  This shell program reads the time period for which streamgage
#  and raingage data are retrieved from ADAPS on the PRIME.
#  All previously existing data are removed before the retrieval.
#  In addition, shell program hyd decides whether hyd.sh1 or
#  hyd.sh2 is run depending on the amount of rainfall recorded.
#  Variables $period and $days are transferred to program hyd.sh1.
#  Shell program hyd.sh2 is run only once, if there is a need to
#  depending on the amount of rainfall recorded since the last run.
#
echo
echo
echo "THIS PROGRAM WILL GENERATE A FILE WITH THE TOTAL"
echo "RAIN ACCUMULATED DURING A PERIOD OF DAYS"
echo "Enter LAST DATE of the period (YYYYMMDD) -> \c"
read period
echo
echo "Enter LENGTH of period (max of 2 days)   -> \c"
read days
echo
echo
rm $HOME/DATA/oq*
rm $HOME/DATA/or*
hyd.sh1 $period $days
echo "Would you like to run this program again (y/n)?"
echo "-> \c"
read answer
if [ "$answer" = y -o "$answer" = Y ]
then
   rm $HOME/DATA/oq*
   rm $HOME/DATA/or*
   hyd.sh2 $period $days
fi
```

Shell program hyd.sh1

```
#
#  Variables specifying directory names in the $HOME directory,
#  HYDRAUX, are initialized in this shell program.
#
DATA=$HOME/DATA
CAGUAS=$HOME/CAGUAS
GURABO=$HOME/GURABO
SLORENZO=$HOME/SLORENZO
UNGAGED=$HOME/UNGAGED
VBLANCA=$HOME/VBLANCA
#
#  Linesubs incorporates the values of variables $period and $days
#  into file getfiles, actual executable program which transfers
#  streamgage and raingage data to the workstation from the PRIME.
#
linesubs $HOME/bin/get_files $HOME/bin/get_files.bak 12 "send $1\r"
linesubs $HOME/bin/get_files.bak $HOME/bin/get_files 14 "send $2\r"
rm $HOME/bin/get_files.bak
get_files
#
#  The only difference between hyd.sh1 and hyd.sh2 is that in hyd.sh2
#  the executable program named filter is substituted for the executable
#  program named filter2.  Executable program filter2 takes into account
#  the time when the last program execution was performed.
#  A file named message is generated by filter in case the rainfall
#  volumes recorded at the stations is minimal and no hydraulic
#  routing is necessary.  If this is the case, the option is left
#  open to the user to route base flow or not.
#
 rm $DATA/message
```

```
 filter
if [ -f $DATA/message ]
then
   line_num=`wc -l $DATA/message`
   if [ "$line_num" -ne 0 ]
   then
      cat message
      echo "\nWould you like to continue (y/n)? -> \c"
      read answer
   fi
   if [ "$answer" = n -o "$answer" = N ]
   then
       exit
   fi
   rm $DATA/message
fi
#
#  Next 5 lines generate lateral influx files for each one of the
#  5 intervening subbasins (XI to XV).
#
slorenzo
gurabo
caguas
vblanca
ungaged
#
#  The GUH-estimated discharge hydrograph is generated for each one of
#  the independent subbasins with names are stored in file geo-files.
#
cd $DATA
while read line
do
  basin=`echo $line | cut -f1 -d' '`
  oqfile=`echo $line | cut -f2 -d' '`
  echo "\nBEGIN RUNNING $basin"
  cp $basin.parguh  geomorphic.parguh
  geomorphic
  mv geomorphic.guh $oqfile
done < geo-files
echo "\nENDED RUNNING geomorphic\n"
#
#  The time-step interval is computed based on the contents of the
#  input file control.dat.
#
DELTAT=`get_deltaT /hydraux/CAGUAS/control.dat`
read SETIME < times
#
#  Executable program get_times calculates time interval of simulation
#  in minutes and starting time in seconds
#
get_times times.chg $DELTAT $SETIME
read TIMEMINS TIMESECS < times.chg
#
#  Composition between the GUH-generated discharge hydrograph and, if availbale,
#  the measured discharge hydrograph is performed using the five-point moving
#  average technique (to avoid stiff discontinuities) for each independent subbasin
#  (I to X) to generate the upstream boundary conditions.
#
appendRt-Obs $DATA/oq50050900  $DATA/oq509    $SLORENZO/oq50050900   0  $SETIME
appendRt-Obs $DATA/oq50051150  $DATA/oq5115   $SLORENZO/oq50051150   0  $SETIME
appendRt-Obs $DATA/oq50051180  $DATA/oq5118   $SLORENZO/oq50051180   0  $SETIME
appendRt-Obs $DATA/oq50051310  $DATA/oq5131   $SLORENZO/oq50051310   0  $SETIME
appendRt-Obs $DATA/oq50053025  $DATA/oq53025  $CAGUAS/oq50053025     0  $SETIME
appendRt-Obs $DATA/oq50055100  $DATA/oq551    $VBLANCA/oq50055100    0  $SETIME
appendRt-Obs $DATA/oq50055390  $DATA/oq5539   $UNGAGED/oq50055390    0  $SETIME
appendRt-Obs $DATA/oq50055750  $DATA/oq5575   $GURABO/oq50055750     0  $SETIME
appendRt-Obs $DATA/oq50056400  $DATA/oq564    $GURABO/oq50056400     0  $SETIME
appendRt-Obs $DATA/oq50058350  $DATA/oq5835   $UNGAGED/oq50058350    0  $SETIME
#
#  Hydraulic routing at intervening subbasins XII and XIV is performed
#  in batch mode to save execution time.  Hydraulic routing at intervening
#  subbasin XI is performed interactively.
#
```

```
remsh dprsj25 exec_subbasın $GURABO    $TIMEMINS $TIMESECS &
remsh dprsȷ20 exec_subbasın $VBLANCA   $TIMEMINS $TIMESECS &
exec_subbasin $SLORENZO  $TIMEMINS $TIMESECS
#
#  Composition between the routed and, if avaılable, the measured discharge
#  hydrographs is performed at intervenıng subbasins XI, XII, and XIV.
#
appendRt-Obs $DATA/oq50057000 $GURABO/nettsq.dat   $UNGAGED/oq50057000 1 $SETIME
appendRt-Obs $DATA/oq50055225 $VBLANCA/nettsq.dat  $UNGAGED/oq50055225 1 $SETIME
appendRt-Obs $DATA/oq50051800 $SLORENZO/nettsq.dat $CAGUAS/oq50051800  1 $SETIME
#
#  Hydraulic routing at ıntervening subbasin XIII is performed after routing
#  at intervening subbasin XI is completed.  Composition of the routed and, if
#  available, the measured hydrographs at intervening subbasın XIII is computeo
#  after hydraulic routing is completed and the result is stored in the directcry
#  used to store all related input files to route flow through intervening
#  subbasin XV.
#
exec_subbasin $CAGUAS    $TIMEMINS $TIMESECS
appendRt-Obs $DATA/oq50055000 $CAGUAS/nettsq.dat   $UNGAGED/oq50055000 1 $SETIME
#
#  Hydraulic routing at intervening subbasin XV (the ungaged subbasin) is
#  performed last, after routing through intervening subbasins ıs completed.
#  Finally, the trapezoid rule is applied to the final routed discharge
#  hydrograph to compute cumulative volumes of water as a function of time,
#  writing final results in unıts of acre-foot.
#
cd $UNGAGED
cp schmat.dat schmat.old
updt_schmat $DATA/oq50059000  schmat.dat schmat.new $SETIME
mv schmat.new schmat.dat
exec_subbasın $UNGAGED   $TIMEMINS $TIMESECS
trapezoide nettsq.dat nettsq.trp
```

Shell program exec_subbasin

```
#
#  The arguments in the statement that run this executable are specified
#  ın the first three lines of this program.  The sımulation time ıs input
#  to this shell program from the calling shell program and is then written
#  to the corresponding line number of files control.dat and chbndlst.dat.
#  The executable netbound is run then.
#
 TIMEMINS=$2
 TIMESECS=$3
 cd $1
 date > FECHA
 strsubs control.dat control 9 8 $TIMEMINS
 mv control control.dat
 strsubs control.dat control 10 10 $TIMESECS
 mv control control.dat
 strsubs chbndlst.dat chbndlst 1 8 $TIMESECS
 mv chbndlst chbndlst.dat
 cp chnlbnd.dat chnlbnd.old
 netbound
#
#  Executable program cmp_dates decides ıf program netprop is run.
#  Program cmp_dates returns the following output: LT, GT, EQ
#  (earlıer than, later than, or at the same time).
#  Only ıf the date when the file rawgeom.dat was created is later
#  than th edate file cxgeom.dat was created, then netprop is run.
#
 COMP=`cmp_dates rawgeom.dat cxgeom.dat`
 if [ "$COMP" = "LT" ]; then
     netprop.950419
 fı
#
#  Hydraulic routıng program HYDRAUX is executed.
#
 hydraux.950518
 date >> FECHA
```

APPENDIX 2. FORTRAN optimization program used to calibrate Green-Ampt infiltration parameters

```
C
C     This program computes the optimal set of Green-Ampt (GA) infiltration parameter
C     values that minimizes the sum, over 5 rainfall events for each subbasin, of
C     absolute differences between the total excess rainfall volume computed from
C     the GA equations for values of eta, eta_e, psi, and K (SOIL(1), SOIL(2), SOIL(3),
C     and SOIL(4), respectively) and the total direct runoff volume computed from an
C     empirically-derived scheme for hydrograph separation.
C     The set of optimal GA parameters that minimize this sum is found using IMSL
C     subroutine BCONF, which implements a quasi-Newton method with a finite-difference
C     gradient computation.
C
C     Main variables used:
C
C     B1            Slope of linear regression
C     B2            Intercept of linear regression
C     BASAR         Subbasin drainage area, in square miles
C     BF            Base flow component of discharge hydrograph
C     BREAK         Breakpoints of the cubic spline coefficients
C     CORR          Correlation coefficient in linear regression analysis
C     CSCOEF        Cubic spline coefficients fitting the shape of the discharge hydrograph
C     DELT          Time interval used for unit values, set to 0.25 hour
C     DQ            Total direct runoff volume per event
C     DQDT          Derivative of surface discharge with respect to time
C     DQDTR         Dependent variable used in DQDT vs QT linear regression
C     ER            Excess rainfall unit values
C     ERC           Total excess rainfall unit values per event
C     HIN           Infiltration loss unit values
C     INUM          Number of events used in calibration (5)
C     ND1           Hydrograph index indicating beginning of direct runoff per event
C     ND2           Hydrograph index of maximum direct runoff
C     ND3           Hydrograph index of beginning of recession curve
C     ND4           Number of discharge unit values
C     NDM           Maximum dimension for number of discharge unit values
C     NR            Number of rainfall unit values
C     NRM           Maximum dimension for number of rainfall unit values
C     QBEG          Discharge at index ND1 used to compute initial soil moisture content
C     QMAX          Maximum base flow used to compute initial soil moisture content
C     QMIN          Minimum base flow used to compute initial soil moisture content
C     QR            Direct runoff component of discharge hydrograph
C     QT            Discharge hydrograph unit values, equal to BF + QR
C     QTR           Independent variable used in DQDT vs QT linear regression
C     RAIN          Rainfall unit values, equal to HIN + ER
C     RI            Rainfall intensity unit values, equal to RAIN/DELT
C     RKONST        Conversion constant from flux in cfs to inches over BASAR during DELT
C     THETA         Soil moisture content
C     TIEMPO        Matrix containing time unit values for all rainfall events
C     TIME          Vector containing time unit values for a given rainfall event
C
      PARAMETER (INUME=6, NDM=200, NRM=192)
C
      REAL QR(INUME,NDM), QT(INUME,NDM), BF(INUME,NDM), QBEG(INUME)
      REAL DQ(INUME), XLB(4), XUB(4), XSCALE(7), STAT(12), CORR(INUME)
      REAL DQDT(INUME,NDM), DQDTR(NDM), QTR(NDM), XSOIL(4)
      REAL RAIN(INUME,NRM), HIN(INUME,NRM), ER(INUME,NRM), ERC(INUME)
      REAL RPARAM(7), THETA(INUME), SOIL(4), RAINS(INUME,NRM,12)
      REAL CSCOEF(4,NDM), BREAK(NDM), TIEMPO(INUME,NDM), TIME(NDM)
      INTEGER ND1(INUME), ND2(INUME), ND3(INUME), ND4(INUME)
      INTEGER NR(INUME), NR1(INUME), NR2(INUME), IPARAM(7)
      LOGICAL DECIDE
C
C     List of IMSL-related variables:
C     XLB, XUB, XSCALE, STAT, XSOIL, RPARAM, CSCOEF, BREAK, IPARAM
C     COMMON variables used in SUBROUTINES VALGA and SVALGA
C
      COMMON /SUELO/ DELT, THMAX, THMIN
      COMMON /GOTAS/ RAIN, HIN, ER, WATER, DQ, QBEG, QMAX, QMIN
      COMMON /IRANG/ NR, NR1, NR2
      COMMON /RITE/ DECIDE
      COMMON /NUMST/ IR, ERC
      COMMON /TOTAL/ RAINS
C
```

```
C     Declare EXTERNAL all SUBROUTINES called by IMSL
C
      EXTERNAL RLINE, IWKIN, BCONF, VALGA, CSAKM, CSDER, SVALGA
C
C     Save storage space needed by IMSL SUBROUTINES
C
      CALL IWKIN(10000)
C
      OPEN(11,FILE='uhyd1.in',STATUS='OLD',ACCESS='SEQUENTIAL')
      OPEN(12,FILE='uhyd1.out',STATUS='UNKNOWN',ACCESS='SEQUENTIAL')
C
C     Read percent of subbasin corresponding to rivers, subbasin area (in square miles),
C     number of rainfall events, and number of raingages within subbasin.
C
      READ(11,*) IOPTI, WATER, BASAR, INUM, IR
C
C     Read minimum soil moisture content for subbasin
C
      READ(11,*) THMIN
      DELT = 0.250
      RKONST = 3.0*DELT/(1936.0*BASAR)
      QMIN = BASAR/5.0
      QMAX = 20.0*BASAR
      PI = 4.0*ATAN(1.0)
      IPARAM(1) = 0
      FSCALE = 1.0
C
C     Read, for each storm, number of unit values to be read for hydrograph and hyetograph
C
      DO 2  K=1,INUM
        READ(11,*) ND1(K), ND2(K), ND3(K), ND4(K), NR(K), NR1(K), NR2(K)
 2    CONTINUE
C
C     Read QT
C
      DO 10  I=1,INUM
        READ(11,*)
      DO 4  N=1,ND4(I)
        READ(11,*) ITIME, QT(I,N)
C
C     Express initial time as hour plus fraction of hour
C
      IF(N .EQ. 1) THEN
        ISAVE1 = ITIME/100
        ISAVE2 = ITIME - 100*ISAVE1
        TIEMPO(I,1) = FLOAT(ISAVE1) + FLOAT(ISAVE2)/60.0
      ELSE
        TIEMPO(I,N) = TIEMPO(I,N-1) + DELT
      END IF
 4    CONTINUE
C
C     Read total rainfall values from all raingages in the basin for each storm.
C
      DO 8  K=1,IR
        READ(11,*)
      DO 6  N=1,NR(I)
        READ(11,*) ITIME, RAINS(I,N,K)
 6    CONTINUE
 8    CONTINUE
 10   CONTINUE
C
      DO 50  I=1,INUM
C
C     Calculate the first derivative of the discharge hydrograph using cubic splines.
C
      NINTV = ND4(I) - 1
      NDATA = ND4(I)
      DO 12  K=1,ND4(I)
        TIME(K) = TIEMPO(I,K)
        QTR(K) = QT(I,K)
 12   CONTINUE
      CALL CSAKM(NDATA, TIME, QTR, BREAK, CSCOEF)
C
```

```
      DO 14  K=1,ND4(I)
        TVAL = TIME(K)
        DQDT(I,K) = CSDER(1, TVAL, NINTV, BREAK, CSCOEF)
 14   CONTINUE
C
C     Generate data to be used in linear regression:
C     DQDT = B1*QT + B2  where DQDT is computed in cfs/hour.
C
      CORD = 0.100
      NSTOP = ND4(I) - 3
      DO 24  NIND=ND3(I),NSTOP
C
      NOBS = ND4(I) - NIND + 1
      DO 16  K=1,NOBS
        KIND = NIND - 1 + K
        QTR(K) = QT(I,KIND)
        DQDTR(K) = DQDT(I,KIND)
 16   CONTINUE
C
      CALL RLINE(NOBS, QTR, DQDTR, B2, B1, STAT)
C
C     Find hydrograph index representing the beginning of depletion curve
C     and the end of surface runoff contribution: KF.
C     KF is computed by finding the index that minimizes the sum of square errors
C     between the measured discharge hydrograph and the analytically computed
C     depletion curve.
C
      ERR = 5.0E+09
      DO 20  K=NIND,NSTOP
        SUM = 0.0
      DO 18  M=NIND,ND4(I)
        XFIT = (QT(I,K) + B2/B1)*EXP(B1*(TIME(M) - TIME(K))) - B2/B1
        SUM = SUM + (QT(I,M) - XFIT)**2
 18   CONTINUE
      IF(SUM .LT. ERR) THEN
        ERR = SUM
        KNUM = K
      END IF
 20   CONTINUE
C
C     Find correlation coefficient between DQDT and QT.
C
      NOBS = ND4(I) - KNUM + 1
      DO 22  K=1,NOBS
        KIND = KNUM + K - 1
        QTR(K) = QT(I,KIND)
        DQDTR(K) = DQDT(I,KIND)
 22   CONTINUE
      CALL RLINE(NOBS, QTR, DQDTR, B2, B1, STAT)
      IF(ABS(STAT(5)) .GT. CORD) THEN
        CORD = ABS(STAT(5))
        KF = KNUM
      END IF
 24   CONTINUE
C
      WRITE(12,82) ND3(I), ND4(I), KF, CORD
      WRITE(6,82) ND3(I), ND4(I), KF, CORD
      CORR(I) = CORD
      ND3(I) = KF
C
C     Find slope of the falling limb of discharge hydrograph.
C     Find slope of the depletion curve of discharge hydrograph from KF to ND4.
C
      NOBS = ND4(I) - KF + 1
      DO 32  K=1,NOBS
        KIND = KF + K - 1
        QTR(K) = TIME(KIND)
        DQDTR(K) = QT(I,KIND)
 32   CONTINUE
      CALL RLINE(NOBS, QTR, DQDTR, B2, B1, STAT)
      SF = B1
C
      J = 0
```

```
      NEND = ND3(I) - 1
      DO 34  K=ND2(I),NEND
        KP1 = K + 1
        IF(QT(I,K) .GT. QT(I,KP1)) THEN
          J = J + 1
        ELSE IF(QT(I,K) .EQ. QT(I,KP1)) THEN
          J = J + 1
          GO TO 36
        ELSE IF(QT(I,K) .LT. QT(I,KP1)) THEN
          J = J + 1
          GO TO 36
        END IF
 34   CONTINUE
C
C     Do a linear regression on at most 10 points starting from the hydrograph peak.
C
 36   IF(J .GE. 10) THEN
        NOBS = 10
      ELSE
        NOBS = J
      END IF
C
      DO 38  K=1,NOBS
        KIND = ND2(I) + K - 1
        QTR(K) = TIME(KIND)
        DQDTR(K) = QT(I,KIND)
 38   CONTINUE
C
      CALL RLINE(NOBS, QTR, DQDTR, B2, B1, STAT)
      CORF = ABS(STAT(5))
      SP = B1
      WRITE(12,*) 'Falling corr. coefficient = ',CORF
      WRITE(12,*) 'Depletion curve slope = ',SF
      WRITE(12,*) 'Falling curve slope = ',SP
C
C     Compute the components of the base flow BF from indices ND3 to ND1.
C
      BF(I,ND1(I)) = QT(I,ND1(I))
      BF(I,ND2(I)) = QT(I,ND3(I)) + SF*(QT(I,ND2(I)) - QT(I,ND3(I)))/SP
      BF(I,ND3(I)) = QT(I,ND3(I))
      NBEG = ND1(I) + 1
      NEND = ND2(I) - 1
      DO 40  K=NBEG,NEND
        TEMP = (QT(I,K) - QT(I,ND1(I)))/(QT(I,ND2(I)) - QT(I,ND1(I)))
        BF(I,K) = BF(I,ND1(I)) + TEMP*(BF(I,ND2(I)) - BF(I,ND1(I)))
 40   CONTINUE
C
      NBEG = ND2(I) + 1
      NEND = ND3(I) - 1
      DO 42  K=NBEG,NEND
        TEMP = (QT(I,K) - QT(I,ND3(I)))/(QT(I,ND2(I)) - QT(I,ND3(I)))
        BF(I,K) = BF(I,ND3(I)) + TEMP*(BF(I,ND2(I)) - BF(I,ND3(I)))
 42   CONTINUE
C
C     The base flow BF plus the direct runoff QR is the total discharge QT
C
      DO 44  N=1,ND4(I)
      IF((N .LT. ND1(I)) .OR. (N .GT. ND3(I))) THEN
        QR(I,N) = 0.0
        BF(I,N) = QT(I,N)
      ELSE
        QR(I,N) = QT(I,N) - BF(I,N)
      END IF
 44   CONTINUE
C
C     Print QT, QR, and BF values from indices ND3 to ND1 for each rainfall event I.
C
      DO 46  K=ND1(I),ND3(I)
        WRITE(12,84) K, TIME(K), QT(I,K), BF(I,K), QR(I,K)
        IF(BF(I,K) .LT. 0.0) THEN
          WRITE(6,84) K, TIME(K), QT(I,K), BF(I,K), QR(I,K)
        END IF
 46   CONTINUE
```

```
C
C     Compute total direct runoff volume DQ for event I, in inches.
C
      SUM = (QR(I,ND1(I)) + QR(I,ND3(I)))/2.0
      NS = ND1(I) + 1
      NF = ND3(I) - 1
      DO 48  K=NS,NF
      SUM = SUM + QR(I,K)
      IF(QR(I,K) .LT. 0.0) THEN
        WRITE(6,*) 'NEGATIVE QR ENTRIES IN EVENT ',I
        WRITE(12,86) I, K, QR(I,K)
        WRITE(6,86) I, K, QR(I,K)
        QR(I,K) = 0.0
        BF(I,K) = QT(I,K)
      END IF
 48   CONTINUE
C
      DQ(I) = RKONST*SUM
      WRITE(12,*)
C
 50   CONTINUE
C
C     Print warning messages concerning QMAX and QMIN potential violations.
C
      DO 52  K=1,INUM
        QBEG(K) = QT(K,ND1(K))
        IF(QBEG(K) .GE. QMAX) THEN
          WRITE(6,*) 'QT(',K,',',ND1(K),') >= QMAX, QMAX WARNING'
          QBEG(K) = 0.80*QMAX
        ELSE IF(QBEG(K) .LE. QMIN) THEN
          WRITE(6,*) 'QT(',K,ND1(K),') <= QMIN, QMIN WARNING'
          QBEG(K) = 1.20*QMIN
        END IF
 52   CONTINUE
C
C     Set up and read some IMSL-related variables.
C
      DO 54  K=1,7
        XSCALE(K) = 1.0
 54   CONTINUE
C
C     Set initial values for SOIL(I), denoted by XSOIL(I):
C        I = 1  Porosity of the top soil
C        I = 2  Effective porosity of the top soil
C        I = 3  Wetting front soil suction head
C        I = 4  Hydraulic conductivity of the top soil
C
      READ(11,*) XUB(1), XLB(1), XUB(2), XLB(2)
      READ(11,*) XSOIL(1), XSOIL(2), XSOIL(3), XSOIL(4)
      XUB(3) = 7.0
      XLB(3) = 1.0
      XUB(4) = 0.700
      XLB(4) = 0.100
      DECIDE = .FALSE.
C
C     Call optimization SUBROUTINE BCONF to compute GA infiltration parameters
C
      CALL BCONF(SVALGA, INUM, XSOIL, 0, XLB, XUB, XSCALE, FSCALE,
     *               IPARAM, RPARAM, SOIL, FVALUE)
C
C     Print excess rainfall and direct runoff values for the optimal
C     GA infiltration parameters.
C
      DECIDE = .TRUE.
      CALL SVALGA(INUM, SOIL, FLS)
C
      WRITE(12,88)
      WRITE(6,88)
      SUM = 0.0
      DO 56  I=1,INUM
        TMP1 = (QBEG(I) - QMIN)/(QMAX - QMIN)
        THETA(I) = THMIN*((THMAX/THMIN)**TMP1)
        WRITE(6,90) DQ(I), ERC(I), CORR(I)
```

```
        WRITE(12,90) DQ(I), ERC(I), CORR(I)
        SUM = SUM + ABS(DQ(I) - ERC(I))
 56   CONTINUE
      ERRMIN = SUM
      CONV = 100.0/39.370
      WRITE(12,92) SOIL(1), SOIL(2), SOIL(3), SOIL(4), ERRMIN
      WRITE(6,92) SOIL(1), SOIL(2), SOIL(3), SOIL(4), ERRMIN
      WRITE(6,93) CONV*SOIL(3), CONV*SOIL(4)
      WRITE(6,94) (THETA(I), I=1,INUM)
      WRITE(12,94) (THETA(I), I=1,INUM)
C
 82   FORMAT(' Interval: (',I3,',',I3,'), runoff ended at: ',I3,
     *       '  and corr. coeff: ',F7.4)
 84   FORMAT(I3,2X,F6.2,3(2X,F7.1))
 86   FORMAT(' QR(',I3,',',I3,') = ',F10.2)
 88   FORMAT(/' Q_runoff  Excess rain    Corr_coeff ',/
     *        '     (in.)      (in.) ')
 90   FORMAT(2X,F8.4,2X,F8.4,5X,F6.4)
 92   FORMAT('  Soil(1)= ',F6.3,'  Soil(2)= ',F6.3,'  Soil(3)= ',F6.3,
     *       '  Soil(4)= ',F6.3,/,'  Sum of Errors = ',F7.4)
 93   FORMAT('                                    Soil(3)= ',F6.3,
     *       '  Soil(4)= ',F6.3)
 94   FORMAT(' Initial soil water contents per event:',8(2X,F5.3))
      STOP
      END
C
      SUBROUTINE SVALGA(INUM, SOIL, FLS)
C
C     Main variables used:
C
C     FC            Vector with cumulative infiltration unit values
C     FR            Vector with infiltration rate unit values
C     Other variables are listed at the beginning of the program.
C
      PARAMETER (INUME=6, NDM=200, NRM=192)
      REAL SOIL(4), DQ(INUME), QBEG(INUME), RAINS(INUME,NRM,12)
      REAL ERS(INUME,NRM)
      REAL RAIN(INUME,NRM), HIN(INUME,NRM), ER(INUME,NRM), ERC(INUME)
      INTEGER NR(INUME), NR1(INUME), NR2(INUME)
C
      COMMON /SUELO/ DELT, THMAX, THMIN
      COMMON /TOTAL/ RAINS
      COMMON /GOTAS/ RAIN, HIN, ER, WATER, DQ, QBEG, QMAX, QMIN
      COMMON /IRANG/ NR, NR1, NR2
      COMMON /NUMST/ IR, ERC
C
      DO 4  I=1,INUM
        ERC(I) = 0.0
        DO 2  N=1,NR(I)
          ERS(I,N) = 0.0
 2      CONTINUE
 4    CONTINUE
C
      DO 14  K=1,IR
        DO 8  I=1,INUM
          DO 6  N=1,NR(I)
            RAIN(I,N) = RAINS(I,N,K)
 6        CONTINUE
 8      CONTINUE
        CALL VALGA(INUM, SOIL)
        DO 12  I=1,INUM
          DO 10  N=1,NR(I)
            ERS(I,N) = ERS(I,N) + ER(I,N)/FLOAT(IR)
 10       CONTINUE
 12     CONTINUE
 14   CONTINUE
C
      DO 18  I=1,INUM
        DO 16  N=NR1(I),NR2(I)
          ERC(I) = ERC(I) + ERS(I,N)
 16     CONTINUE
 18   CONTINUE
C
```

```
      FLS = 0.0
      DO 20  I=1,INUM
        FLS = FLS + ABS(DQ(I) - ERC(I))
 20   CONTINUE
C
      DO 24  I=1,INUM
        DO 22  N=1,NR(I)
          RAIN(I,N) = 0.0
 22     CONTINUE
 24   CONTINUE
C
      DO 30  K=1,IR
        DO 28  I=1,INUM
          DO 26  N=1,NR(I)
            RAIN(I,N) = RAIN(I,N) + RAINS(I,N,K)/FLOAT(IR)
 26       CONTINUE
 28     CONTINUE
 30   CONTINUE
C
      DO 34  I=1,INUM
        DO 32  N=1,NR(I)
          HIN(I,N) = RAIN(I,N) - ERS(I,N)
 32     CONTINUE
 34   CONTINUE
C
      RETURN
      END
C
      SUBROUTINE VALGA(INUM, SOIL)
      PARAMETER (INUME=6, NDM=200, NRM=192)
      REAL RC(NRM), RI(NRM), FR(NRM), FC(NRM), DTHETA(INUME)
      REAL THETA(INUME), SOIL(4), DQ(INUME), QBEG(INUME)
      REAL RAIN(INUME,NRM), HIN(INUME,NRM), ER(INUME,NRM)
      INTEGER NR(INUME), NR1(INUME), NR2(INUME)
      LOGICAL DECIDE
C
      COMMON /SUELO/ DELT, THMAX, THMIN
      COMMON /GOTAS/ RAIN, HIN, ER, WATER, DQ, QBEG, QMAX, QMIN
      COMMON /IRANG/ NR, NR1, NR2
      COMMON /RITE/ DECIDE
C
C     Compute moisture content for each event
C
      THMAX = SOIL(2) - 0.010
      DO 2   I=1,INUM
      TMP1 = (QBEG(I) - QMIN)/(QMAX - QMIN)
      THETA(I) = THMIN*((THMAX/THMIN)**TMP1)
 2    CONTINUE
C
      DO 40  I=1,INUM
      IF(DECIDE) THEN
        WRITE(12,100) I
        WRITE(12,102)
      END IF
C
      CHECK = SOIL(1) - SOIL(2)
      SE = (THETA(I) - CHECK)/SOIL(2)
      DTHETA(I) = (1.0 - SE)*SOIL(2)
C
      IF(RAIN(I,1) .EQ. 0.0) THEN
        FC(1) = 0.0
        RI(1) = 0.0
        RC(1) = 0.0
        FR(1) = SOIL(4)*(SOIL(3)*DTHETA(I)/0.010 + 1.0)
      ELSE
        RI(1) = RAIN(I,2)/DELT
        RC(1) = RAIN(I,1)
        FCP = RAIN(I,1)
C
C     Calculate tentative infiltration rate
C
        FRP = SOIL(4)*(SOIL(3)*DTHETA(I)/FCP + 1.0)
        IF(FRP .GT. RI(1)) THEN
```

```
          FC(1) = FCP
          FR(1) = FRP
        ELSE
          FCP = SOIL(4)*SOIL(3)*DTHETA(I)/(RI(1) - SOIL(4))
          DTP = FCP/RI(1)
          DT = DELT - DTP
C
C     Compute FC(1)
C
          FOLD = FCP
 6        RNUM = FOLD + SOIL(3)*DTHETA(I)
          DENO = FCP + SOIL(3)*DTHETA(I)
          FUNC = FCP + SOIL(3)*DTHETA(I)*ALOG(RNUM/DENO) +
     *           SOIL(4)*DT - FOLD
          FPRI = -FOLD/RNUM
          FNEW = FOLD - FUNC/FPRI
          IF(ABS(FNEW-FOLD) .GT. 0.001) THEN
            FOLD = FNEW
            GO TO 6
          ELSE
            FC(1) = FNEW
            FR(1) = SOIL(4)*(SOIL(3)*DTHETA(I)/FC(1) + 1.0)
          END IF
        END IF
      END IF
C
      ER(I,1) = RC(1) - FC(1)
      IF((ER(I,1) .EQ. 0.0) .AND. (RAIN(I,1) .GT. 0.0)) THEN
        ER(I,1) = RAIN(I,1)*WATER
      END IF
C
C     Compute infiltration loss from RAIN and ER
C
      JJ = 0
      HIN(I,1) = RAIN(I,1) - ER(I,1)
      IF(ER(I,1) .NE. 0.0) THEN
        JJ = JJ + 1
      END IF
C
      SUM = ER(I,1)
      IF(DECIDE) THEN
        IF(NR1(I) .EQ. 1) THEN
          TIM = DELT
          WRITE(12,104) TIM, RC(1), RI(1), FC(1)
        END IF
      END IF
C
C     Calculate excess rainfall for remaining time INTERVALS
C
      DO 34  N=2,NR(I)
      RC(N) = RC(N-1) + RAIN(I,N)
      IF(N .LT. NR(I)) THEN
        RI(N) = RAIN(I,N+1)/DELT
      END IF
C
      IF((RAIN(I,N) .EQ. 0.0) .AND. (FC(N-1) .EQ. 0.0)) THEN
        FC(N) = 0.0
        FR(N) = SOIL(4)*(SOIL(3)*DTHETA(I)/0.010 + 1.0)
      ELSE IF((RAIN(I,N) .GT. 0.0) .AND. (FC(N-1) .EQ. 0.0)) THEN
        FCP = RAIN(I,N)
        FRP = SOIL(4)*(SOIL(3)*DTHETA(I)/FCP + 1.0)
        IF(FRP .GT. RI(N-1)) THEN
          FC(N) = FCP
          FR(N) = FRP
        ELSE IF(FRP .LE. RI(N-1)) THEN
          FCP = SOIL(4)*SOIL(3)*DTHETA(I)/(RI(N-1) - SOIL(4))
          DTP = FCP/RI(N-1)
          DT = DELT - DTP
C
C     Compute FC(N) from nonlinear Green-Ampt equation
C
          FOLD = FCP
 12       RNUM = FOLD + SOIL(3)*DTHETA(I)
```

```
            DENO = FCP + SOIL(3)*DTHETA(I)
            FUNC = FCP + SOIL(3)*DTHETA(I)*ALOG(RNUM/DENO) +
     *           SOIL(4)*DT - FOLD
            FPRI = -FOLD/RNUM
            FNEW = FOLD - FUNC/FPRI
            IF(ABS(FNEW-FOLD) .GT. 0.001) THEN
              FOLD = FNEW
              GO TO 12
            ELSE
              FC(N) = FNEW
              FR(N) = SOIL(4)*(SOIL(3)*DTHETA(I)/FC(N) + 1.0)
            END IF
          END IF
        ELSE IF(FC(N-1) .GT. 0.0) THEN
          IF(FR(N-1) .GT. RI(N-1)) THEN
C
C     Compute fcprime and compare resulting frprime with RI(N-1)
C
            FCP = FC(N-1) + RI(N-1)*DELT
            FRP = SOIL(4)*(SOIL(3)*DTHETA(I)/FCP + 1.0)
            IF(FRP .GT. RI(N-1)) THEN
              FC(N) = FCP
              FR(N) = FRP
            ELSE
              FCP = SOIL(4)*SOIL(3)*DTHETA(I)/(RI(N-1) - SOIL(4))
              DTP = (FCP - FC(N-1))/RI(N-1)
              DT = DELT - DTP
C
C     Compute FC(N) from cumulative infiltration equation using Newton's method.
C
              FOLD = FCP
 30           RNUM = FOLD + SOIL(3)*DTHETA(I)
              DENO = FCP + SOIL(3)*DTHETA(I)
              FUNC = FCP + SOIL(3)*DTHETA(I)*ALOG(RNUM/DENO) +
     *             SOIL(4)*DT - FOLD
              FPRI = -FOLD/RNUM
              FNEW = FOLD - FUNC/FPRI
              IF(ABS(FNEW-FOLD) .GT. 0.001) THEN
                FOLD = FNEW
                GO TO 30
              ELSE
                FC(N) = FNEW
                FR(N) = SOIL(4)*(SOIL(3)*DTHETA(I)/FC(N) + 1.0)
              END IF
            END IF
          ELSE
            FOLD = FC(N-1) + 0.10
 32         RNUM = FOLD + SOIL(3)*DTHETA(I)
            DENO = FC(N-1) + SOIL(3)*DTHETA(I)
            FUNC = FC(N-1) + SOIL(3)*DTHETA(I)*ALOG(RNUM/DENO) +
     *           SOIL(4)*DELT - FOLD
            FPRI = -FOLD/RNUM
            FNEW = FOLD - FUNC/FPRI
            IF(ABS(FNEW-FOLD) .GT. 0.001) THEN
              FOLD = FNEW
              GO TO 32
            ELSE
              FC(N) = FNEW
              FR(N) = SOIL(4)*(SOIL(3)*DTHETA(I)/FC(N) + 1.0)
            END IF
          END IF
        END IF
C
        ER(I,N) = RC(N) - FC(N) - (RC(N-1) - FC(N-1))
        IF((ER(I,N) .EQ. 0.0) .AND. (RAIN(I,N) .GT. 0.0)) THEN
          ER(I,N) = RAIN(I,N)*WATER
        END IF
C
C     Compute infiltration loss from excess rainfall and total rainfall
C
        HIN(I,N) = RAIN(I,N) - ER(I,N)
C               .
        SUM = SUM + ER(I,N)
```

```
      FC(N) = RC(N) - SUM
      IF(DECIDE) THEN
        IF((N .GE. NR1(I)) .AND. (N .LE. NR2(I))) THEN
          TM = DELT*FLOAT(N)
          WRITE(12,106) TM,RAIN(I,N),RC(N),RI(N),FR(N),FC(N),SUM,ER(I,N)
        END IF
      END IF
 34   CONTINUE
C
 40   CONTINUE
C
 100  FORMAT(/' RAINFALL EVENT NUMBER ',I2,/)
 102  FORMAT('           RAINFALL              INFILTRATION     EXCESS',
     *' RAINFALL',/,
     *       '-------------------------------------------------------',
     *'---------',/,
     *       'TIME   INCR.   CUMU.  INTEN.    RATE     CUMU.    CUMU. ',
     *'  INCR.  ',/,
     *       '(MIN)   (IN)   (IN)  (IN/HR)   (IN/HR)    (IN)    (IN)  ',
     *'  (IN)   ',/,
     *       '-------------------------------------------------------',
     *'---------')
 104  FORMAT(F6.2,1X,5X,2X,F5.2,1X,F6.4,5X,5X,3X,F6.4)
 106  FORMAT(F6.2,1X,F5.2,2X,F5.2,2X,F5.2,3X,F7.4,3X,F6.4,3X,F6.4,3X,
     *F7.4)
C
      RETURN
      END
```

APPENDIX 3. FORTRAN Program Geomorphic.f

```
C
C     Program geomorphic.f computes the estimated direct runoff hydrograph
C     for each independent subbasins (upstream boundary conditions for HYDRAUX)
C     using the Geomorphic Unit Hydrograph technique explained in a subsection
C     of section WATERSHED MODELING.
C
C     Main variables used in the program:
C
C     AREA          Vector of NORDR components with total catchment areas of streams
C     BASAR         Total subbasin area in square miles
C     DELT          Time step discretization, set to 0.25 hour
C     ERSUM         Variable used to compute average excess rainfall unit values over subbasin
C     GUH           Vector of NSTP components with geomorphic unit hydrograph ordinates
C     ICNT          Vector of NUMSTR entries with number of available rainfall unit values
C     IND           Number of nonzero runoff pulses due to INR excess rainfall intervals
C     INDEX         Index of starting position of each individual rainfall burst
C     INDR          Number of rainfall bursts within each event
C     INR           Number of nonzero excess rainfall intervals in each rainfall burst
C     MVAL          Number of nonzero GUH ordinates, variable M in equation 12
C     NORDR         Order of subbasin
C     NR1           Time index indicating beginning of simulation period
C     NR2           Time index indicating end of simulation period
C     NRF           Time index indicating last rainfall unit value available
C     NSTP          Number of unit values in the hydrograph
C     NUM           Vector of NORDR components with number of streams per order
C     NUMSTR        Number of raingages within subbasin
C     QBASE         Base flow estimate for subbasin when streamgage is not operational
C     QE            Estimated discharge hydrograph unit values
C     QSAVE         Observed discharge hydrograph unit values
C     RAINS         Variable used to compute average rainfall unit values over subbasin
C     RKONST        Conversion factor needed to express GUH in cfs/hr units
C     RSTR          Matrix containing all raingage data for each one of the NUMSTR stations
C     SPEED         Streamflow velocity unit value estimated from equation 13 of paper
C     TIMES         Time equal to one unit value less than beginning of rainfall
C     TIMEF         Time when discharge estimation ends, in hr.
C     VEL           Geometric mean streamflow velocity value
C     XONE          Variable to evaluate sum of GUH ordinates times RKONST
C
C     Variables already defined in Appendix 2 are:
C     RAIN, HIN, ER, SOIL
C
C     Variables used in SUBROUTINE GEOMOR:
C     AREA, DELT, GUH, NORDR, NSTP, NUM, P, PHI
C     RKONST, RLA, RLAVE, SA, SD, OMEGA, VAL
C
      PARAMETER (NSTP=100, NDM=250, NORMAX=10, NPO=1024, NMAX=50)
C
      REAL RAIN(NDM), HIN(NDM), ER(NDM), ERSUM(NDM), RAINS(NDM)
      REAL AREA(NORMAX), RLAVE(NORMAX), RSTR(NMAX,NDM), SOIL(4)
      REAL SPEED(NDM), XONE(NMAX), QSAVE(NDM), QE(NDM), GUH(NSTP)
      INTEGER NUM(NORMAX), INR(NMAX), IND(NMAX), INDEX(NMAX)
      INTEGER ICNT(NMAX)
      CHARACTER*24 STQ, STR
      CHARACTER*72 NAME
      LOGICAL FLAG
C
C     Declare COMMON statements to be used in SUBROUTINES GEOMOR and VALGA
C
      COMMON /NPROB/ NORDR
      COMMON /SPACE/ AREA, RLAVE, GUH
      COMMON /RAPID/ DELT, RKONST, XUNIT, VEL
      COMMON /SUELO/ THMAX, THMIN
      COMMON /GOTAS/ RAIN, HIN, ER, WATER, QBEG, QMAX, QMIN
      COMMON /IRANG/ NR
C
C     Open times file to read simulation time
C
      OPEN(10,FILE='/hydraux/DATA/times',STATUS='OLD')
      READ(10,*) TIMES, TIMEF
      NR1 = INT(3600.0*TIMES)/900
      NR2 = INT(3600.0*TIMEF)/900
```

```
      NRF = NR2 - 24
      ITOT = NR2 - NR1 + 1
C
C     Conversion factors from meters to feet and from inches to cm
C
      CONV = 39.370/12.0
      CONVIN = 100.0/39.370
C
C     Open file containing geomorphic parameters
C
      OPEN(11,FILE='/hydraux/DATA/geomorphic.parguh',STATUS='OLD')
C
C     Read geomorphic data
C
      READ(11,80) NAME
      WRITE(6,82) NAME
      READ(11,106) STQ
      READ(11,*) NUMSTR
      IUNIT = 11
      DO 2  I=1,NUMSTR
        READ(11,106) STR
        IUNIT = IUNIT + 1
        OPEN(IUNIT,FILE=STR,STATUS='OLD')
 2    CONTINUE
      READ(11,*) NORDR
      READ(11,84) (RLAVE(K), K=1,NORDR)
      READ(11,84) (AREA(K), K=1,NORDR)
      READ(11,*) (NUM(K), K=1,NORDR)
      READ(11,*) WATER, THMIN, (SOIL(K), K=1,4)
C
C     Determine total basin area BASAR, in square miles from vector AREA
C     Determine average length of streams of the same order
C
      BASAR = 0.0
      DO 4  I=1,NORDR
        BASAR = BASAR + AREA(I)
        RLAVE(I) = RLAVE(I)/FLOAT(NUM(I))
 4    CONTINUE
      BASAR = BASAR*CONV*CONV/(5280.0*5280.0)
C
C     Determine total stream channel length and read slope and
C     intercept to be used in equation 13 of paper
C
      DELT = 0.250
      READ(11,*) NINT
      XLEN = 0.0
      DO 6  I=1,NINT
        READ(11,*) XINT, DUMMY
        XINT = CONV*XINT
        XLEN = XLEN + XINT
 6    CONTINUE
      READ(11,*) IDUMY1, RINTER, SLOPE, DUMY2
C
C     If measured discharge hydrograph is available, read discharge unit values
C     else estimate QSAVE at hydrograph index NR1
C
      ICNTQ = 0
      INQUIRE(FILE=STQ,EXIST=FLAG)
      IF(FLAG) THEN
        OPEN(29,FILE=STQ,STATUS='OLD')
        DO 10  I=1,NDM
          READ(29,*,END=12) ITIME, QSAVE(I)
          ICNTQ = I
 10     CONTINUE
      ELSE
        QSAVE(NR1) = BASAR/5.0
        ICNTQ = 0
      END IF
 12   QBEG = QSAVE(NR1)
C
C     Set maximum and minimum discharge values used to compute
C     initial soil moisture content
C
```

```
      QMIN = BASAR/5.0
      QMAX = 20.0*BASAR
      IF(QBEG .GE. QMAX) THEN
        QBEG = 0.80*QMAX
      ELSE IF(QBEG .LE. QMIN) THEN
        QBEG = 1.20*QMIN
      END IF
C
C     Read rainfall data for all NUMSTR stations
C
      IUNIT = 11
      DO 16  I=1,NUMSTR
        IUNIT = IUNIT + 1
        DO 14  N=1,NDM
          READ(IUNIT,*,END=16) ITIME, RSTR(I,N)
          ICNT(I) = N
 14     CONTINUE
 16   CONTINUE
C
C     Calculate average rainfall unit values from available data.
C     Estimate initial soil moisture content from empirical equation 27 in paper
C     Then call Green-Ampt infiltration subroutine.
C
      DO 18  I=1,NDM
        ERSUM(I) = 0.0
        RAINS(I) = 0.0
 18   CONTINUE
C
      DO 24  J=1,NUMSTR
        DO 20  I=1,ICNT(J)
          RAIN(I) = RSTR(J,I)
 20     CONTINUE
        NR = ICNT(J)
        CALL VALGA(SOIL)
        DO 22  I=1,ICNT(J)
          ERSUM(I) = ERSUM(I) + ER(I)
          RAINS(I) = RAINS(I) + RAIN(I)
 22     CONTINUE
 24   CONTINUE
C
C     NR  is the minimum number of rainfall unit values available from all data sets
C     NRM is the maximum number of rainfall unit values available from all data sets
C
      NR = ICNT(1)
      NRM = ICNT(1)
      DO 26  I=1,NUMSTR
        IF(ICNT(I) .LE. NR) THEN
          NR = ICNT(I)
        END IF
        IF(ICNT(I) .GE. NRM) THEN
          NRM = ICNT(I)
        END IF
 26   CONTINUE
C
      DO 28  I=1,NR
        ER(I) = ERSUM(I)/FLOAT(NUMSTR)
        RAIN(I) = RAINS(I)/FLOAT(NUMSTR)
        HIN(I) = RAIN(I) - ER(I)
 28   CONTINUE
C
      IF(NRM .GT. NR) THEN
        NRP = NR + 1
        DO 32  I=NRP,NRM
          ISUM = 0
          DO 30  J=1,NUMSTR
            IF(ICNT(J) .GE. I) THEN
              ISUM = ISUM + 1
            END IF
 30       CONTINUE
          ER(I) = ERSUM(I)/FLOAT(ISUM)
          RAIN(I) = RAINS(I)/FLOAT(ISUM)
          HIN(I) = RAIN(I) - ER(I)
 32     CONTINUE
```

```
        NR = NRM
      END IF
C
      IF(NRM .LT. NRF) THEN
        NRMP = NRM + 1
        DO 34  I=NRMP,NRF
          RAIN(I) = 0.0
          HIN(I) = 0.0
          ER(I) = 0.0
 34     CONTINUE
        NR = NRF
      END IF
C
C     Discretize the total stream channel length in uniform DX intervals.
C
      DX = XLEN/FLOAT(NPO)
C
C     Open rainfall, infiltration, measured discharge, and GUH files.
C
      OPEN(30,FILE='/hydraux/DATA/geomorphic.out',STATUS='UNKNOWN')
      OPEN(31,FILE='/hydraux/DATA/geomorphic.guh',STATUS='UNKNOWN')
C
C     Determine the indices of the beginning and end of each rainfall burst
C     occurring between indices NR1 and NRF
C
      INDR = 1
      J = NR1
      ICOUNT = 0
      DO WHILE (J .LE. NRF)
        IF(RAIN(J) .GT. 0.0) THEN
          INDEX(INDR) = J
          DO WHILE (((ER(J) .GE. 0.010) .AND. (J .LE. NRF)) .OR.
     *              (ICOUNT .LT. 3))
            ICOUNT = ICOUNT + 1
            J = J + 1
          END DO
          INR(INDR) = ICOUNT
          ICOUNT = 0
          INDR = INDR + 1
        ELSE
          J = J + 1
        END IF
      END DO
      IF(INR(INDR) .EQ. 0) THEN
        INDR = INDR - 1
      END IF
C     WRITE(6,108) INDR
C     WRITE(6,108) (INR(K), K=1,INDR)
C     WRITE(6,108) (INDEX(K), K=1,INDR), INDEX(INDR+1)
      WRITE(30,108) INDR
      WRITE(30,108) (INR(K), K=1,INDR)
      WRITE(30,108) (INDEX(K), K=1,INDR), INDEX(INDR+1)
C
C     Re-group excess rainfall bursts in sets greater or equal to 2
C     Excess rainfall values smaller than 0.01 inch are considered to be zero
C     Write re-grouped excess rainfall bursts
C
      K = 0
 36   K = K + 1
      IF(K .LE. INDR) THEN
        ISTAR = INDEX(K)
        IEND = INDEX(K) + INR(K) - 1
        ISUM = 0
        DO 38  I=ISTAR,IEND
          IF(ER(I) .GE. 0.010) THEN
            ISUM = ISUM + 1
          END IF
 38     CONTINUE
        IF(ISUM .LE. 1) THEN
          IF(K .EQ. 1) THEN
            INR(1) = INR(2) + INDEX(2) - INDEX(1)
            IEND = INDR - 1
            INDR = INDR - 1
```

```
            K = K - 1
            DO 40  I=2, IEND
              INR(I) = INR(I+1)
              INDEX(I) = INDEX(I+1)
 40         CONTINUE
          ELSE
            INR(K-1) = INR(K) + INDEX(K) - INDEX(K-1)
            IEND = INDR - 1
            INDR = INDR - 1
            DO 42  I=K, IEND
              INR(I) = INR(I+1)
              INDEX(I) = INDEX(I+1)
 42         CONTINUE
            K = K - 1
          END IF
        END IF
        GO TO 36
      END IF
      INDEX(INDR+1) = INDEX(INDR) + INR(INDR) - 1
      WRITE(6,108) INDR
      WRITE(6,108) (INR(K), K=1,INDR)
      WRITE(6,108) (INDEX(K), K=1,INDR), INDEX(INDR+1)
      WRITE(30,108) INDR
      WRITE(30,108) (INR(K), K=1,INDR)
      WRITE(30,108) (INDEX(K), K=1,INDR), INDEX(INDR+1)
      WRITE(30,80) NAME
C
C     Define conversion factor RKONST
C
      RKONST = 12.0*DELT*3600.0/(5280.0*5280.0*BASAR)
C
C     Compute total excess rainfall from index NR1 to index NRF
C
      SUM = 0.0
      DO 44  J=NR1,NRF
        SUM = SUM + ER(J)
 44   CONTINUE
      ERC = SUM
C
C     Set estimated discharge unit values QE initially to base flow values.
C
      DO 46  N=1,NDM
        QE(N) = QSAVE(NR1)
 46   CONTINUE
C
C     QBASE is computed based on average lateral influx under base flow conditions
C
      IF(ICNTQ .GT. 0) THEN
        IF(ICNTQ .GE. NR1) THEN
          TEMP = QSAVE(NR1)
        ELSE
          TEMP = QSAVE(ICNTQ)
        END IF
        ERADD = TEMP/(5280.0*5280.0*BASAR)
        QBASE = ERADD*5280.0*5280.0*BASAR*DX*FLOAT(NPO)/XLEN
      ELSE IF(ICNTQ .EQ. 0) THEN
        ERADD = QSAVE(NR1)/(5280.0*5280.0*BASAR)
        QBASE = ERADD*5280.0*5280.0*BASAR*DX*FLOAT(NPO)/XLEN
      END IF
C
C     Compute the geometric mean streamflow velocity for each one of the
C     INDR excess rainfall bursts
C
      DO 74  I=1,INDR
C
      I1 = INDEX(I)
      I2 = INDEX(I) + INR(I) - 1
C
C     Compute SPEED(NR1) to SPEED(NR).
C
      DO 56  J=I1,I2
        SQI = ER(J)/(12.0*DELT*3600.0) + ERADD
        QNTRY = SQI*BASAR*5280.0*5280.0
```

```
C
C     Linear regression was done between discharge Q and velocity v:
C     ln v = SLOPE * ln Q + RINTER
C     and values for RINTER and SLOPE were read earlier.
C     Given values Q, SLOPE, and RINTER, v is computed from
C     v = e^{SLOPE * ln Q + RINTER}
C
        SPEED(J) = EXP(SLOPE*ALOG(QNTRY) + RINTER)
 56   CONTINUE
C
      VEL = 1.0
      ISUM = 0
      DO 58  J=I1,I2
        IF(ER(J) .GE. 0.010) THEN
          VEL = VEL*SPEED(J)
          ISUM = ISUM + 1
        END IF
 58   CONTINUE
      IF(ISUM .NE. 0) THEN
        VEL = VEL**(1.0/FLOAT(ISUM))
      ELSE
        ERMAX = 0.0
        IMAX = 0
        DO 60  J=I1,I2
          IF(ER(J) .GE. ERMAX) THEN
            ERMAX = ER(J)
            IMAX = J
          END IF
 60     CONTINUE
        VEL = SPEED(IMAX)
      END IF
      WRITE(30,102) VEL/CONV, ISUM
      WRITE(6,102) VEL/CONV, ISUM
C
C     Convert geometric mean streamflow velocity VEL to meters/hr
C     and call GUH subroutine.
C
      VEL = 3600.0*VEL/CONV
      CALL GEOMOR
C
C     Calculate MVAL, the number of "nonzero" GUH ordinates, that is,
C     the number of GUH values that are greater than 0.5
C
      MVAL = 1
      DO 62  N=NSTP,2,-1
        GUH(N) = GUH(N-1)
        IF(GUH(N) .GT. 0.500) THEN
          MVAL = MVAL + 1
        END IF
 62   CONTINUE
      GUH(1) = 0.0
      MVALP = MVAL + 1
      IND(I) = MVAL + INR(I) - 1
C
C     Write computed GUH ordinates to a file
C
      WRITE(30,88)
      DO 64  N=1,NSTP
        TIM = TIMES + DELT*FLOAT(N - 1 + INDEX(I) - NR1)
        WRITE(30,90) TIM, GUH(N)
C       WRITE(6,90) TIM, GUH(N)
 64   CONTINUE
      XONE(I) = XUNIT
C
C     Compute the GUH for each one of the INDR excess rainfall bursts and
C     then superimpose the individual results according to equation 12
C     to obtain the final estimated discharge values QE
C     GUH-estimated unit hydrograph values are computed first for
C     indices from 1 to MVAL, that is, the first sum in equation 12
C
      INDICE = IND(I) - MVAL + 1
      DO 68  N=1,MVAL
        KEND = MIN0(N,INDICE)
```

```
      DO 66   K=1,KEND
        KR = INDEX(I) + K - 1
        NN = INDEX(I) + N - 1
        QE(NN) = QE(NN) + ER(KR)*GUH(N-K+1)
 66   CONTINUE
 68   CONTINUE
C
      IF(I .EQ. INDR) THEN
        NEND = ITOT
      ELSE
        NEND = IND(I)
      END IF
C
C     GUH-estimated unit hydrograph values are computed then for
C     indices greater than MVAL, that is, the second sum in equation 12
C
      DO 72  N=MVALP,NEND
        INDICE = IND(I) - N + 1
        KEND = MIN0(MVAL,INDICE)
      DO 70  K=1,KEND
        KR = INDEX(I) + K - 1 + N - MVAL
        NN = INDEX(I) + N - 1
        QE(NN) = QE(NN) + ER(KR)*GUH(MVAL-K+1)
 70   CONTINUE
 72   CONTINUE
        QBASE = QE(NEND + INDEX(I) - 1)
 74   CONTINUE
C
C     Write total and excess rainfall as well as estimated and measured (if availbale)
C     discharge hydrograph unit values
C
      WRITE(30,94)
      WRITE(30,96)
      DO 75  N=NR1,NRF
        TIM = TIMES + DELT*FLOAT(N - NR1)
        WRITE(30,98) TIM, RAIN(N), HIN(N), QSAVE(N), QE(N)
C       WRITE(6,98) TIM, RAIN(N), HIN(N), QSAVE(N), QE(N)
 75   CONTINUE
      NRFP = NRF + 1
      DO 76  N=NRFP,NR2
        TIM = TIMES + DELT*FLOAT(N - NR1)
        WRITE(30,100) TIM, QSAVE(N), QE(N)
C       WRITE(6,100) TIM, QSAVE(N), QE(N)
 76   CONTINUE
C
C     Compute RMSE values between measured and simulated discharge hydrographs
C     Write total excess rainfall, total direct runoff, and values of XONE
C
      RKONST = 12.0*DELT*3600.0/(5280.0*5280.0*BASAR)
      SUM = 0.0
      RMSE = 0.0
      DO 78  N=NR1,NR2
        TIM = TIMES + DELT*FLOAT(N - NR1)
        WRITE(31,100) TIM, QE(N)
C       WRITE(6,100) TIM, QE(N)
        RMSE = RMSE + (QSAVE(N) - QE(N))**2
        SUM = SUM + QE(N)
 78   CONTINUE
      SUM = SUM - (QE(NR1) + QE(NR2))/2.0
      DQ = SUM*RKONST
      RMSE = SQRT(RMSE/FLOAT(ITOT))
      WRITE(30,104) RMSE
      WRITE(30,92) (XONE(I), I=1,INDR)
      WRITE(30,86) DQ, ERC
C
 80   FORMAT(A72)
 82   FORMAT(1X,A72)
 84   FORMAT(7F11.1)
 86   FORMAT(' ROUT AREA = ',F6.4,' (in) EXC. RAIN = ',F6.4,' (in)')
 88   FORMAT('      Time   GUH Ordinates  ',/,'     (Hrs.)    (Cfs/in)')
 90   FORMAT(5X,F5.2,4X,F9.3)
 92   FORMAT(' Unity constant:  ',7(F8.6,2X))
 94   FORMAT('   Time  Rainfall Infiltration   Observed    Derived')
```

```
 96   FORMAT('    Hr.    In.        In.          Cfs         Cfs  ')
 98   FORMAT(2X,F5.2,2X,F7.4,4X,F7.4,4X,F9.2,2X,F9.2)
 100  FORMAT(2X,F5.2,24X,F9.2,2X,F9.2)
 102  FORMAT(' Mean Vel.: ',F5.3,' m/s and ISUM=',I2)
 104  FORMAT(' RMSE FROM GUH METHOD: ',F7.1,' cfs')
 106  FORMAT(A24)
 108  FORMAT(1X,25(I3,1X))
      STOP
      END
C
      SUBROUTINE GEOMOR
C
C     OMEGA        Vector of NORDR entries with GUH areal coefficients, shown in equation 16
C     P            NORDR by NORDR semi-Markovian transition probability matrix
C     PHI          NORDR by NSTP matrix containing functions on left hand side of equation 21
C     RLA          Vector of NORDR entries with lambda values in equation 21
C     RLAVE        Vector of NORDR entries with average length of streams
C     SA           NORDR by NORDR matrix with script a values shown in equation 19
C     SD           NORDR by NORDR matrix with script d values shown in equation 18
C
      PARAMETER (NSTP=100, NMAX=10, NDM=250)
      REAL SD(NMAX,NMAX), P(NMAX,NMAX), SA(NMAX,NMAX)
      REAL PHI(NMAX,NSTP), AREA(NMAX)
      REAL RLAVE(NMAX), RLA(NMAX), GUH(NSTP), OMEGA(NMAX)
      INTEGER NUM(NMAX)
C
      COMMON /NPROB/ NORDR
      COMMON /SPACE/ AREA, RLAVE, GUH
      COMMON /RAPID/ DELT, RKONST, XUNIT, VEL
C
      NP1 = NORDR + 1
      CONV = 39.370/12.0
C
      SUM = 0.0
      DO 2  K=1,NORDR
        SUM = SUM + AREA(K)
2     CONTINUE
      TAREA = SUM
      DO 4  K=1,NORDR
        OMEGA(K) = AREA(K)/TAREA
4     CONTINUE
C
C     Define matrices P, SA, and SD which are of upper triangular form
C
      DO 8  J=1,NP1
      DO 8  I=1,NP1
      IF(I .EQ. J) THEN
        IF(J .EQ. NP1) THEN
          P(I,J) = 1.0
        ELSE
          P(I,J) = 0.0
        END IF
      ELSE IF(I .GT. J) THEN
        P(I,J) = 0.0
      ELSE IF(I .LT. J) THEN
        IF((I .EQ. NORDR) .AND. (J .EQ. NP1)) THEN
          P(I,J) = 1.0
        ELSE IF((I .LT. NORDR) .AND. (J .EQ. NP1)) THEN
          P(I,J) = 0.0
        ELSE IF(J .LT. NP1) THEN
          IP1 = I + 1
          SUM = 0.0
          DO 6  K=IP1,NORDR
          SUM = SUM + AREA(K)
6         CONTINUE
          P(I,J) = AREA(J)/SUM
        END IF
      END IF
8     CONTINUE
C
      DO 12  J=1,NP1
      DO 10  I=1,NP1
      IF(I .GT. J) THEN
```

```
        SA(I,J) = 0.0
        SD(I,J) = 0.0
      END IF
      IF(J .EQ. NP1) THEN
        SD(I,J) = 1.0
      END IF
      IF(I .EQ. J) THEN
        SA(I,J) = 1.0
        SD(I,J) = 1.0
      END IF
10    CONTINUE
12    CONTINUE
C
      DO 34  K=1,NORDR
        RLA(K) = VEL/RLAVE(K)
34    CONTINUE
C
      DO 52  N=1,NSTP
        TIM = DELT*FLOAT(N)
C
      DO 40  J=2,NORDR
        JM1 = J - 1
      DO 38  I=JM1,1,-1
        SUM = 0.0
        IP1 = I + 1
      DO 36 K=IP1,J
        SUM = SUM + RLA(I)*P(I,K)*SD(K,J)/(RLA(I) - RLA(J))
36    CONTINUE
      SD(I,J) = SUM
38    CONTINUE
40    CONTINUE
C
      DO 46  I=1,NORDR
        IP1 = I + 1
      DO 44  J=IP1,NP1
        SUM = 0.0
        JM1 = J - 1
      DO 42  K=I,JM1
        SUM = SUM - SA(I,K)*SD(K,J)
42    CONTINUE
      SA(I,J) = SUM
44    CONTINUE
46    CONTINUE
C
      DO 50  I=1,NP1
      IF(I .EQ. NP1) THEN
        PHI(I,N) = 1.0
      ELSE IF(I .LT. NP1) THEN
        SUM = 0.0
        DO 48  K=I,NP1
        IF(K .EQ. NP1) THEN
          SUM = SUM + 1.0
        ELSE IF(K .LT. NP1) THEN
          SUM = SUM + SD(I,K)*SA(K,NP1)*EXP(-RLA(K)*TIM)
        END IF
48      CONTINUE
        PHI(I,N) = SUM
      END IF
50    CONTINUE
52    CONTINUE
C
      GUH(1) = 0.00
      DO 54  K=1,NORDR
        GUH(1) = GUH(1) + OMEGA(K)*PHI(K,1)/DELT
54    CONTINUE
      GUH(1) = DELT*GUH(1)/RKONST
      SUM = GUH(1)
C
      DO 58  N=2,NSTP
        GUH(N) = 0.0
      DO 56  K=1,NORDR
        GUH(N) = GUH(N) + OMEGA(K)*(PHI(K,N) - PHI(K,(N-1)))/DELT
56    CONTINUE
```

```
      GUH(N) = DELT*GUH(N)/RKONST
      SUM = SUM + GUH(N)
58    CONTINUE
      XUNIT = RKONST*SUM
C
      RETURN
      END
C
      SUBROUTINE VALGA(SOIL)
C
C     This subroutine is already listed in Appendix 2
C
```

APPENDIX 4. Channel Cross Sections

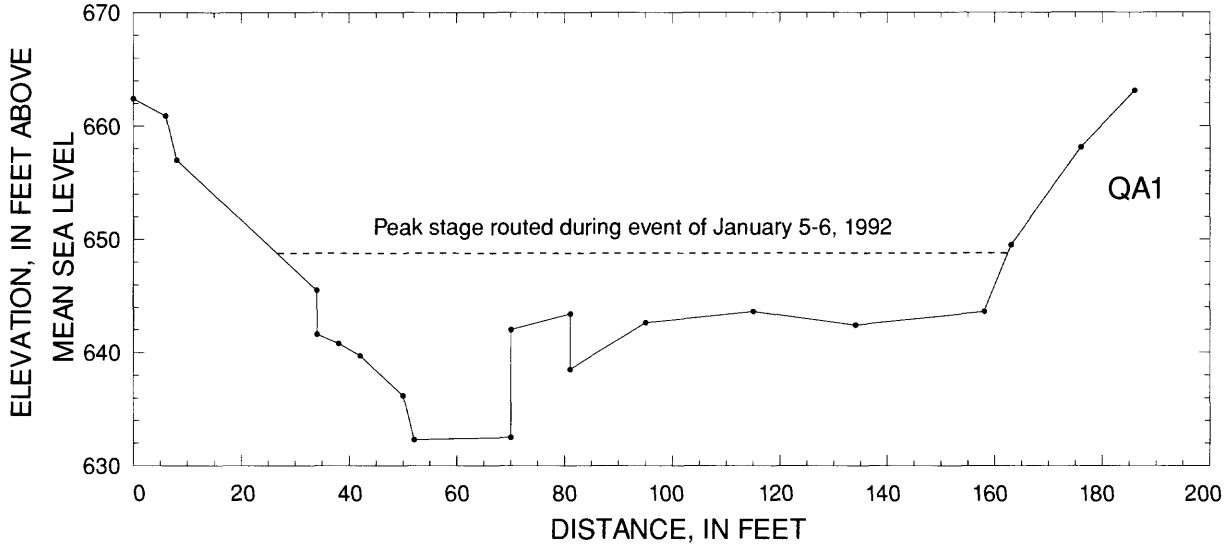

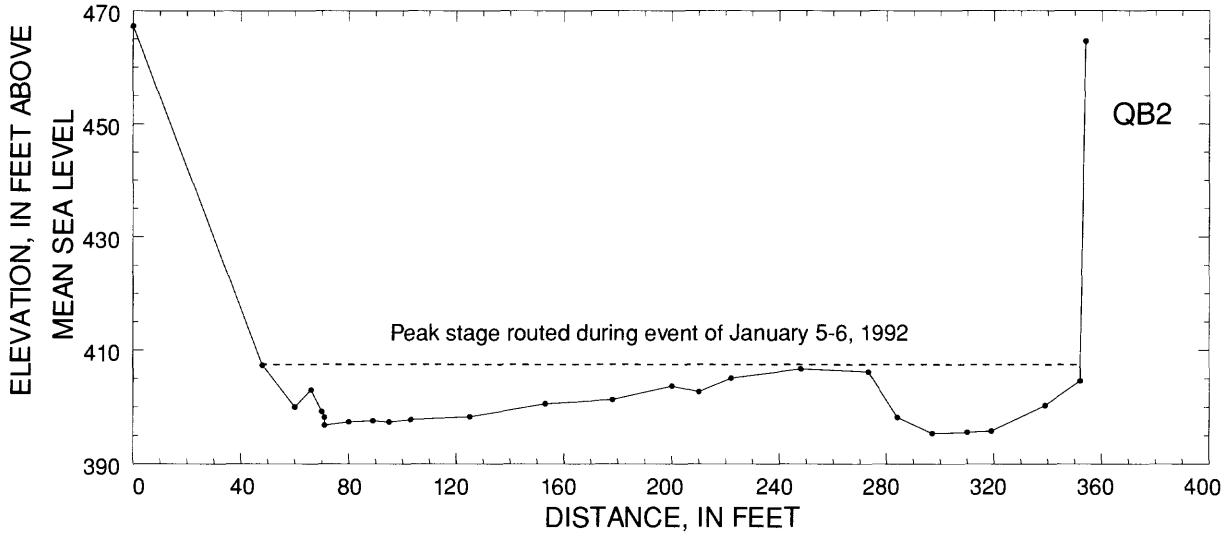

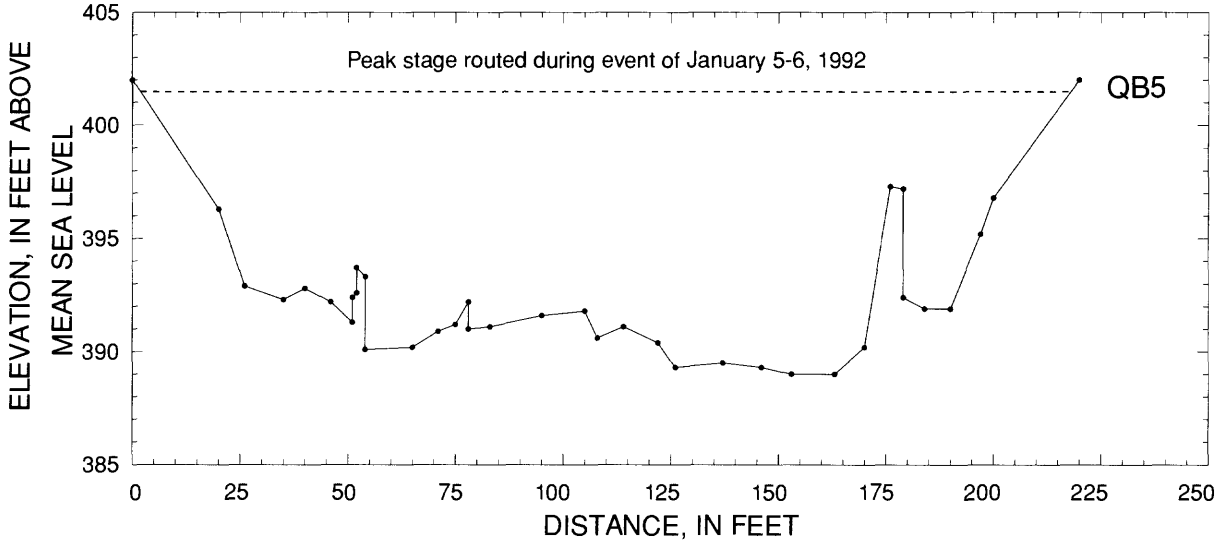

Cross sections QA1, QB2, and QB5

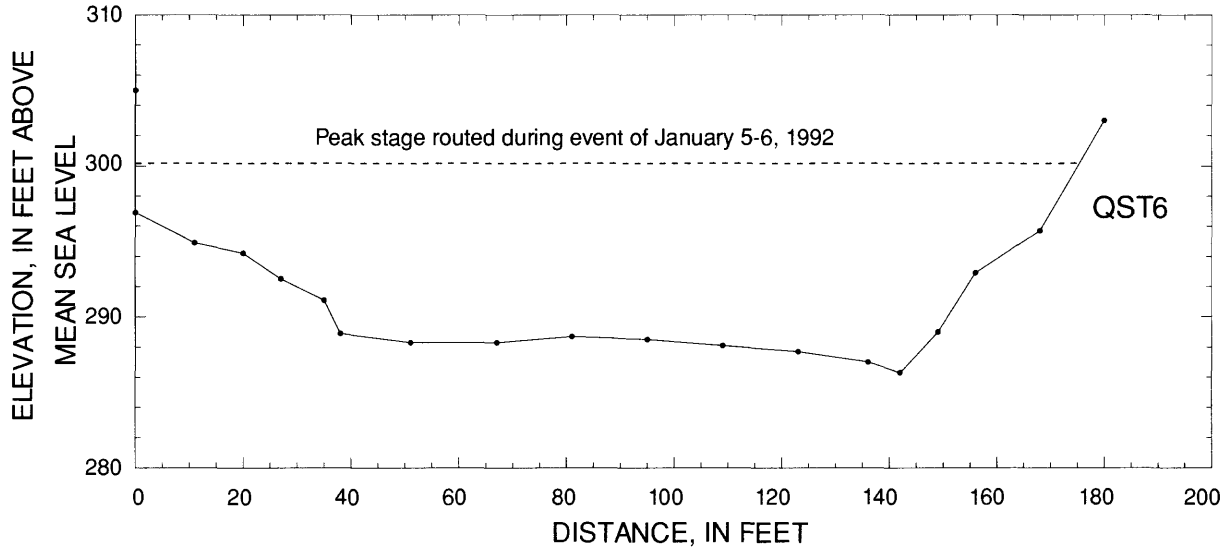

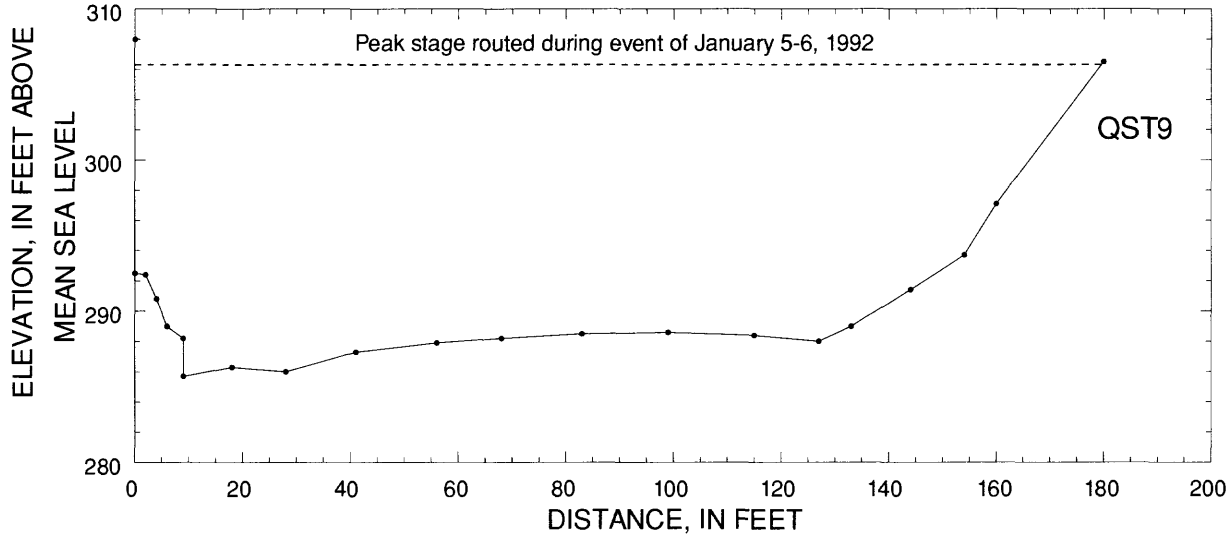

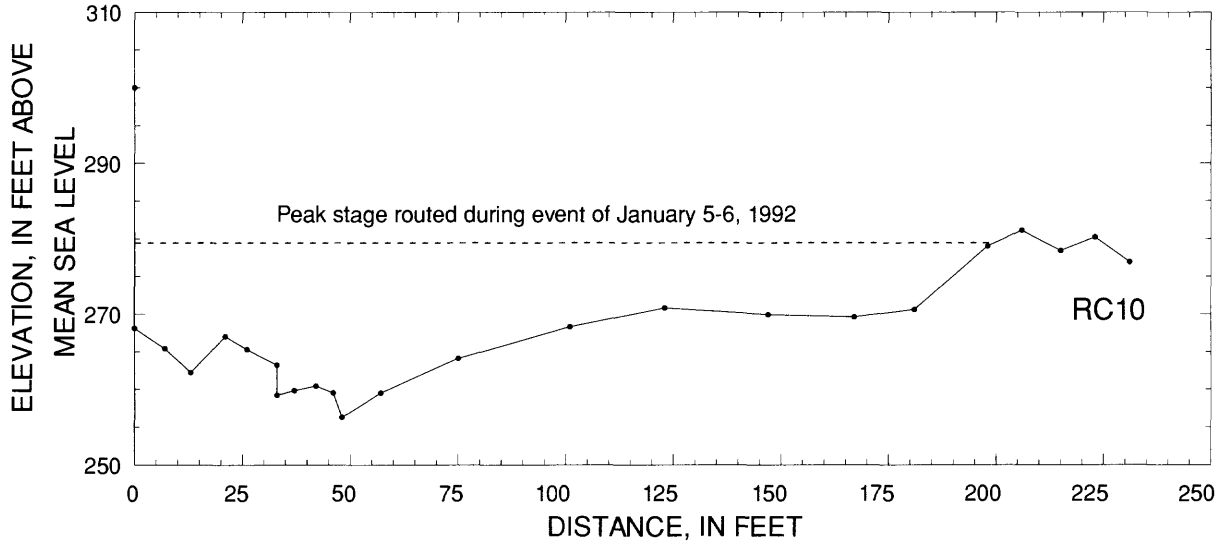

Cross sections QST6, QST9, and RC10

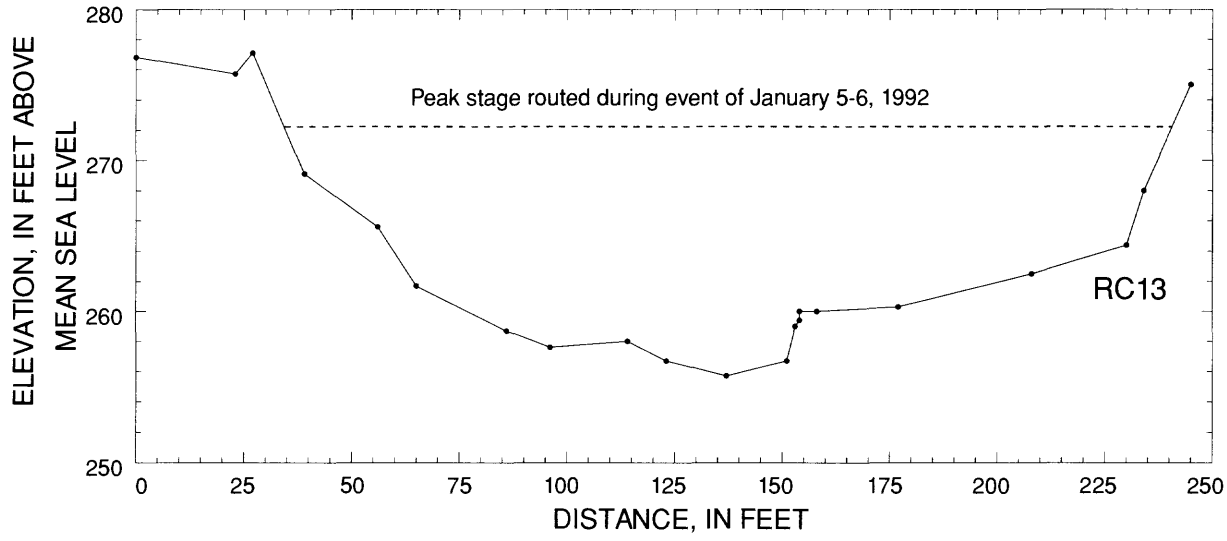

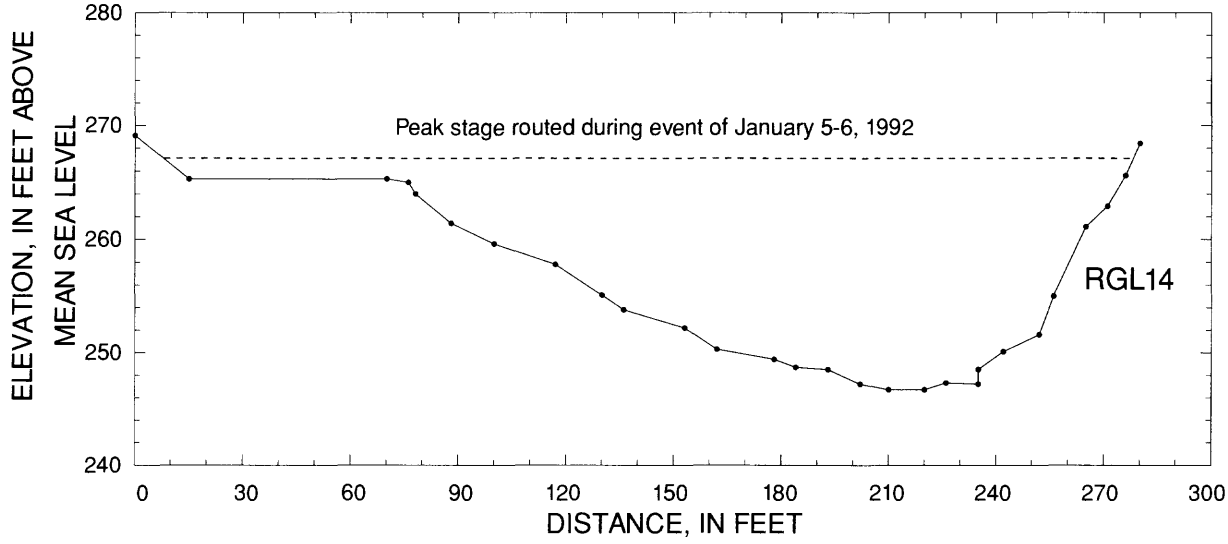

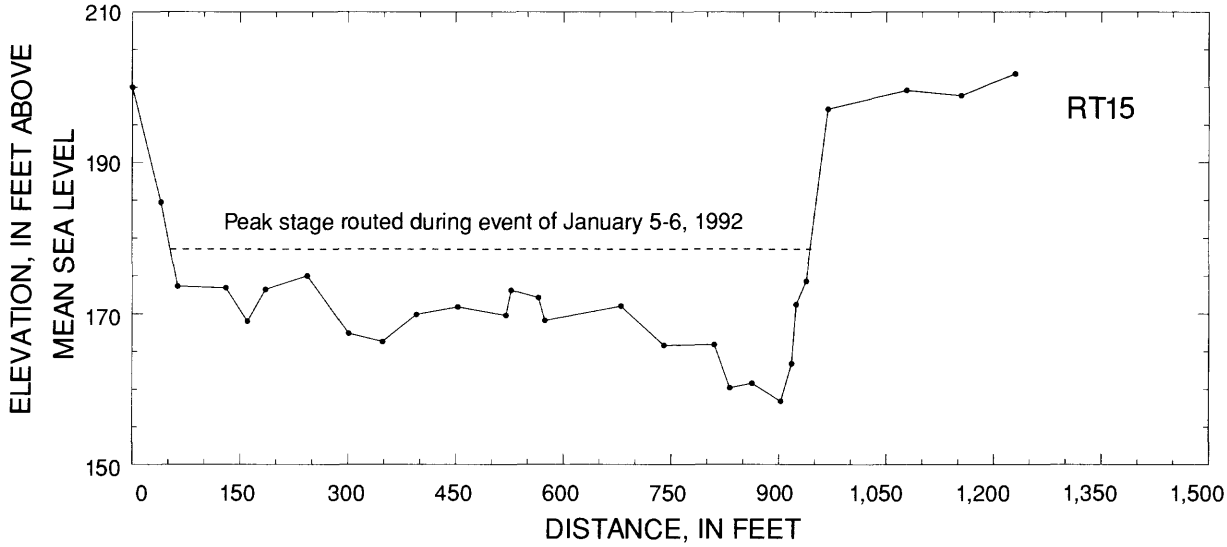

Cross sections RC13, RGL14, and RT15

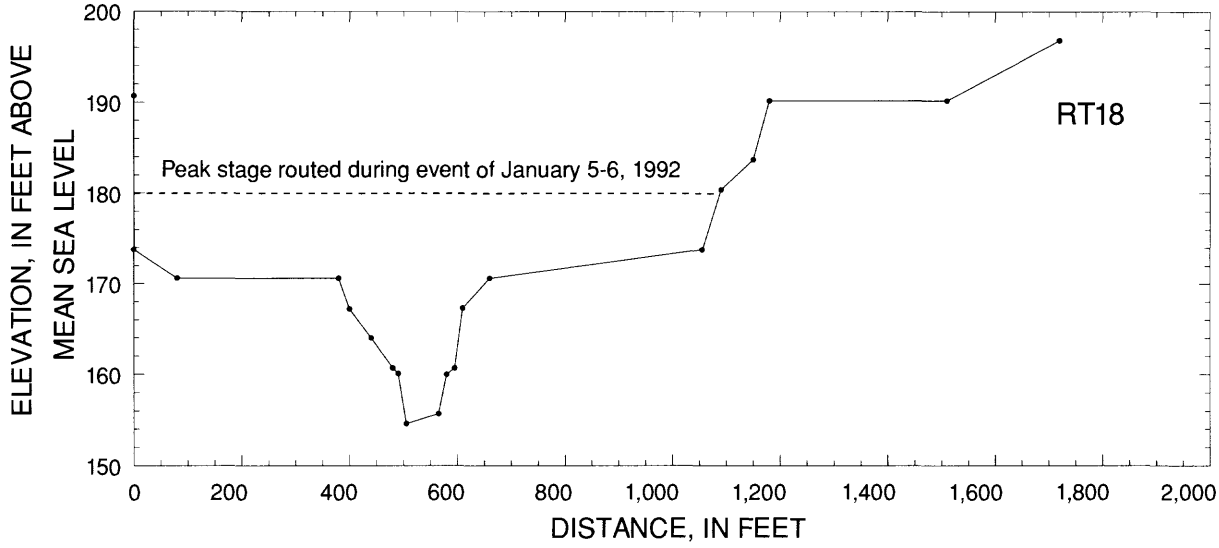

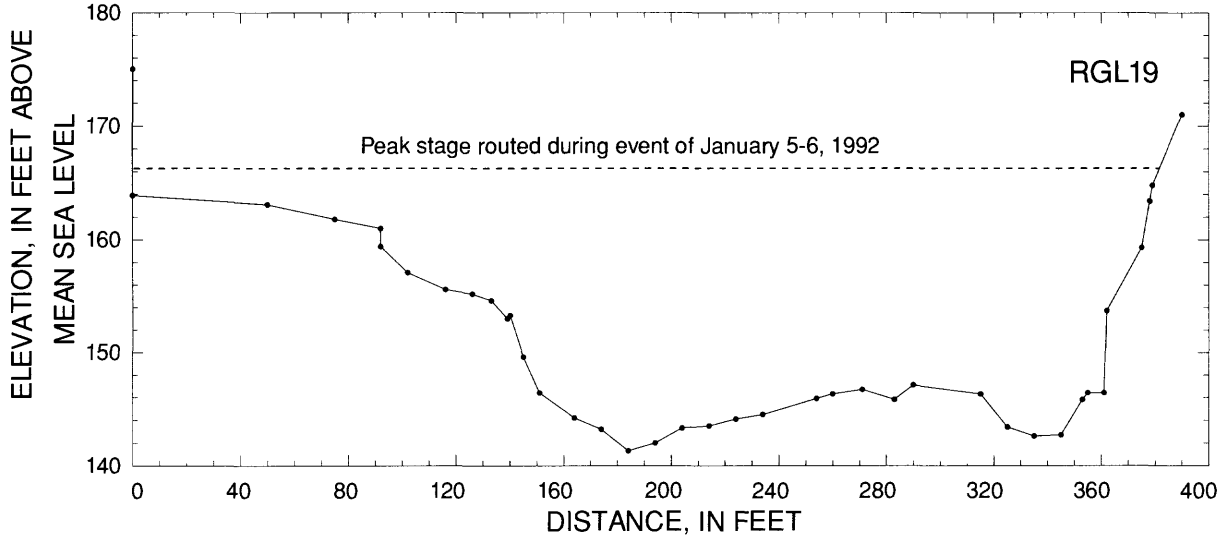

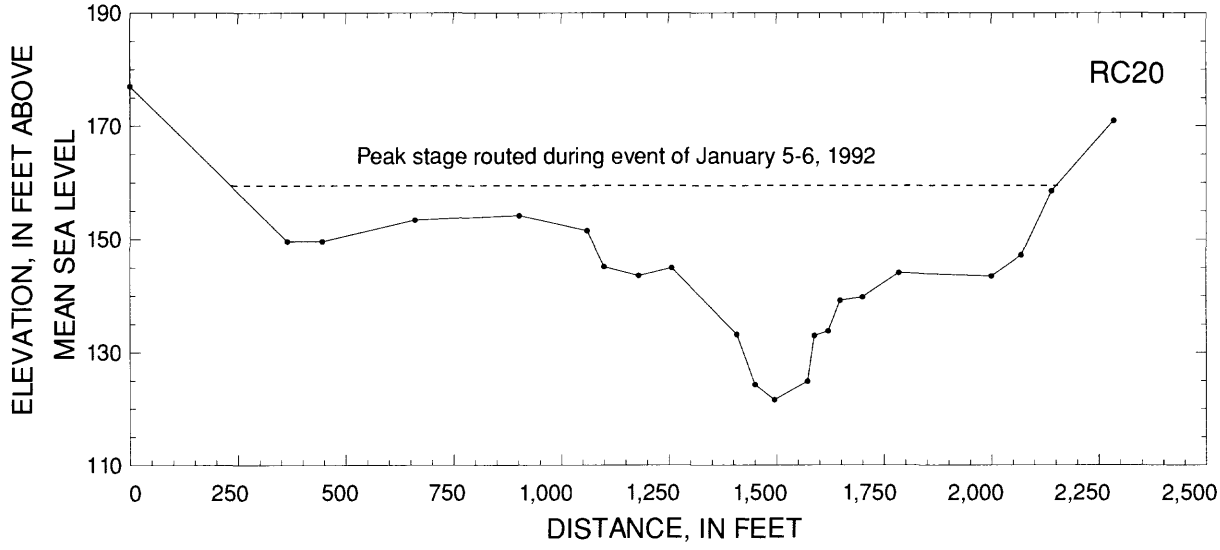

Cross sections RT18, RGL19, and RC20

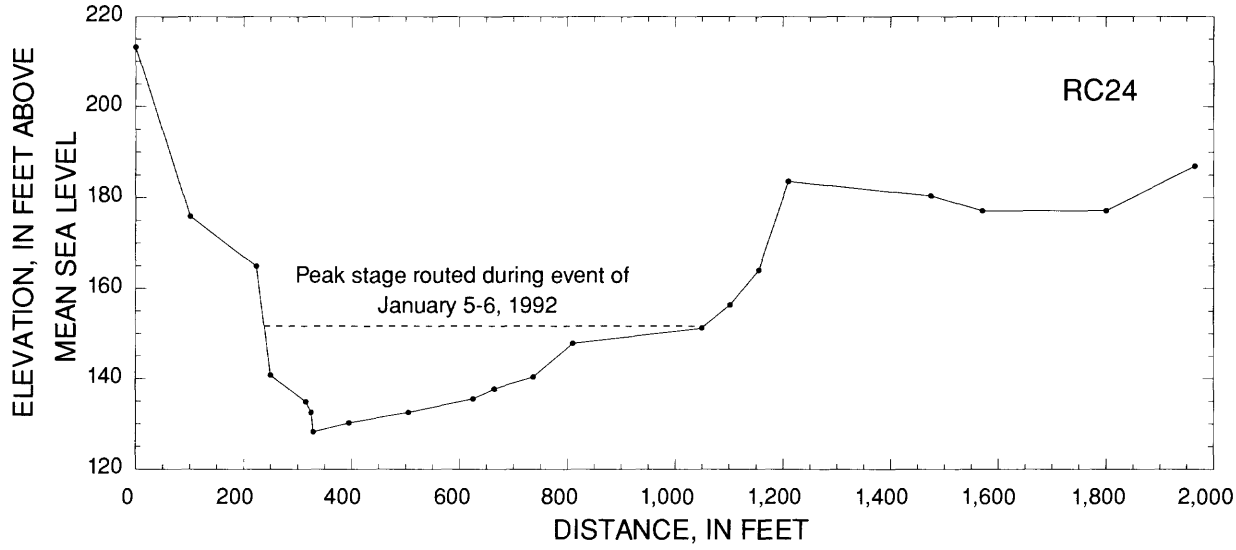

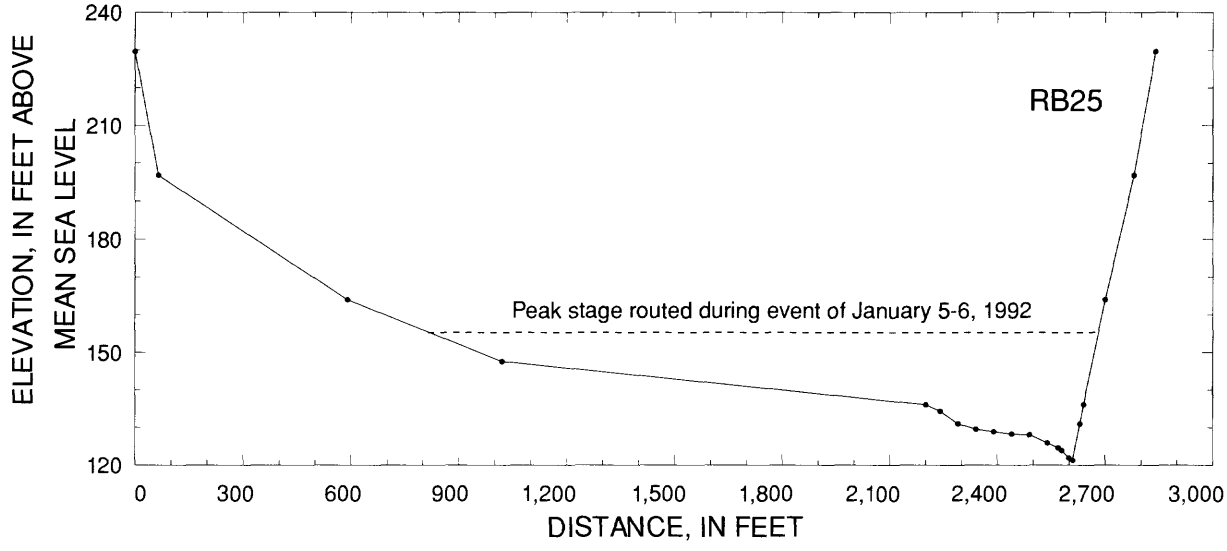

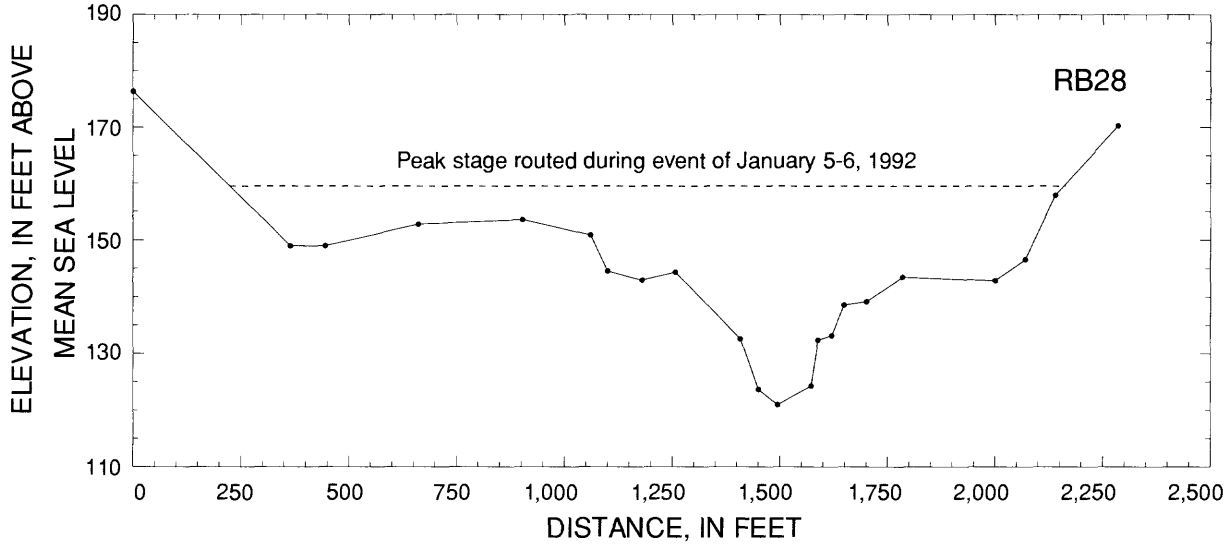

Cross sections RC24, RB25, and RB28

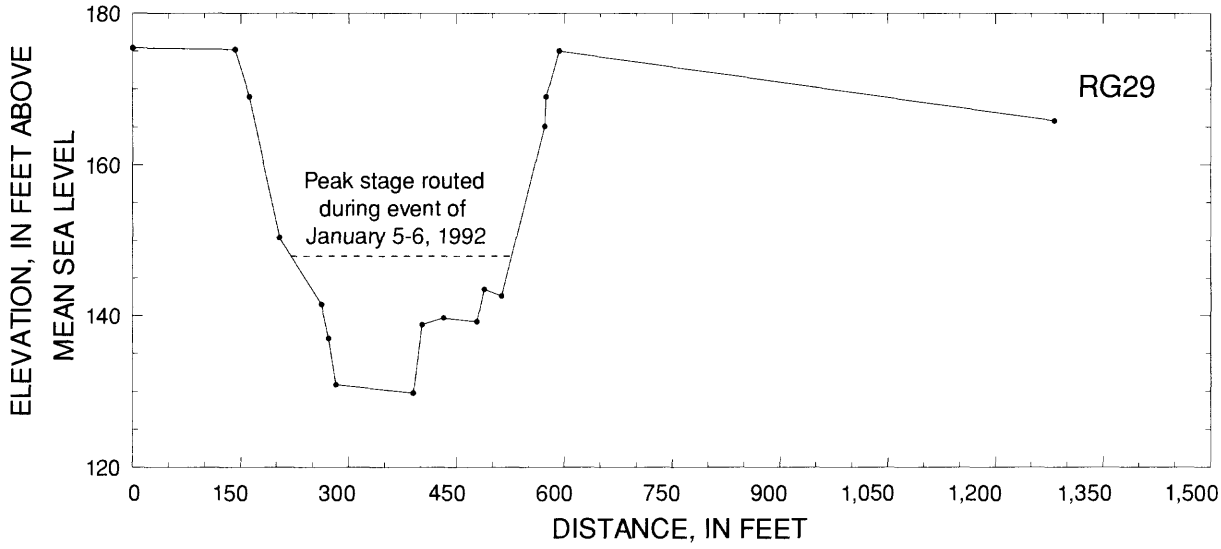

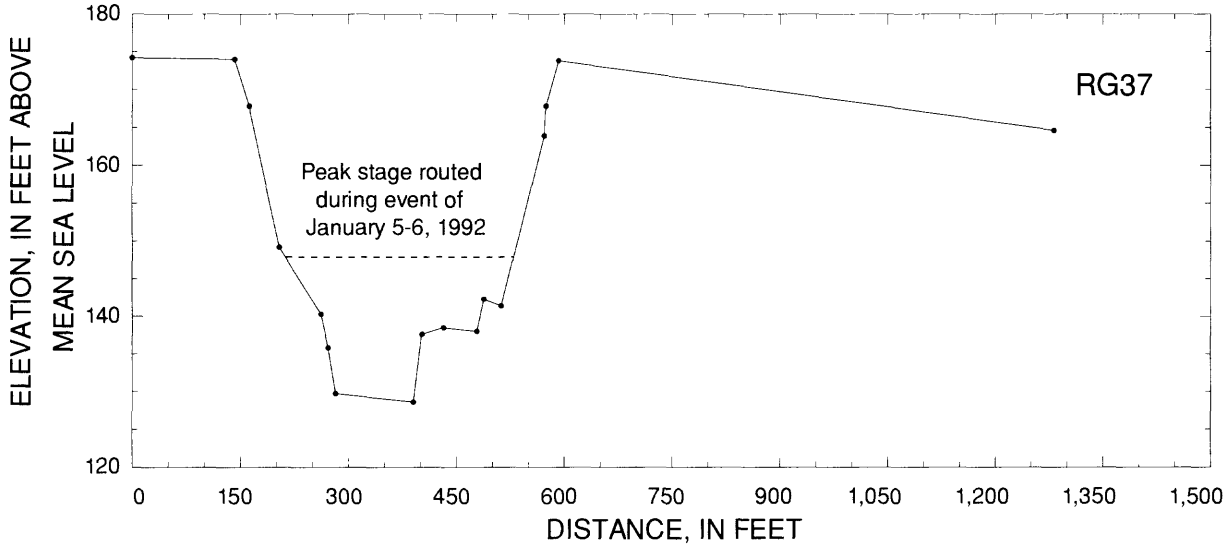

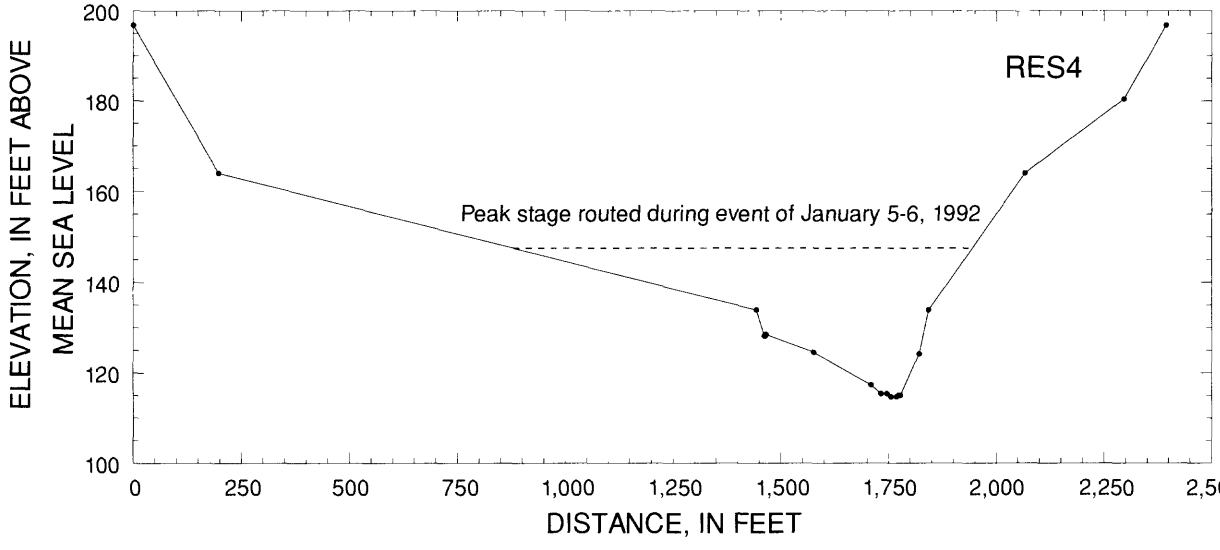

Cross sections RG29, RG37, and RES4

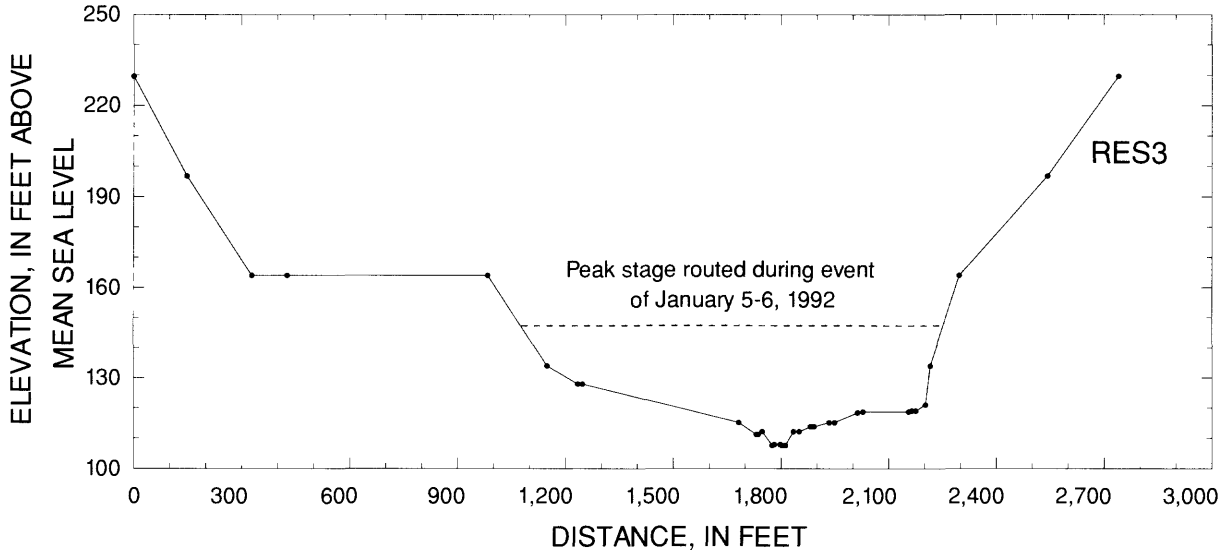

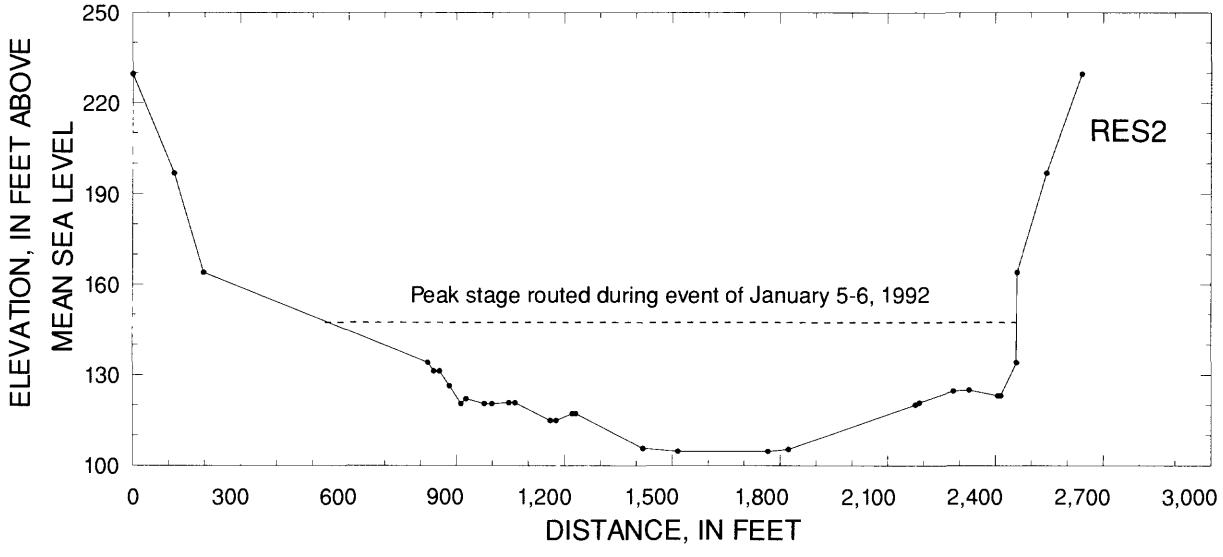

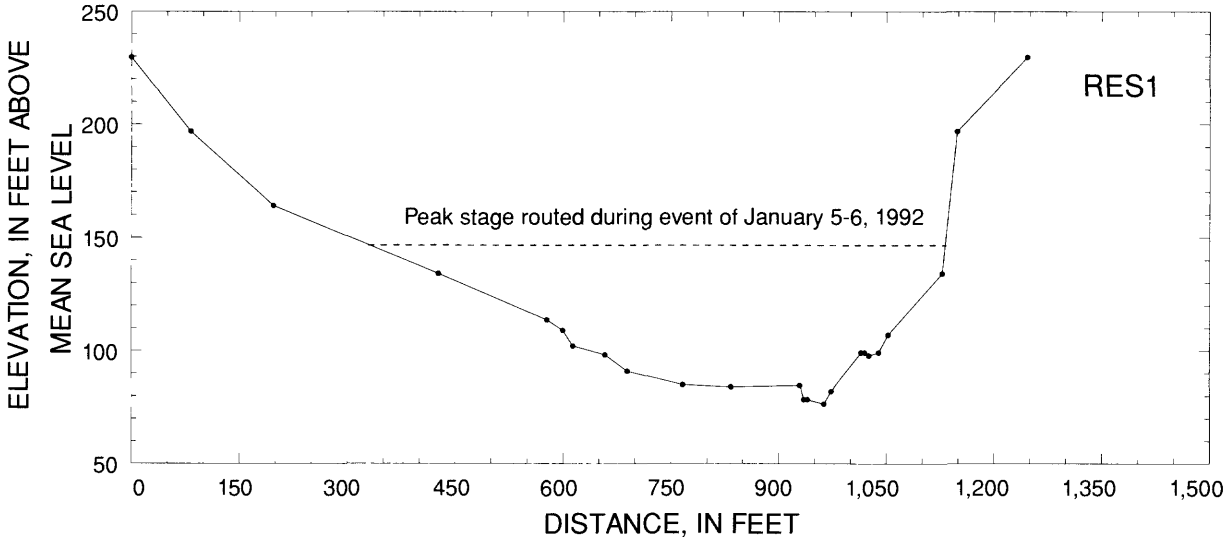

Cross sections RES3, RES2, and RES1

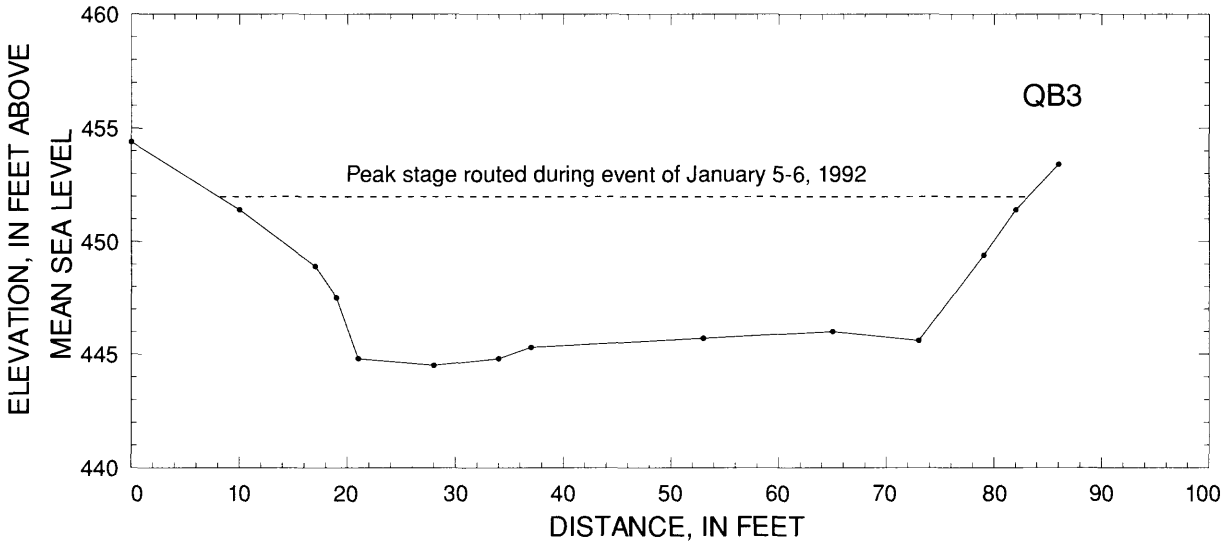

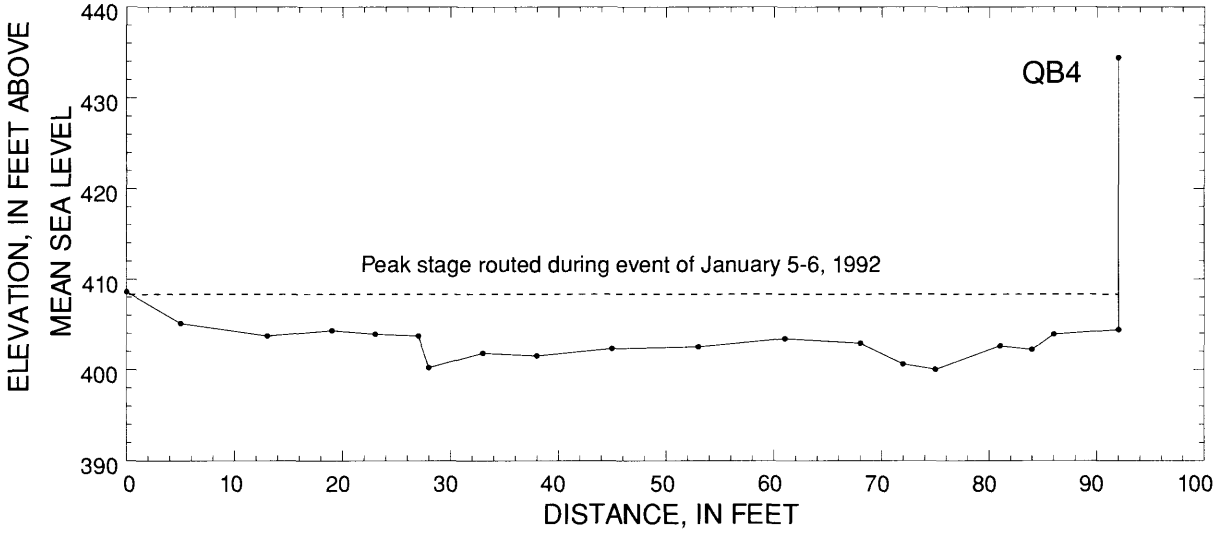

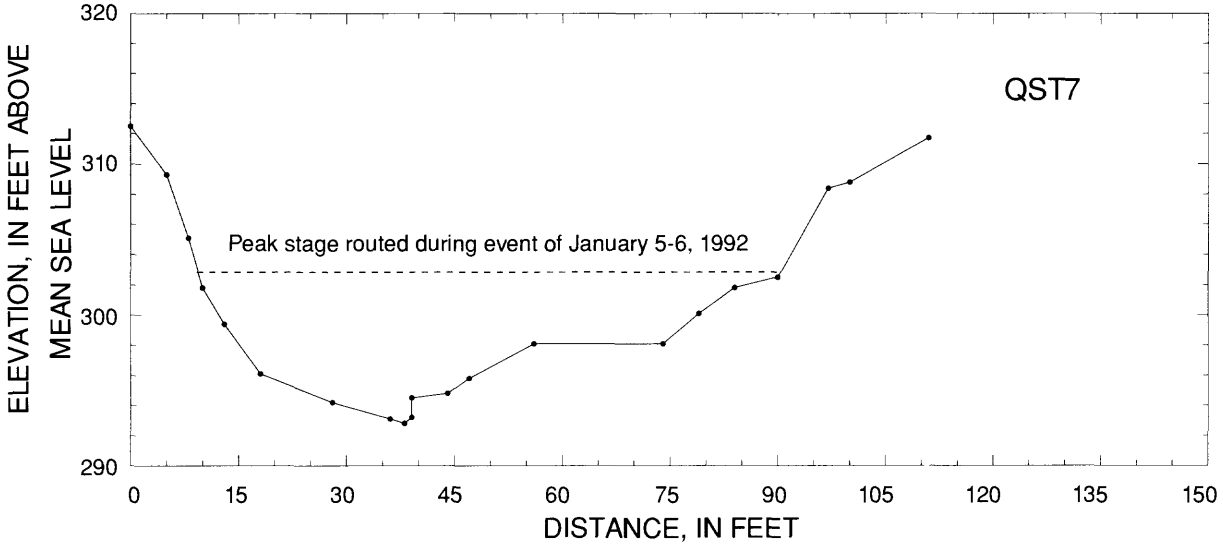

Cross sections QB3, QB4, and QST7

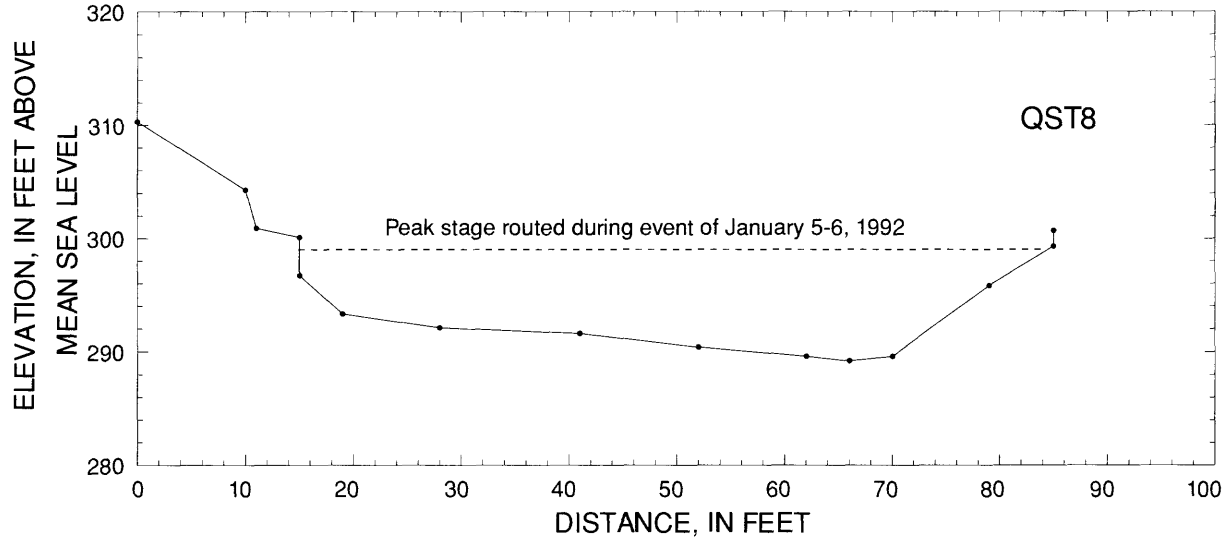

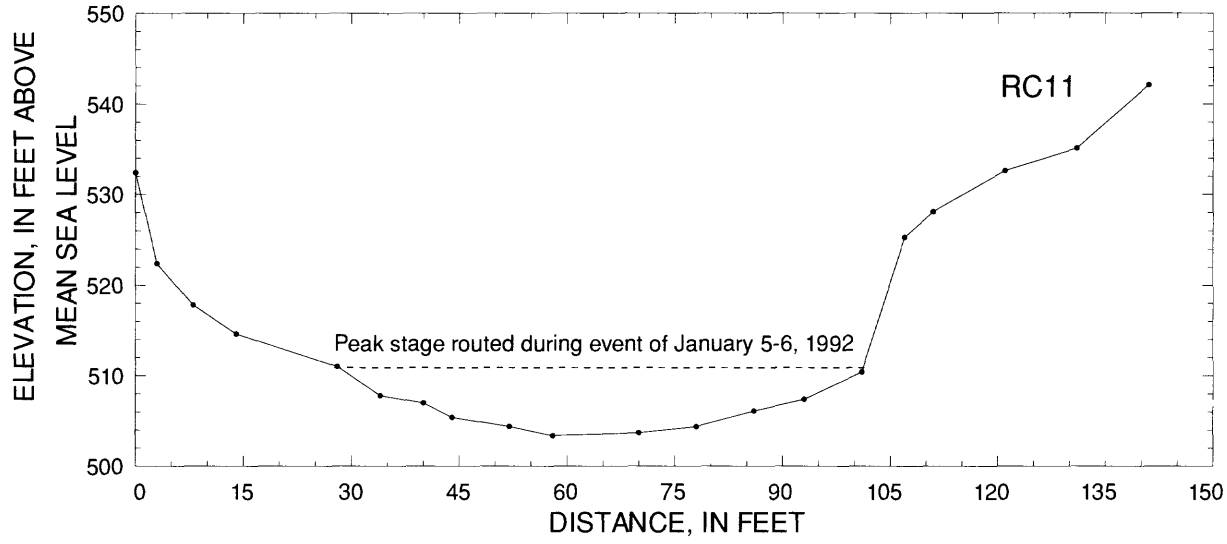

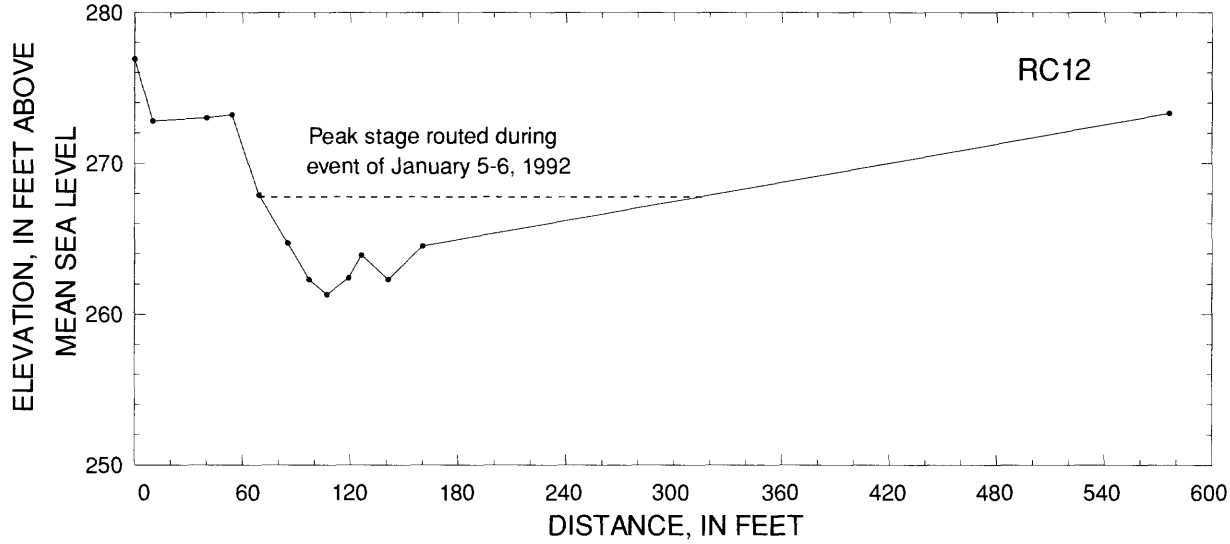

Cross sections QST8, RC11, and RC12

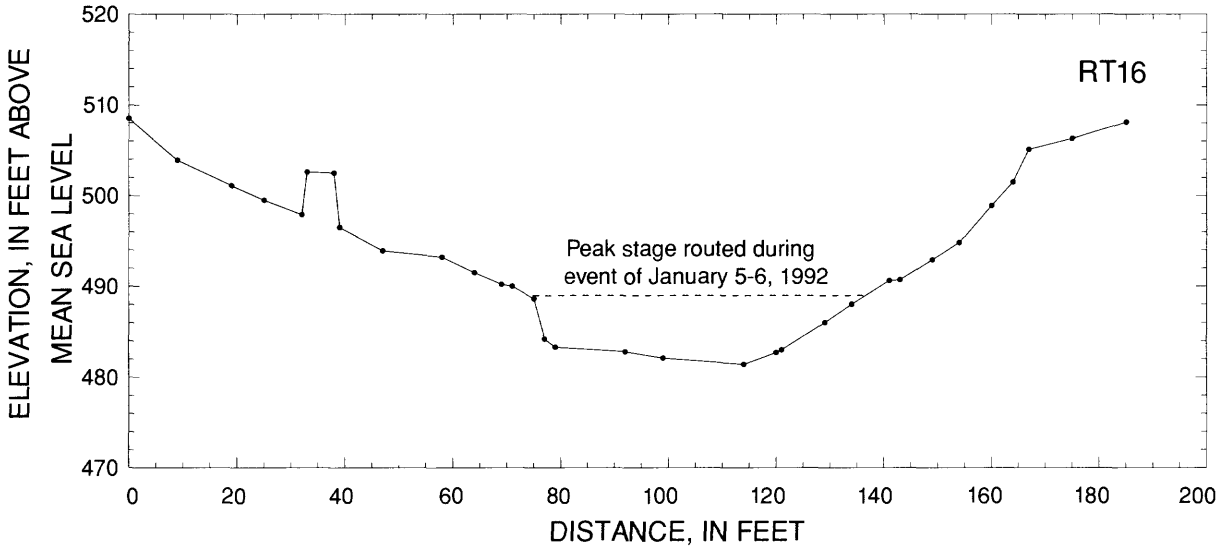

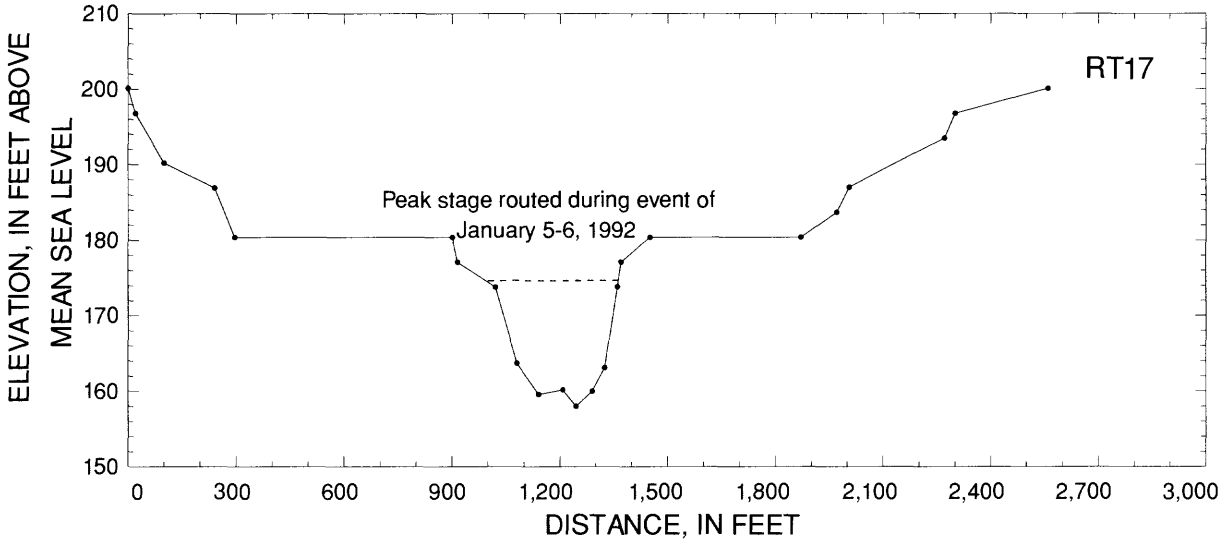

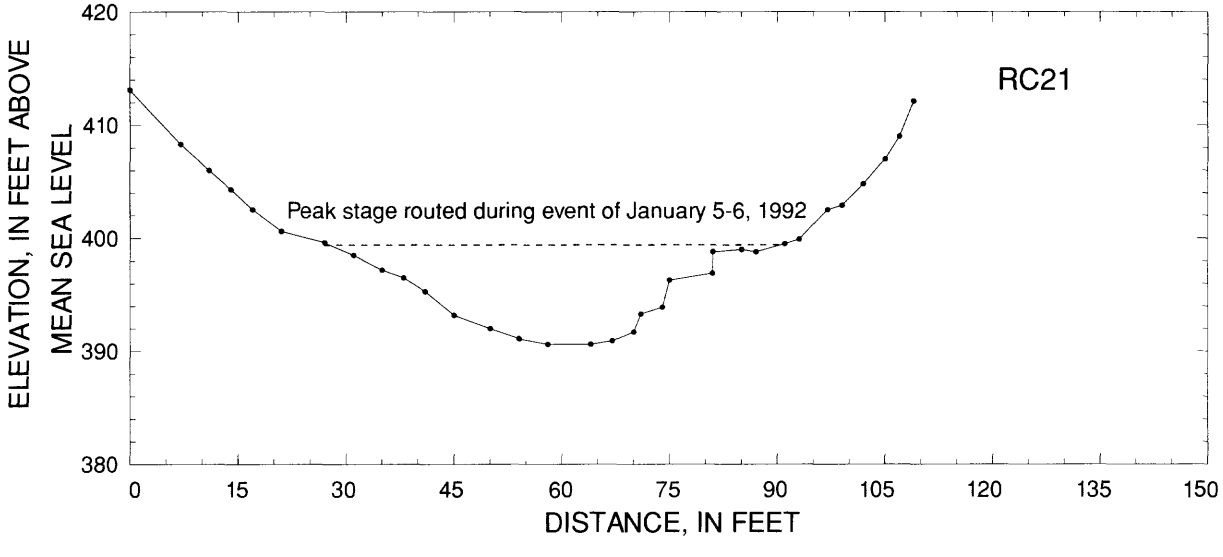

Cross sections RT16, RT17, and RC21

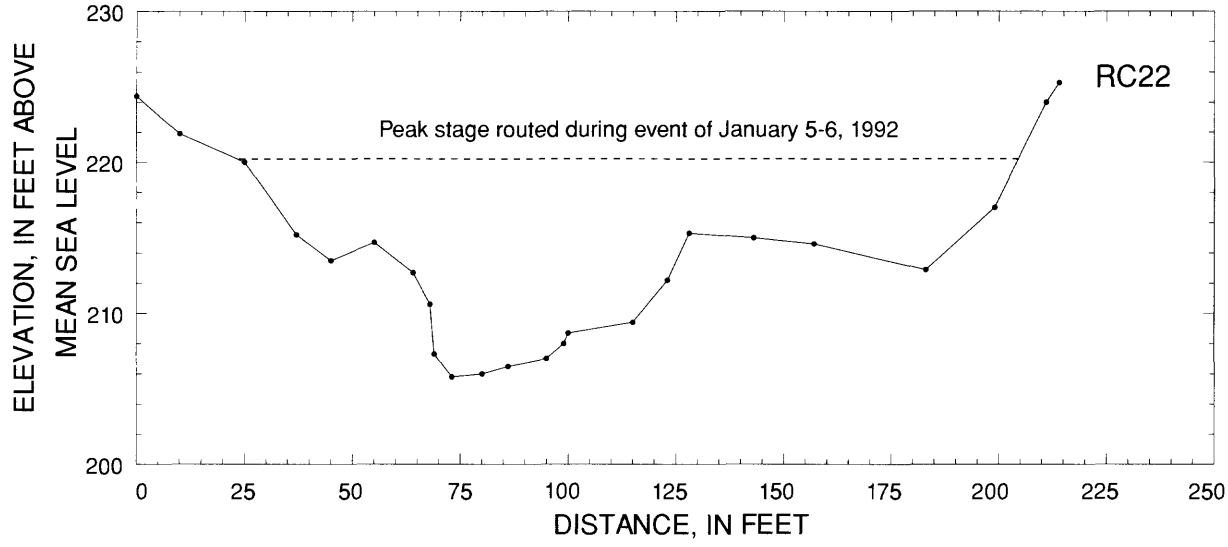

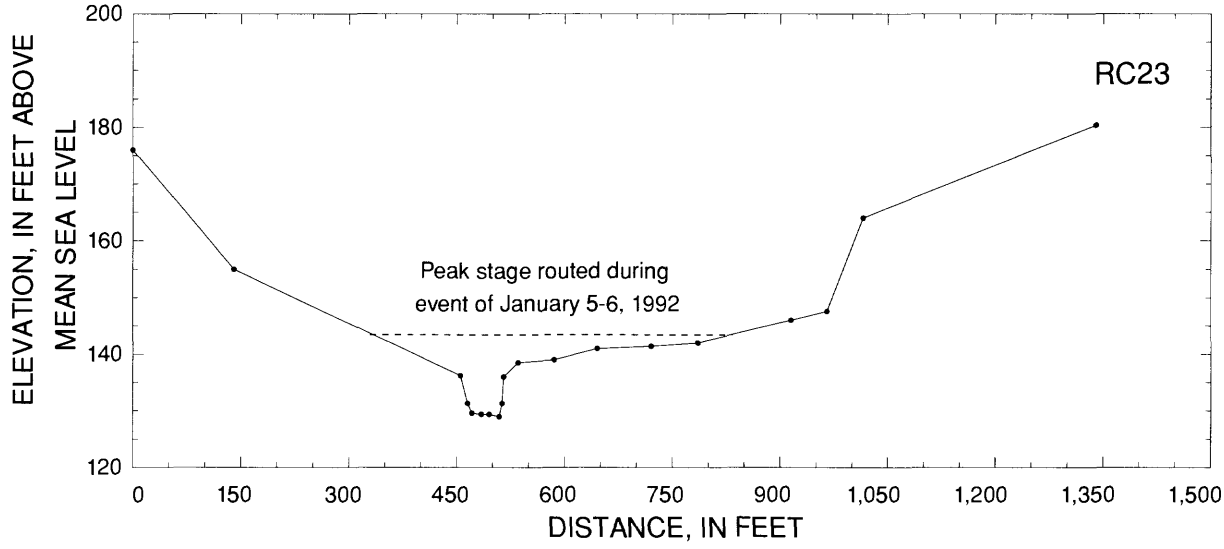

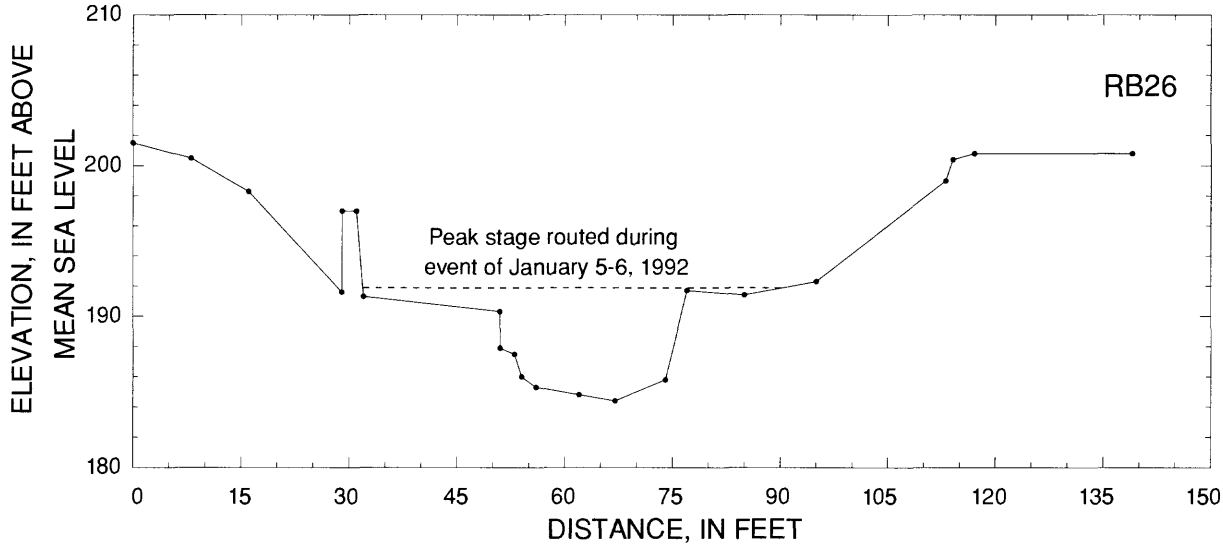

Cross sections RC22, RC23, and RB26

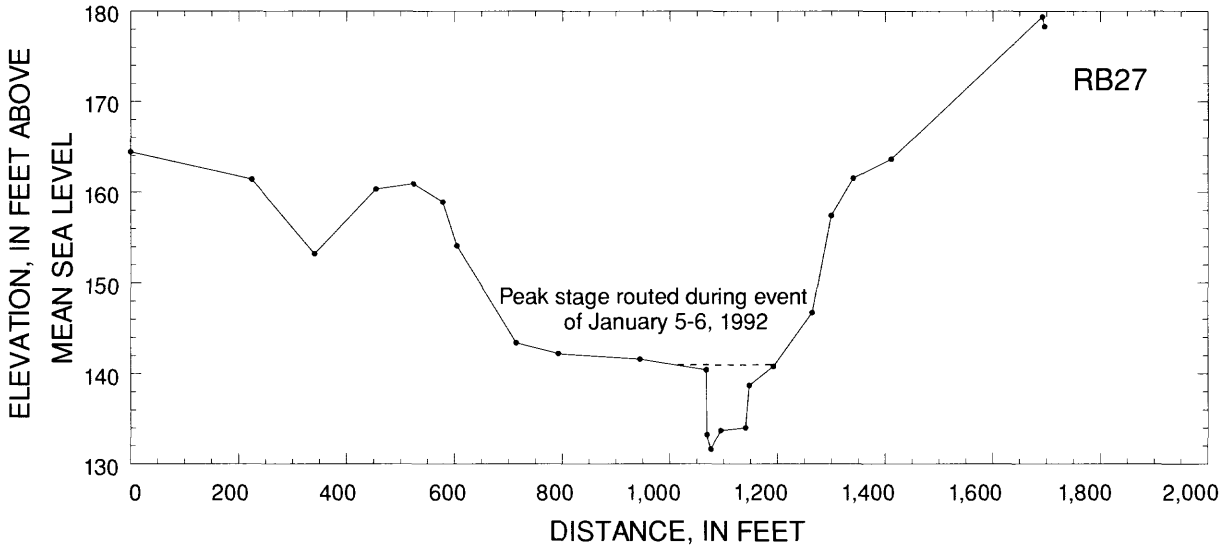

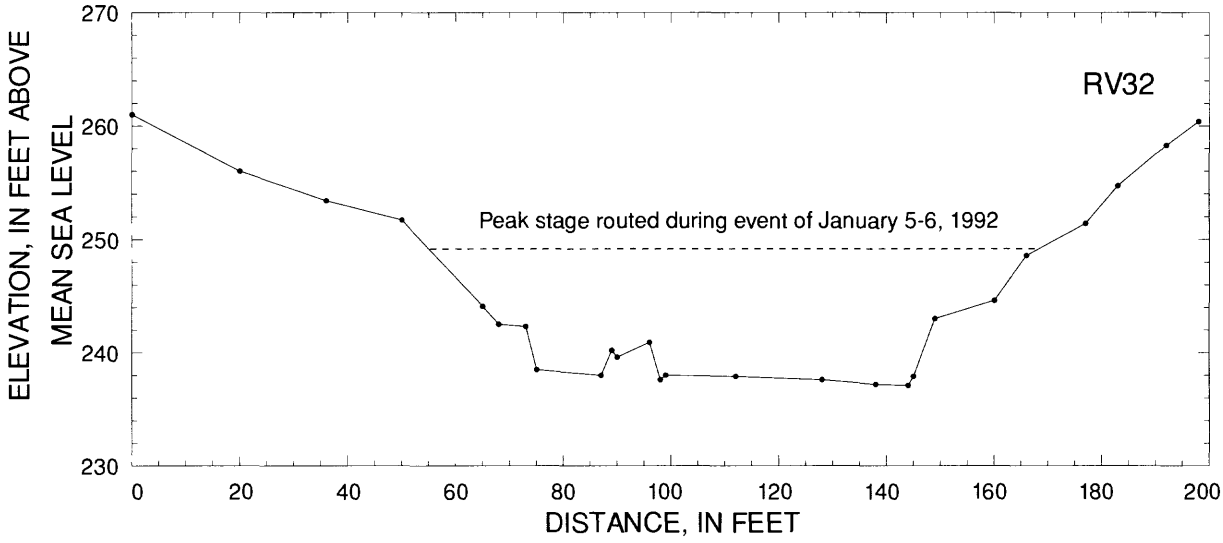

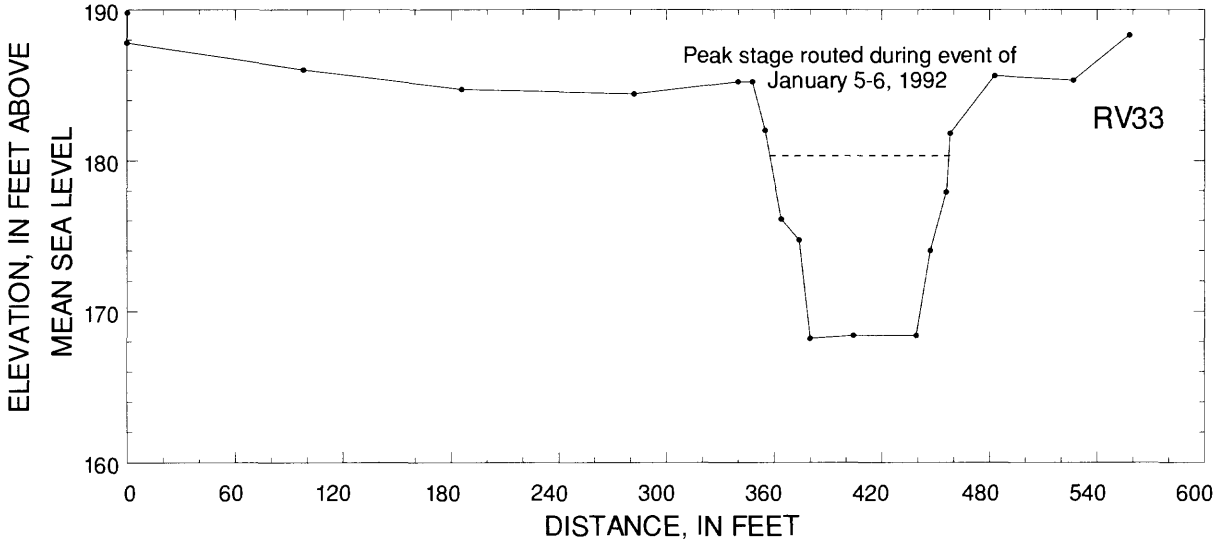

Cross sections RB27, RV32, and RV33

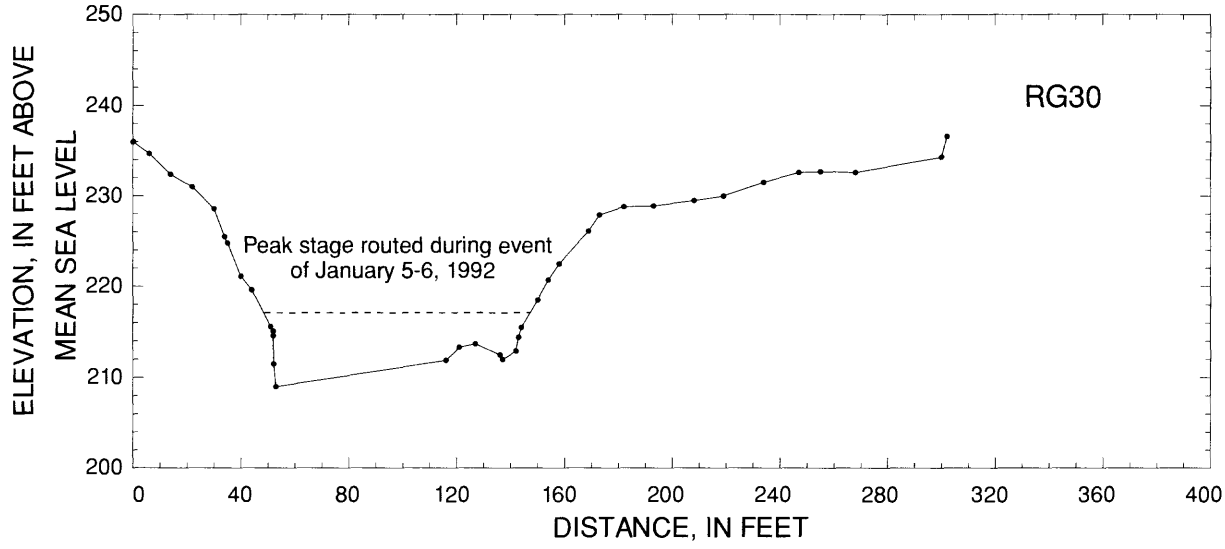

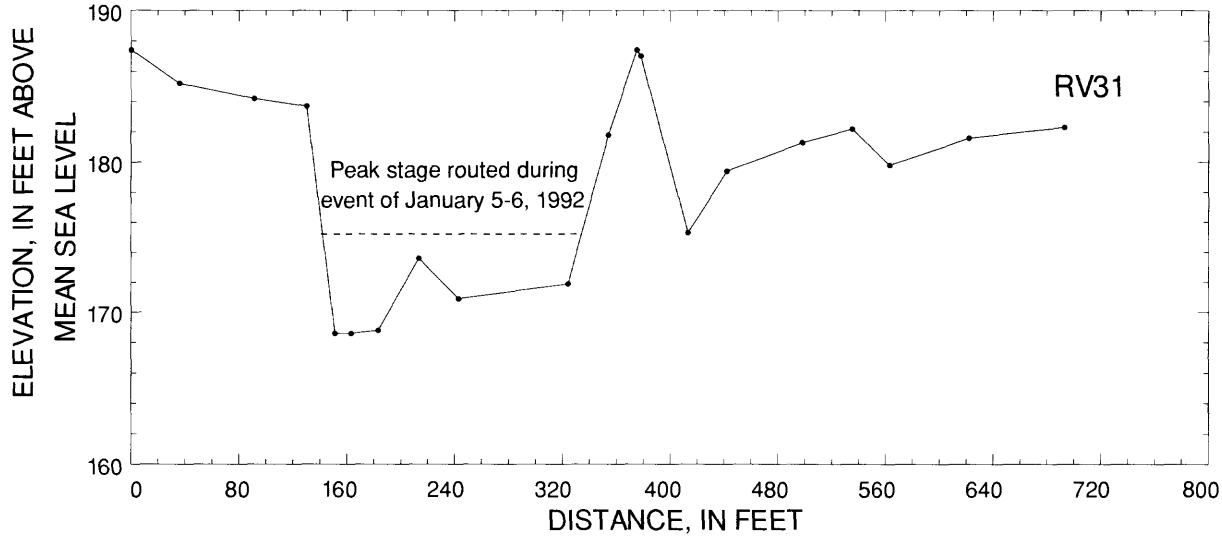

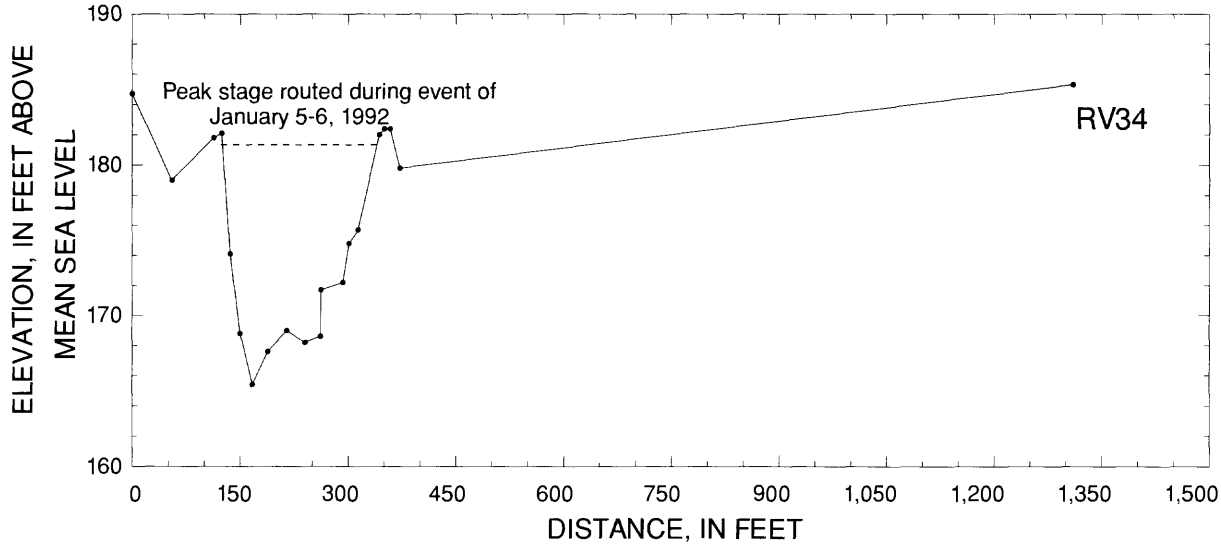

Cross sections RG30, RV31, and RV34

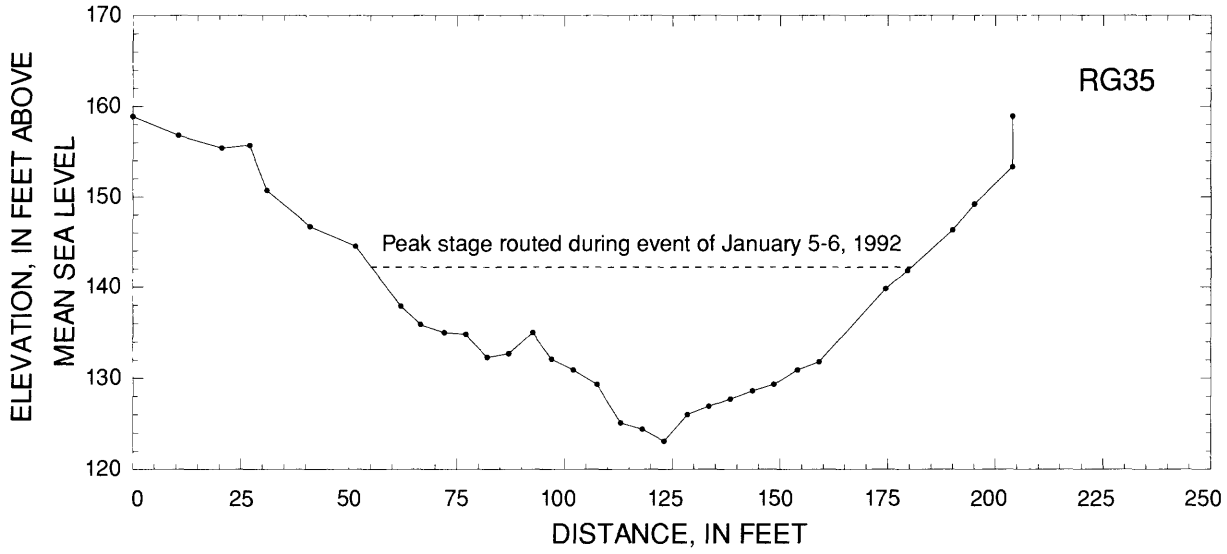

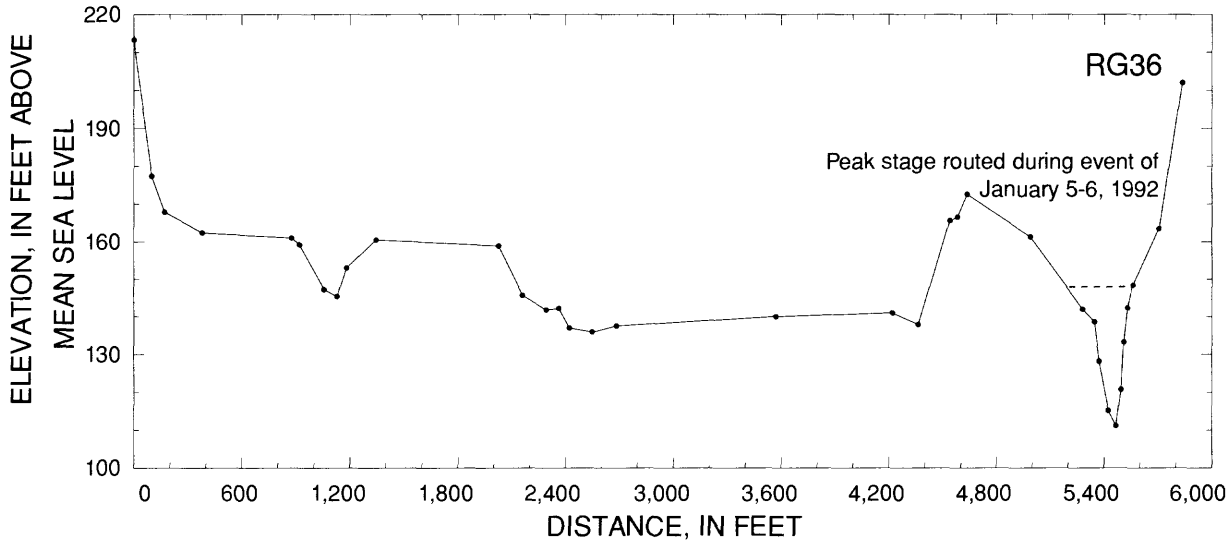

Cross sections RG35 and RG36

APPENDIX 5. HYDRAUX Input and Output Data File Samples

Boundary Values - chbndlst.dat

Boundary values data are supplied to HYDRAUX at the upstream end of channels where the inflow discharge is known. The preprocessor program called NETBOUND reads the input file chbndlst.dat and creates the boundary file chnlbnd.dat used by HYDRAUX. The chbndlst.dat input file contains the starting time when boundary values are applied, the time step at which these boundary values are given, the channel number where the boundary values are applied, the location of the boundary values with respect to the channel (upstream or downstream), and the file name where the boundary unit values are located. The input file chbndlst.dat used for subbasin XV is listed here to show its specific format.

```
25200   / starting time, in seconds
900     / time-series time step
11       / channel number, + upstream, - downstream
oq50055000
13       / channel number, + upstream, - downstream
oq50055225
15       / channel number, + upstream, - downstream
oq50055390
20       / channel number, + upstream, - downstream
oq50057000
21       / channel number, + upstream, - downstream
oq50058350
```

Control Program - control.dat

The control.dat input file establishes which terms in equation (24) will be included in the numerical solution, the level of output to be printed, the number of time steps to be simulated, the time increment, and the time-weighting factor. The input file control.dat used for subbasin XV follows to show an example of its specific format.

```
              Loiza Basin Simulation
    "UNGAGED" Subbasin XV, Channels 11,13,14,15,16,20,21.
1          / Terms, 1=dynamic, 2=diffusion, 3=kinematic
0          / 0 = constant density, 1 = variable density.
0          / 0 = constant sinuosity, 1 = variable sinuosity.
1          / 0 = do not read boundary values, 1 = read values.
0          / 0 = perturbation inactive, 1 = perturbation active.
32.2       / acceleration due to gravity.
940        / MaxTimeSteps, maximum number of time steps.
25200     / NetStartTime, atarting elapse time, in seconds.
180      / DT, time step, in seconds.
1.0       / Theta, time-weighting factor.
0.21132486541, 0.5,
0.78867513459, 0.5
           / local ( 0 to 1 ) quadrature-point coordinate and weight, paired.
5          / MaxIterations, maximum number of iterations per time step.
1          / LuInc, interval for complete forward eliminations.
0.005      / ToleranceQ, tolerance for closure on discharge.
0.005      / ToleranceZ, tolerance for closure on water-surface elevation.
1          / PrintLevel, amount of printing, 0 to 9, increasing with number.
-99/0          / PrintCount, initial value of print counter.
900        / PrintInc, print increment.
0          / TimeSeriesCount, initial value of time-series counter.
5           / TimeSeriesInc, time-series increment.
21, -30801.0
21,  -164.00
           / Requested time-series output, paired channel no. & downstream distance.
0          / SpaceCount, initial value of spatial-series output counter.
900        / SpaceInc, spatial-series increment.
1          / RestartFile, if 1, write restart file.

11         / ChannelNumber, for equation boundary (+ upstream, - downstream).
```

```
1          / Number of sinusoidal components.
5.0        / Base, base value for equation boundary condition.

 00.0      / Amplitude.
6.0        / Period, in hours.
3.0        / Phase angle, in hours.
0.0        / EqStart, time at which equation takes effect.
 999999.0     / EqStop, time at which equation is no longer effective.

-11        / Channel number for equation boundary (+ upstream, - downstream)
0          / Number of sinusoidal components.
-0.000637   / Base, base value for equation boundary condition.
0.0        / EqStart, time at which equation takes effect.
 999999.0    / EqStop, time at which equation is no longer effective.

13        / ChannelNumber, for equation boundary (+ upstream, - downstream).
0         / Number of sinusoidal components.
5.        / Base, base value for equation boundary condition.
0.0       / EqStart, time at which equation takes effect.
 999999.0   / EqStop, time at which equation is no longer effective.

-13        / ChannelNumber, for equation boundary (+ upstream, - downstream).
0          / Number of sinusoidal components.
-0.012901/  -0.00227    / Base, base value for equation boundary condition.
0.0        / EqStart, time at which equation takes effect.
 999999.0    / EqStop, time at which equation is no longer effective.

  ...  information for channels 14, 15, 16, and 20 goes between these lines

-21         / Channel number for equation boundary (+ upstream, - downstream)
0           / Number of sinusoidal components.
-0.00100     / Base, base value for equation boundary condition.
0.0         / EqStart, time at which equation takes effect.
 999999.0     / EqStop, time at which equation is no longer effective.
```

Channel Properties - cxgeom.dat

Channel properties data is generated by a preprocessor program called NETPROP. NETPROP reads two input files: rawgeom.dat and schmat.dat. The file rawgeom.dat contains the necessary cross sections to define the geometry of the channels. The output of NETPROP, a file named cxgeom.dat, provides the channel properties to HYDRAUX. The cxgeom.dat file generated for subbasin XV is listed next.

```
 0
CH        11
HY RGL19               47490.0     141.30
DP       0.00  0.000000E+00  0.000000E+00  1.00  0.00  0.00     0.0     0.0
DP       2.50  0.763873E+02  0.278933E+04  1.00  1.00  1.00    75.2    75.8
DP       5.00  0.362886E+03  0.228414E+05  1.00  1.00  1.00   157.4   159.2
DP       7.50  0.878045E+03  0.804289E+05  1.00  1.00  1.00   214.8   219.4
DP      10.00  0.142065E+04  0.175590E+06  1.00  1.00  1.00   219.0   226.5
DP      12.50  0.197441E+04  0.295131E+06  1.00  1.00  1.00   226.2   236.7
DP      15.00  0.257463E+04  0.421040E+06  1.00  1.00  1.00   258.6   269.7
DP      17.50  0.325027E+04  0.590036E+06  1.00  1.00  1.00   279.2   291.1
DP      20.00  0.395912E+04  0.793775E+06  1.00  1.00  1.00   290.8   305.5
DP      22.50  0.476147E+04  0.920546E+06  1.00  1.00  1.00   372.0   388.1
DP      25.00  0.570830E+04  0.122167E+07  1.00  1.00  1.00   379.0   399.4
DP      27.50  0.665580E+04  0.156498E+07  1.00  1.00  1.00   379.0   404.4
DP      30.00  0.760330E+04  0.193770E+07  1.00  1.00  1.00   379.0   409.4
DP      32.50  0.855080E+04  0.233765E+07  1.00  1.00  1.00   379.0   414.4
DP      35.00  0.949830E+04  0.276295E+07  1.00  1.00  1.00   379.0   419.4
DP      37.50  0.104458E+05  0.321195E+07  1.00  1.00  1.00   379.0   424.4
DP      40.00  0.113933E+05  0.368319E+07  1.00  1.00  1.00   379.0   429.4
DP      42.50  0.123408E+05  0.417537E+07  1.00  1.00  1.00   379.0   434.4
DP      45.00  0.132883E+05  0.468733E+07  1.00  1.00  1.00   379.0   439.4
DP      47.50  0.142358E+05  0.521799E+07  1.00  1.00  1.00   379.0   444.4
DP      50.00  0.151833E+05  0.576640E+07  1.00  1.00  1.00   379.0   449.4
HY  RC24               38944.0     128.20
DP       0.00  0.000000E+00  0.000000E+00  1.00  0.00  0.00     0.0     0.0
DP       2.50  0.107885E+03  0.196682E+04  1.00  1.00  1.00    92.2    93.4
DP       5.00  0.489721E+03  0.151725E+05  1.02  1.00  1.00   210.9   212.9
DP       7.50  0.115679E+04  0.489268E+05  1.11  1.00  1.00   322.4   324.7
```

```
DP      10.00  0.205522E+04  0.103462E+06  1.15  1.00  1.00   399.7   402.2
DP      12.50  0.317145E+04  0.179332E+06  1.18  1.00  1.00   488.9   491.5
DP      15.00  0.443035E+04  0.282142E+06  1.17  1.00  1.00   517.3   521.0
DP      17.50  0.575795E+04  0.406371E+06  1.16  1.00  1.00   544.8   549.5
DP      20.00  0.715905E+04  0.544018E+06  1.17  1.00  1.00   596.4   602.2
DP      22.50  0.887324E+04  0.681402E+06  1.24  1.00  1.00   774.9   781.7
DP      25.00  0.109140E+05  0.885694E+06  1.23  1.00  1.00   833.7   841.5
DP      27.50  0.130341E+05  0.112515E+07  1.22  1.00  1.00   862.5   871.4
DP      30.00  0.152199E+05  0.139488E+07  1.20  1.00  1.00   884.6   894.6
DP      32.50  0.174564E+05  0.169222E+07  1.19  1.00  1.00   904.6   915.8
DP      35.00  0.197428E+05  0.201559E+07  1.18  1.00  1.00   924.6   936.9
DP      37.50  0.220766E+05  0.236242E+07  1.17  1.00  1.00   945.6   959.0
DP      40.00  0.244841E+05  0.272577E+07  1.17  1.00  1.00   980.4   994.3
DP      42.50  0.269785E+05  0.312148E+07  1.16  1.00  1.00  1015.1  1029.6
DP      45.00  0.295598E+05  0.354791E+07  1.16  1.00  1.00  1049.9  1064.9
DP      47.50  0.322279E+05  0.400432E+07  1.16  1.00  1.00  1084.6  1100.1
DP      50.00  0.352413E+05  0.408195E+07  1.24  1.00  1.00  1380.3  1396.7

  ...  information for channels 14, 15 and 20 goes between these lines

CH        21
HY RG37                30801.0     128.60
DP       0.00  0.000000E+00  0.000000E+00  1.00  0.00  0.00     0.0     0.0
DP       6.20  0.657147E+03  0.647100E+05  1.00  1.00  1.00   124.6   128.1
DP      12.40  0.171366E+04  0.214034E+06  1.00  1.00  1.00   227.5   233.9
DP      18.60  0.343969E+04  0.556324E+06  1.00  1.00  1.00   310.4   318.6
DP      24.80  0.550331E+04  0.112275E+07  1.00  1.00  1.00   349.5   359.8
DP      31.00  0.776477E+04  0.187964E+07  1.00  1.00  1.00   380.0   392.8
DP      37.20  0.102656E+05  0.282724E+07  1.00  1.00  1.00   496.5   513.7
DP      43.40  0.148689E+05  0.414421E+07  1.12  1.00  1.00   993.1  1019.6
DP      49.60  0.223863E+05  0.604304E+07  1.23  1.00  1.00  1282.0  1319.3
DP      55.80  0.303347E+05  0.850291E+07  1.25  1.00  1.00  1282.0  1331.7
DP      62.00  0.382831E+05  0.114066E+08  1.24  1.00  1.00  1282.0  1344.1
DP      68.20  0.462315E+05  0.147036E+08  1.23  1.00  1.00  1282.0  1356.5
DP      74.40  0.541799E+05  0.183595E+08  1.21  1.00  1.00  1282.0  1368.9
DP      80.60  0.621283E+05  0.223479E+08  1.20  1.00  1.00  1282.0  1381.3
DP      86.80  0.700766E+05  0.266479E+08  1.19  1.00  1.00  1282.0  1393.7
DP      93.00  0.780250E+05  0.312418E+08  1.19  1.00  1.00  1282.0  1406.1
DP      99.20  0.859734E+05  0.361148E+08  1.18  1.00  1.00  1282.0  1418.5
DP     105.40  0.939218E+05  0.412538E+08  1.18  1.00  1.00  1282.0  1430.9
DP     111.60  0.101870E+06  0.466475E+08  1.17  1.00  1.00  1282.0  1443.3
DP     117.80  0.109819E+06  0.522857E+08  1.17  1.00  1.00  1282.0  1455.7
DP     124.00  0.117767E+06  0.581595E+08  1.17  1.00  1.00  1282.0  1468.1
HY RES4                29028.0     114.70
DP       0.00  0.000000E+00  0.000000E+00  1.00  0.00  0.00    13.0     0.0
DP       6.20  0.569457E+03  0.651795E+05  1.00  1.00  1.00   161.9   162.8
DP      12.40  0.204082E+04  0.345015E+06  1.00  1.00  1.00   323.0   325.0
DP      18.60  0.436149E+04  0.106534E+07  1.00  1.00  1.00   395.8   399.9
DP      24.80  0.760280E+04  0.189231E+07  1.00  1.00  1.00   673.0   677.7
DP      31.00  0.127137E+05  0.348404E+07  1.00  1.00  1.00   975.7   981.0
DP      37.20  0.197019E+05  0.604155E+07  1.00  1.00  1.00  1278.5  1284.2
DP      43.40  0.285672E+05  0.974322E+07  1.00  1.00  1.00  1581.3  1587.5
DP      49.60  0.393084E+05  0.148062E+08  1.00  1.00  1.00  1875.4  1882.1
DP      55.80  0.513204E+05  0.221241E+08  1.00  1.00  1.00  1999.4  2006.9
DP      62.00  0.641014E+05  0.307868E+08  1.00  1.00  1.00  2123.5  2131.7
DP      68.20  0.776265E+05  0.410231E+08  1.00  1.00  1.00  2227.5  2236.6
DP      74.40  0.916678E+05  0.529378E+08  1.00  1.00  1.00  2302.0  2312.0
DP      80.60  0.106171E+06  0.661880E+08  1.00  1.00  1.00  2376.4  2387.5
DP      86.80  0.121002E+06  0.816759E+08  1.00  1.00  1.00  2394.4  2415.1
DP      93.00  0.135848E+06  0.987132E+08  1.00  1.00  1.00  2394.4  2427.5
DP      99.20  0.150693E+06  0.116941E+09  1.00  1.00  1.00  2394.4  2439.9
DP     105.40  0.165538E+06  0.136304E+09  1.00  1.00  1.00  2394.4  2452.3
DP     111.60  0.180384E+06  0.156752E+09  1.00  1.00  1.00  2394.4  2464.7
DP     117.80  0.195229E+06  0.178240E+09  1.00  1.00  1.00  2394.4  2477.1
DP     124.00  0.210074E+06  0.200728E+09  1.00  1.00  1.00  2394.4  2489.5

  ...  information for cross sections RES3 and RES2 between these lines

HY RES1                  164.0      76.48
DP       0.00  0.000000E+00  0.000000E+00  1.00  0.00  0.00     0.0     0.0
DP       6.20  0.182914E+03  0.225964E+05  1.00  1.00  1.00    42.9    46.6
DP      12.40  0.132991E+04  0.186933E+06  1.00  1.00  1.00   273.3   279.3
DP      18.60  0.324652E+04  0.724647E+06  1.00  1.00  1.00   333.0   340.8
DP      24.80  0.554165E+04  0.151194E+07  1.00  1.00  1.00   420.6   430.4
```

```
DP      31.00  0.826306E+04  0.279793E+07  1.00  1.00  1.00   451.4   464.2
DP      37.20  0.111845E+05  0.435656E+07  1.00  1.00  1.00   494.5   509.2
DP      43.40  0.144451E+05  0.616419E+07  1.00  1.00  1.00   557.3   573.6
DP      49.60  0.180952E+05  0.835933E+07  1.00  1.00  1.00   620.1   637.9
DP      55.80  0.221348E+05  0.109700E+08  1.00  1.00  1.00   683.0   702.2
DP      62.00  0.265431E+05  0.140915E+08  1.00  1.00  1.00   736.3   759.5
DP      68.20  0.312622E+05  0.176745E+08  1.00  1.00  1.00   785.9   814.0
DP      74.40  0.362886E+05  0.217026E+08  1.00  1.00  1.00   835.5   868.5
DP      80.60  0.416225E+05  0.261915E+08  1.00  1.00  1.00   885.1   922.9
DP      86.80  0.472637E+05  0.311571E+08  1.00  1.00  1.00   934.7   977.4
DP      93.00  0.531498E+05  0.370829E+08  1.00  1.00  1.00   961.4  1009.5
DP      99.20  0.591841E+05  0.435298E+08  1.00  1.00  1.00   985.1  1038.6
DP     105.40  0.653656E+05  0.504306E+08  1.00  1.00  1.00  1008.9  1067.7
DP     111.60  0.716943E+05  0.577832E+08  1.00  1.00  1.00  1032.6  1096.7
DP     117.80  0.781700E+05  0.655865E+08  1.00  1.00  1.00  1056.4  1125.8
DP     124.00  0.848043E+05  0.736767E+08  1.00  1.00  1.00  1086.2  1159.2
```

Input/Output File Names - master.fil

File master.fil specifies the input and output file names used by HYDRAUX as well as the unit numbers assigned to each file. The implementation of HYDRAUX requires data files for program control (control.dat), schematic description and initial values (schmat.dat), channel properties and boundary values (chbndlst.dat and chnlbnd.dat), and constraint properties (strmcnst.dat). These sets of data are the input file requirements for the hydraulic rounting model.

The output data files generated by HYDRAUX are: the general results file netprint.dat, the file containing initial conditions for restarting netrstrt.dat, discharge space series netspcq.dat, depth of flow space series netspcz.dat, discharge time series nettsq.dat, and water surface elevation time series nettsz.dat. The master.fil file used for subbasin XV is shown next.

```
netspc.tmp    netspc.tmp     32
dbgspace.dat  dbgspace.dat   33
chbndlst.dat  chbndlst.dat   34
wtshdbnd.dat  wtshdbnd.dat   35
control.dat   control.dat    36
schemat.dat   schmat.dat     37
rawgeom.dat   rawgeom.dat    38
cxgeom.dat    cxgeom.dat     39
netspch.dat   netspch.dat    40
chnlbnd.dat   chnlbnd.dat    41
netts.tmp     netts.tmp      42
temp.txt      temp.txt       43
neterror.dat  neterror.dat   44
netspcq.dat   netspcq.dat    45
netprint.dat  netprint.dat   46
nettsq.dat    nettsq.dat     47
nettsz.dat    nettsz.dat     48
netrstrt.dat  netrstrt.dat   49
strmcnst.dat  strmcnst.dat   55
```

Output Data - nettsq.dat

The file nettsq.dat contains the routed hydrograph. Time series hydrographs can be printed at pre-specified points in the channel. The following output is an abbreviated version of the hydrographs obtained at the confluence of channels 16 and 20 and at the spillway.

```
Time      -30801.00       -164.00
           9.00          142.45          0.00
           9.25          143.80          0.00
           9.50          139.81          0.00
           9.75          130.34          0.00
          10.00          127.29          0.00
          10.25          123.62          0.00
          10.50          116.96          0.00
```

```
          10.75          112.01           0.00
          11.00          110.36           0.00

          ...

          17.00         7769.25         323.34
          17.25         9156.55         642.89
          17.50        11954.86        1141.58

          ...
```

Schematic Description - schmat.dat

The schematic description date relates individual channel attributes such as channel geometry specified by cross sections, number of cross sections defining the channel, the nature of connections among channels, boundary condition codes, and type of approximation to be used to determine initial values for the unknowns. Initial values for discharge and water surface elevation in this HYDRAUX application are specified in the schmat.dat file. The schmat.dat input file used for subbasin XV is listed to show its format.

```
Channel
Hydraux
     11    / branch number   (Bet. RGDL @ Caguas & Rio Caguitas)
        2,500.00, 1, 7, 0   / no. of cx, dx, NKEEP, ICNDAP, NVAL
RGL19                       / cx ID
        143.8    70.0       / 143.00,          5.0     / WS, Q
RC24                        / cx ID
        134.08   70.0       /129.50,           5.0     / cx no., WS, Q
 2                     /condition code     upstream
  0                    /connections
 05                    /condition code     downstream
  1                    /connections
 +14                   /connecting branch

Watershed
11           / watershed number
72747328.0   / contributing drainage area, L^2
Distributed  / type of connection
2            / distance-area pairs following
0.0000      0.0000   / channel distance, & area, cumulative fractions
1.0000      1.0000


11           / channel receiving runoff

  ...  information for channels 13, 14, 15, 16, and 20 goes between these lines

Channel
Hydraux
     21    / branch number (Bet. Rio Gurabo Conf. W/RGDL & Rio Canas)
        5,500.00, 1, 6, 0/ no. of cx, dx, NKEEP, ICNDAP, NVAL
RG37                      / cx ID
        134.08, 85.0      / WS, Q
RES4                      / cx ID
        134.08, 85.0      / cx no., WS, Q
RES3                      / cx ID
        134.08, 85.0      / cx no., WS, Q
RES2                      / cx ID
        134.08, 85.0      / cx no., WS, Q
RES1                      / cx ID
        134.08, 85.0      / cx no., WS, Q

 62                   /condition code     upstream
  2                   /connections
  -16                 /connecting branch
  -20                 /connecting branch
 10352                /condition code     downstream
  0                   /connections

Watershed
```

```
21                      / watershed number
269411100.0             / contributing drainage area, L^2
Distributed             / type of connection
2                       / distance-area pairs following
0.0000      0.0000      / channel distance, & area, cumulative fractions
1.0000      1.0000

21                      / channel receiving runoff
```

Constraint Properties - strmcnst.dat

The constraint properties data file strmcnst.dat used in this application provides HYDRAUX with three parameter relation describing the specific hydraulic condition of flow over a spillway. The rating curve of the Carraizo reservoir spillway is defined by three parameters. These data is supplied to HYDRAUX in the input file strmcnst.dat applying a boundary condition code for the channel where the constraint is applied. An example of this file is listed next.

```
begin       /beginning of data for a log-rating constraint
10352       /boundary-condition code, log relation, for Q
637.59      /a
1.6988      /b
134.51      /Zo
end         / end of data for a specific constraint
```

Watershed Data - wtshdbnd.dat

The lateral influx term in equation (23) is provided as unit values applied to each channel in the input file wtshdbnd.dat. The results obtained from applying calibrated Green-Ampt infiltration parameters are converted in units of feet per hour and prepared in the following format:

```
 25200          / starting elapse time, in seconds
   900          / time step, in seconds
     7          / values to be read each time step
    11          / channel no. 11
    13          / channel no. 13
    14          / channel no. 14
    15          / channel no. 15
    16          / channel no. 16
    20          / channel no. 20
    21          / channel no. 21
0.2582644E-04   / excess rainfall, feet per hour
0.2582644E-04   / excess rainfall, feet per hour
0.2582645E-04   / excess rainfall, feet per hour
0.2582645E-04   / excess rainfall, feet per hour
0.2582644E-04   / excess rainfall, feet per hour
0.2582644E-04   / excess rainfall, feet per hour
0.2582644E-04   / excess rainfall, feet per hour
0.2582644E-04   / excess rainfall, feet per hour
0.1341985E-03   / excess rainfall, feet per hour
0.1341985E-03   / excess rainfall, feet per hour
0.1341985E-03   / excess rainfall, feet per hour
0.1341985E-03   / excess rainfall, feet per hour
0.1341985E-03   / excess rainfall, feet per hour
0.1341985E-03   / excess rainfall, feet per hour
0.1341985E-03   / excess rainfall, feet per hour

         ...

0.2582644E-04   / excess rainfall, feet per hour
0.2582644E-04   / excess rainfall, feet per hour
0.2582645E-04   / excess rainfall, feet per hour
0.2582645E-04   / excess rainfall, feet per hour
0.2582644E-04   / excess rainfall, feet per hour
0.2582644E-04   / excess rainfall, feet per hour
0.2582644E-04   / excess rainfall, feet per hour
```